NUSC Technical Report 7925
14 May 1987

Global Model for Sound Absorption in Sea Water Part II: Geosecs PH Data Analysis

R. H. Mellen
PSI - Marine Sciences

P. M. Scheifele
Combat Systems Analysis Staff

D. G. Browning
Surface Ship Sonar Department

Naval Underwater Systems Center
Newport, Rhode Island / New London, Connecticut

DTIC
ELECTE
JUN 2 3 1987
E

87

Preface

This report was prepared for the Naval Underwater Systems Center, Principal Investigator LT P. M. Scheifele (Code 61M). The report was prepared in large part by Dr. R. H. Mellen, Planning Systems Incorporated - Marine Sciences and co-authored by LT P. M. Scheifele, and D. G. Browning of the Naval Underwater Systems Center, New London Laboratory.

The authors wish to acknowledge T. Bell, B. Fisch, G. Smith, Dr. D. Klingbeil, J. Hanrahan, C. DeVoe, J. Doebler, and J. Dlubac for their guidance and assistance with the direction and format of the reports.

Reviewed and Approved: 14 May 1987

L. Freeman
Head, Surface Ship Sonar Department

J. Keil
Head, Combat Systems Analysis Staff

AD-A181 689

REPORT DOCUMENTATION PAGE

1a. REPORT SECURITY CLASSIFICATION UNCLASSIFIED	1b. RESTRICTIVE MARKINGS
2a. SECURITY CLASSIFICATION AUTHORITY	3. DISTRIBUTION / AVAILABILITY OF REPORT
2b. DECLASSIFICATION / DOWNGRADING SCHEDULE	Approved for public release; distribution is unlimited.
4. PERFORMING ORGANIZATION REPORT NUMBER(S) TR 7925	5. MONITORING ORGANIZATION REPORT NUMBER(S)

6a. NAME OF PERFORMING ORGANIZATION Naval Underwater Systems Center	6b. OFFICE SYMBOL (If applicable) Code 61M	7a. NAME OF MONITORING ORGANIZATION
6c. ADDRESS (City, State, and ZIP Code). New London Laboratory New London, CT 06320		7b. ADDRESS (City, State, and ZIP Code)

8a. NAME OF FUNDING / SPONSORING ORGANIZATION	8b. OFFICE SYMBOL (If applicable)	9. PROCUREMENT INSTRUMENT IDENTIFICATION NUMBER

8c. ADDRESS (City, State, and ZIP Code)

10. SOURCE OF FUNDING NUMBERS			
PROGRAM ELEMENT NO.	PROJECT NO.	TASK NO.	WORK UNIT ACCESSION NO.

11. TITLE (Include Security Classification)
GLOBAL MODEL FOR SOUND ABSORPTION IN SEA WATER - PART II: GEOSECS PH DATA ANALYSIS

12. PERSONAL AUTHOR(S)
R. H. Mellen (PSI), P. M. Schiefele and D. G. Browning (NUSC)

13a. TYPE OF REPORT	13b. TIME COVERED FROM _____ TO _____	14. DATE OF REPORT (Year, Month, Day) 1987 MAY 14	15. PAGE COUNT

16 SUPPLEMENTARY NOTATION

17	COSATI CODES		18. SUBJECT TERMS (Continue on reverse if necessary and identify by block number)
FIELD	GROUP	SUB-GROUP	

19 ABSTRACT (Continue on reverse if necessary and identify by block number)

Ionic relaxations involving magnesium sulfate, boric acid and magnesium carbonate are now known to account for sound absorption in sea water. The mechanisms of the three relaxations have been determined by laboratory measurements and are well understood.

Regional dependence of sound absorption has been shown to be caused mainly by the pH-dependence of the boric acid relaxation. In the nominal sea water pH range 7.7-8.3, the magnitude can be expected to vary over nearly a factor of four at lower frequencies.

20 DISTRIBUTION / AVAILABILITY OF ABSTRACT ☐ UNCLASSIFIED/UNLIMITED ☒ SAME AS RPT ☐ DTIC USERS	21. ABSTRACT SECURITY CLASSIFICATION UNCLASSIFIED
22a. NAME OF RESPONSIBLE INDIVIDUAL P. M. Schiefele	22b. TELEPHONE (Include Area Code) (203) 440-6589 22c. OFFICE SYMBOL Code 61M

DD FORM 1473, 84 MAR 83 APR edition may be used until exhausted SECURITY CLASSIFICATION OF THIS PAGE
All other editions are obsolete.

19. ABSTRACT (Cont'd.)

A simplified 3-relaxation absorption model, based on both laboratory and sea experiments, has already been developed. Estimates based on archival pH values have been shown to agree with available sound-channel data. Since pH varies with depth as well as location, net absorption will also depend on the ray paths. An interim global model, based on published pH contours for the World Ocean, has been proposed. Correction factors for the sound-channel, convergence-zone and surface-duct modes are provided by individual contour charts. However, if there is no clearly dominant propagation mode, integration of loss over all ray paths may be indicated, which requires profiles of correction-factor vs depth. *Part 2 reports analysis,* Analysis of pH data obtained during the GEOSECS expeditions 1972-1978, is reported in this work. The purpose is to check the accuracy of the global model contour charts and to investigate methods of estimating profiles of correction-factor vs depth. PH profiles for all the stations reported in the Atlantic, Pacific and Indian Oceans are presented graphically and derived correction factors are listed in tables. Correction-factor contour charts at depths 0, 0.5, 1, 2, and 4 km are also developed and agreement with the earlier versions appears to be within expected experimental error.

The five values provided by the contour charts should permit reasonably accurate estimation of the correction-factor profiles in most of the World Ocean. A graphic method of generating the profiles is simply to connect the points with a fair curve that approximates actual profiles. A computer curve-fitting procedure has also been tested and found to be give good results. An alternative method is to do a computer-search of the library of profiles and select the one with least-square error for the five points in question. Any of the methods are suitable for adaptation to propagation loss programs.

Table of contents

page

Introduction

Accurate prediction of sound absorption in sea water is essential to the effective design and operation of sonar systems and has been recognized as a serious problem for many years. By the end of WWII, it had become clear that absorption at sonar frequencies is an order of magnitude greater than that in fresh water. Subsequent propagation experiments provided accurate estimates of the magnitude. By the early 1950's, laboratory resonator experiments had identified the cause as a magnesium sulfate relaxation and details of the mechanism and relaxation parameters had been worked out [1,2]. In 1962, Schulkin and Marsh proposed a formula for sea water absorption based on field experiments in the frequency range 2-30 kHz and the measured relaxation parameters [3].

In 1965, Thorp [4] reported sound-channel propagation experiments in the Bermuda-Eleuthera area indicating an anomaly at lower frequencies. The excess loss was fitted by addition of a 1 kHz component to the S&M formula. The result became known as the "Thorp formula" [5].

Mediterranean experiments were reported by Leroy [6], showing a similar anomaly but with somewhat higher magnitude and relaxation frequency. Experiments carried over the next two decades in other areas confirmed the high degree of variability of the extra loss and regional dependence has therefore become much more critical. The major factor involved in this variability has been identified as pH [7].

The principal chemical relaxation responsible for the pH-dependent loss has been shown to involve boric acid [8]. The chemical mechanism has been identified as the boric acid/carbonate equilibrium and the parameters have been measured in the laboratory, all by means of the resonator method [9]. The laboratory investigations also revealed a pH-dependent relaxation involving magnesium carbonate, which has been found to play a minor but significant role in sea water absorption [10].

An absorption formula, based solely on known chemical processes would be far too complex and the accuracy would be limited as well. However, since the range of environmental parameters in the World Ocean is very limited, simplifying approximations can be made; namely, that the losses for both pH-dependent relaxations increase exponentially with pH and the relaxation frequencies increase exponentially with temperature. Thorp's formula can then simply be modified by adding the third relaxation and including the required pH and temperature corrections.

A 3-relaxation formula has already been developed. Predictions based on archival pH data have been tested against all the available sound-channel with good results [11,12].

Absorption Model

$$A = A_1(MgSO_4) + A_2(B(OH)_3) + A_3(MgCO_3)$$
$$A_n = a_n f^2 f_n / (f^2 + f_n^2)$$

$$a_1 = 0.5 \times 10^{-d(km)/20} \qquad f_1 = 50 \times 10^{T/60}$$
$$a_2 = 0.1 \times 10^{(pH-8)} \qquad f_2 = 0.9 \times 10^{T/70}$$
$$a_3 = 0.03 \times 10^{(pH-8)} \qquad f_3 = 4.5 \times 10^{T/30}$$

Atlantic 4°C pH 8.0
$$A = 0.007f^2 + 0.1 f^2/(1+f^2) + 0.18 f^2/(6^2+f^2)$$

N.Pacific 4°C pH 7.7
$$A = 0.007f^2 + 0.05f^2/(1+f^2) + 0.09 f^2/(6^2+f^2)$$

Mediterranean 14°C pH 8.3
$$A = 0.006f^2 + 0.26f^2/(1.4^2+f^2) + 0.78f^2/(12^2+f^2)$$

Red Sea 22°C pH 8.2
$$A = 0.004f^2 + 0.27f^2/(1.8^2+f^2) + 1.1f^2/(24^2+f^2)$$

sub-Arctic -1°C pH 8.3
$$A = 0.01f^2 + 0.17 f^2/(0.85^2+f^2) + 0.24f^2/(4^2+f^2)$$

Figure 1: Simplified absorption formulae.

In the 3-relaxation formula of Figure 1, A is in dB/km, frequency f and relaxation frequencies f_n are in kHz, temperature T is in °C and pH=8.0 is the reference value. The pure water term is neglected, making the formula valid for frequencies less than roughly 100 kHz. PH values in the World Ocean vary roughly from 7.7 to 8.3, which corresponds to an absorption ratio of as much as 4/1 at the lower frequencies.

The magnesium sulfate term includes the depth factor D(km), which is adopted from the pressure correction of Fisher and Simmons [12]. Depth dependencies of the other two relaxations are not yet known; however, measurements indicate that boric acid effects are negligible. Magnesium carbonate depth effects can be neglected because its contribution is so small. Salinity dependence will be considered later..

Specific coefficients for several experimental areas, are shown in the bottom box. Note that the magnesium sulfate terms are approximations valid only for frequencies much less than the relaxation frequencies f_1.
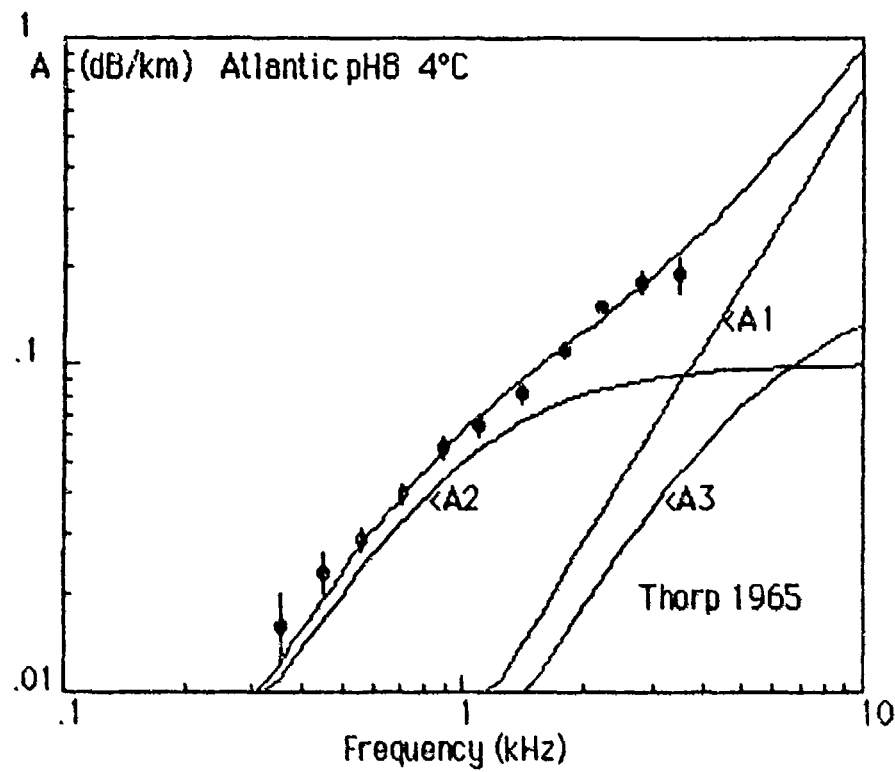
Figure 2: Thorp's data and 3-relaxation model.

Figure 2 shows Thorp's data compared to the 3-relaxation model. The individual components are identified and the top curve is their sum. The overall fit to the data is seen to be as good or better than with Thorp's 2-component formula.

Note that the boric acid (A2) coefficient is lower than that in the Thorp formula by some 10%; i.e., the coefficient in dB/km becomes equal to the value in Thorp's equation, which was given in dB/kyd. Differences in the total absorption at lower frequencies are then made up by the magnesium carbonate component (A3).

The parameter adjustment is mainly justified on the basis of data-fit, the third component being essential to the model. When the sea-water resonator data were fitted with a 2-relaxation model, there were serious discrepencies at higher pH values. Correction of Thorp's equation for pH8.5 gave values that were much too low at the lower frequencies, which was clear evidence of the existence of a third component. Sea water synthesis experiments were then carried out. The mechanism was identified as a magnesium carbonate relaxation and the relaxation parameters, including temperature and pH dependence, were measured.

- 3 -
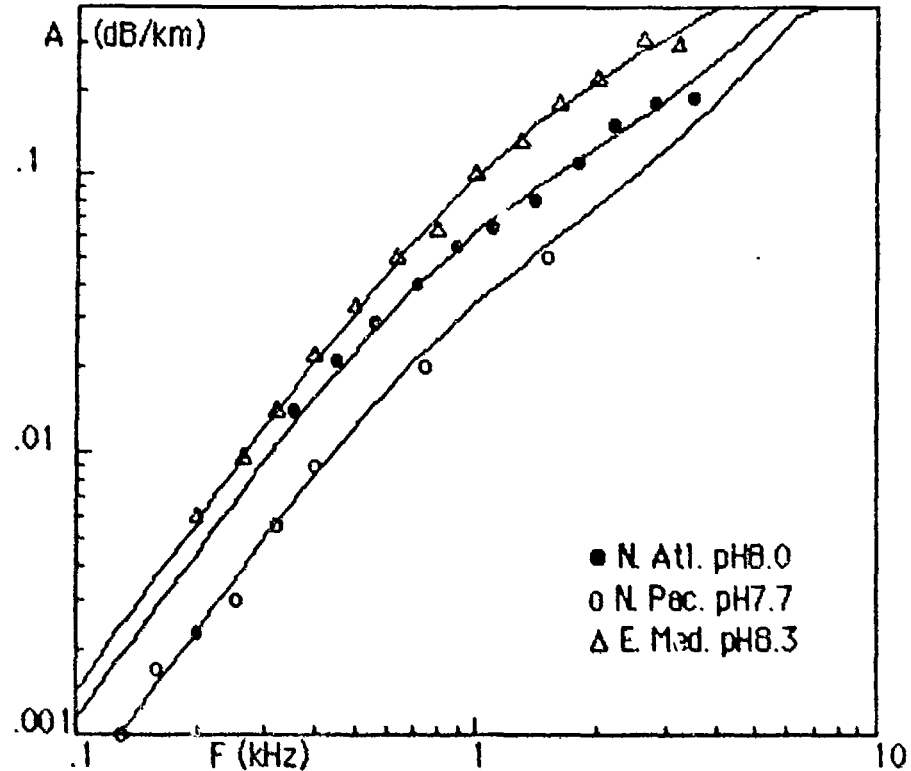
Figure 3: Model and data comparison.

Figure 3 compares the 3-component relaxation model predictions and data from sound-channel experiments in the Mediterranean, North Pacific and North Atlantic (Thorp).

In the North Pacific case [14], the lower value pH≈7.7 reduces both the boric acid (A2) and the magnesium carbonate (A3) coefficients by a factor of two compared to the N. Atlantic. Relaxation frequency depends only on temperature and remains the same.

In the Mediterranean case [15], the higher value pH≈8.3 increases both the boric acid (A2) and the magnesium carbonate (A3) coefficients by a factor of two compared to the N. Atlantic. However, since the relaxation frequency is higher, the curves do not differ by as large a large factor at the lower frequencies.

The value pH 8.0 has been assumed for Thorp's experiment and is used as reference value for the 3-relaxation model. Predictions based on archival pH values then show agreement within experimental limits for all regions examined. Although no discrepencies are now apparent, small adjustments of any of the parameters can be made whenever new absorption and pH data indicate the need.
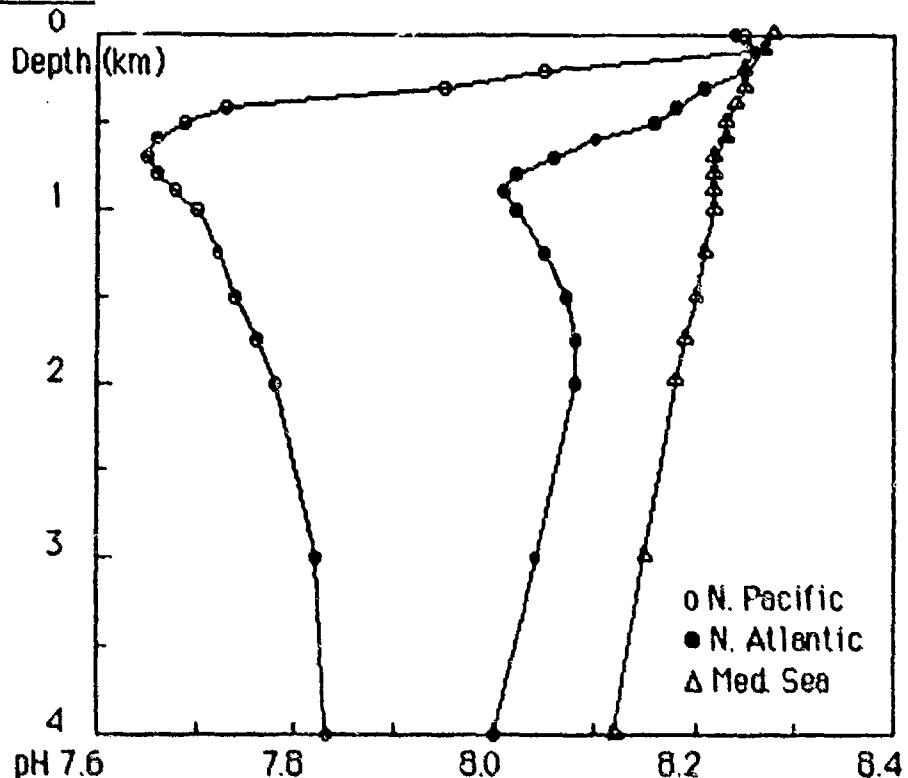
Figure 4: PH profiles.

Typical pH profiles for the North Atlantic and North Pacific Oceans and the Mediterranean Sea,obtained from the GEOSECS expedition reports [16], are shown in Figure 4.

The most striking features are the relative constancy of the pH values at the surface and the slow variations at great depths. Variability with depth means that net absorption realized for the various propagation modes will also depend very strongly on the pH profile and the particular ray paths involved.

In the analysis of sound-channel propagation experiments, axial values of pH and temperature have proved to give adequate approximations, within expected limits of experimental error. Axial depths at mid-latitudes are near 1 km, where the regional variability tends to be greatest. At higher latitudes, the sound-channel axis rises nearer to the surface where the pH values are uniformly high. For convergence-zone propagation, integration of loss over the ray paths by numerical methods has shown that the 2 km depth values give accurate estimates except for possible errors at higher latitudes. Surface values are obviously appropriate for the surface duct. The interim global model has been based on these approximations.

Global Model

$$A = A_1(MgSO_4) + A_2(B(OH)_3) + A_3(MgCO_3)$$

$$A_n = (S/35)\, a_n f^2 f_n /(f^2 + f_n^2)$$

$$a_1 = 0.5 \times 10^{-D(km)/20} \qquad f_1 = 50 \times 10^{T/60}$$

$$a_2 = 0.1\,K \qquad f_2 = 0.9 \times 10^{T/70}$$

$$a_3 = 0.03\,K \qquad f_3 = 4.5 \times 10^{T/30}$$

Figure 5: Global model absorption formula.

Variability of pH is clearly the major limiting factor in the accuracy of the absorption model. In the proposed global model of Figure 5, the pH parameter $K = 10^{(pH-8)}$ has been substituted in the absorption formula of Figure 1. Salinity dependence is taken as S/35 with the caveats noted [11]; i.e. errors probably become excessive outside the range 30-40 ppt since the changes in relaxation frequency must then be considered. This could require analysis of constituents, which is beyond the present scope.

The interim model is based on estimation of the effective K values for specific propagation modes. From the earlier analysis, axial values of K and temperature T (°C) are appropriate for the sound-channel mode and 2 km depth values for CZ and other deep modes. Errors at high latitudes can be reduced by interpolation, depending on the ray paths. Temperature is not a problem since it can be derived from the SVP or XBT data.

Contours of pH for the surface and for depths 0.5 km and 1 km are shown in the World Ocean Atlas of Gorshkov [17]. Contours for 2 km depth are also included in Vol. 2. The contour intervals are 0.1 pH unit and interpolation is required. Correction to *in-situ* pressure is also necessary.

The GEOSECS data have also been used to estimate the 2 km contours in parts of the Pacific Ocean not covered by the Russian work. Discrepencies between the data sets have been arbitrarily resolved by adjustment of the contours to minimize effects on estimation error.

The sound-channel K contour chart of Figure 6 is based on the analysis of Russian pH contours by Lovett [18]. The CZ and surface charts, derived mainly from the Russian report, are shown in Figures 7 and 8, respectively. The CZ chart is a modification of the earlier 2 km chart with corrections for high-latitude effects. Effective K values were obtained by integration over appropriate ray paths.
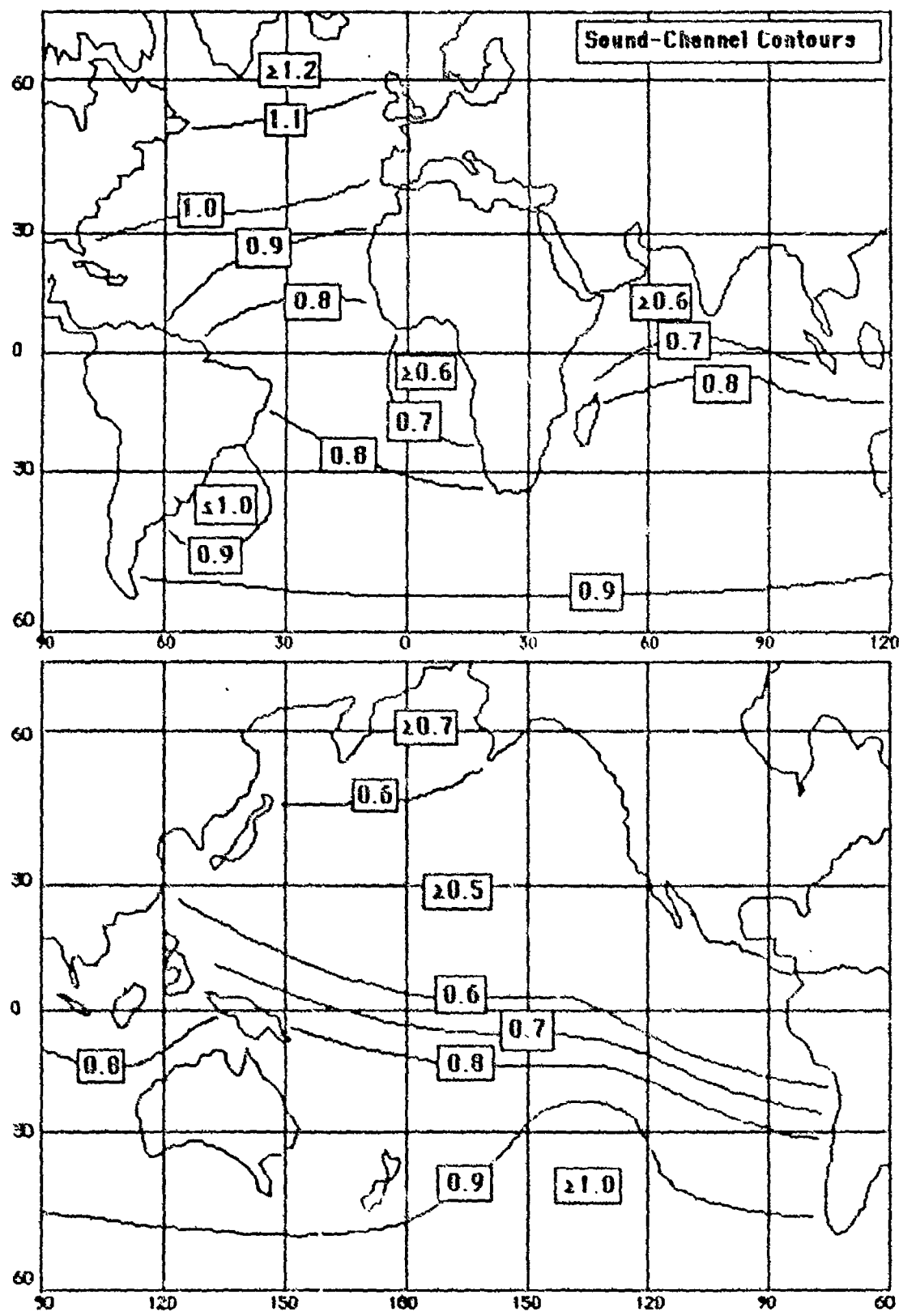
Figure 6. Deep sound-channel K contours.
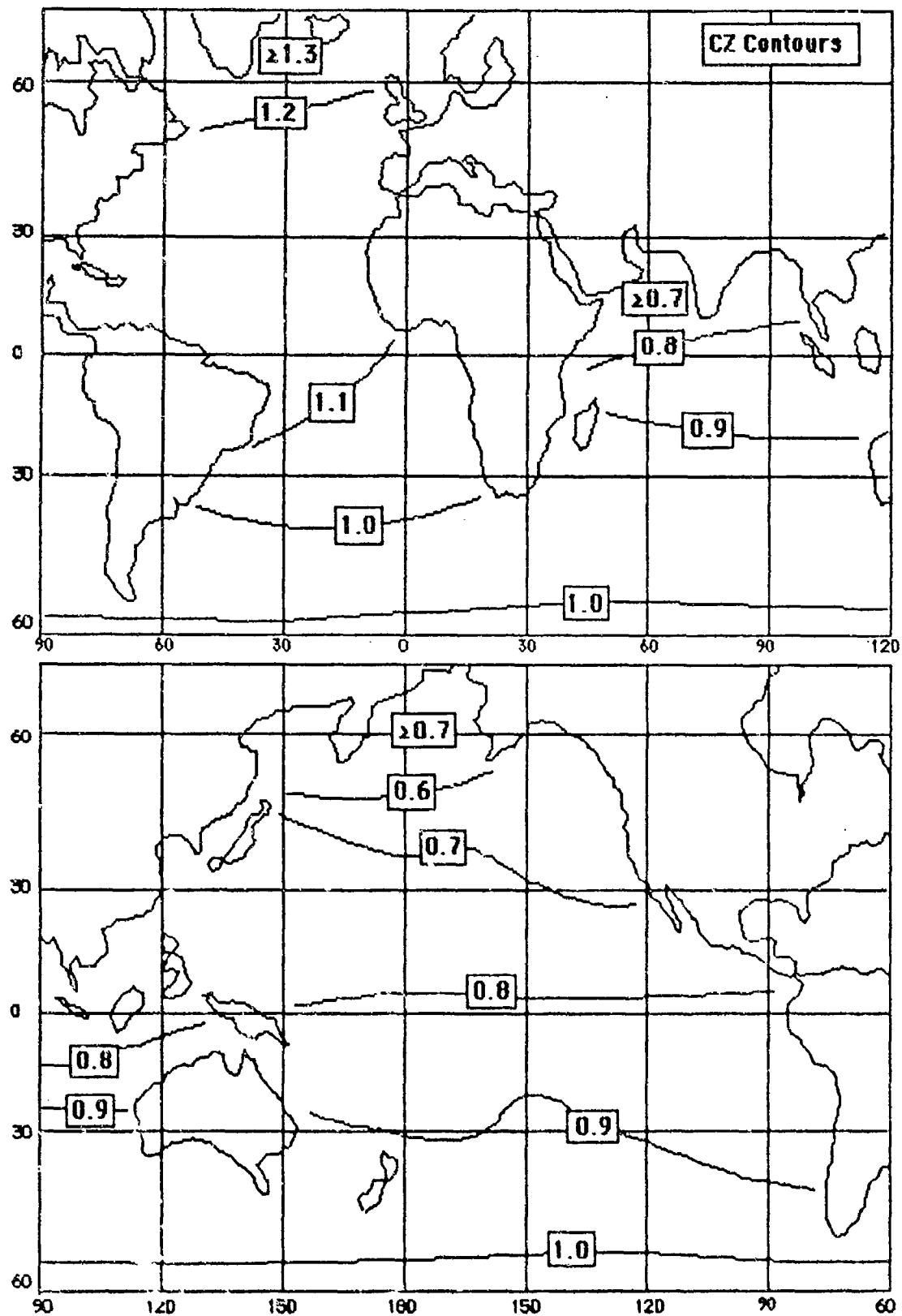
Figure 7: Effective K contours for CZ mode.
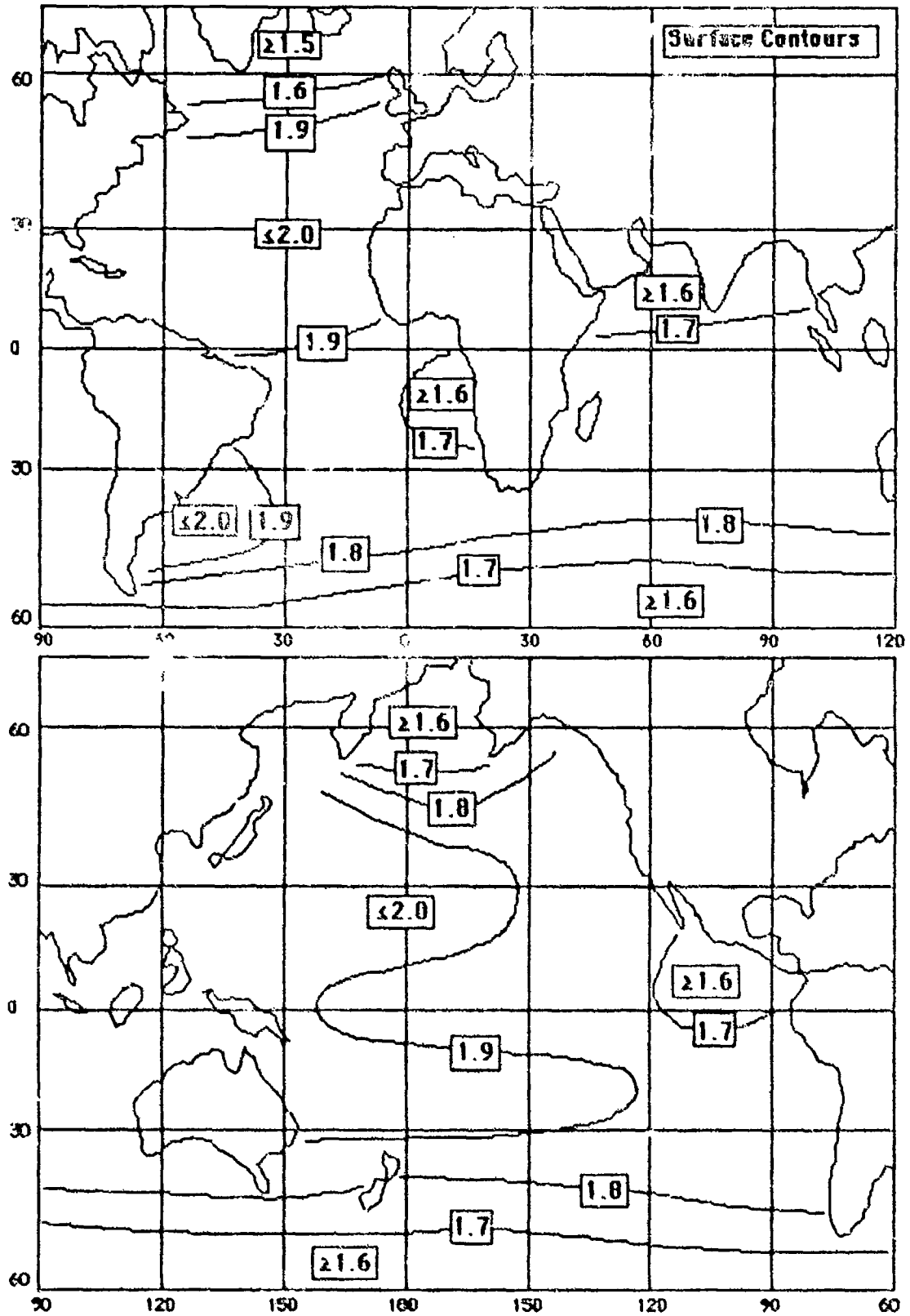
Figure 6: Surface K contours.

The absorption formula of Figure 5 has been based on the results of both laboratory and sound-channel experiments. Because the frequency range of the resonator was limited to 10-100 kHz, it was not possible to measure the boric acid relaxation parameters by this means. The field data were primarily used in determining the absorption spectra at lower frequencies. Thorp's data of Figure 2, considered to be the most accurate, was heavily weighted in the analysis.

The pH data for the sound-channel experiments was archival and errors are estimated to be of the order ±0.05 units, which corresponds to ±12% error in magnitude at lower frequencies. Therefore, the absolute accuracy of the pH-dependent part of the formula is expected to be of this order. The accuracy of the pH-independent part is as good or better. Resonator studies of sea-water absorption in the low kHz range have been carried out recently at the Academia Sinica laboratories and measurements over the pH range of interest confirm overall formula predictions with equivalent accuracy [19,20].

Accuracy of field predictions will, in general, be limited by the pH data. The K contours of Figures 6-8 should provide reasonably good estimates of absolute pH effects for the three propagation modes throughout most of the World Ocean. Possible exceptions are regions where some significant discrepencies between the Russian and GEOSECS values have been noted and also regions where pH profile changes are rapid. Questions can also arise when there is no clearly dominant propagation mode.

While the global model can certainly account for gross regional changes in absorption, the overall accuracy may be inadequate in some cases. For example, it can be difficult to determine what values to use for arbitrary ray paths. Interpolation between the sound-channel, convergence-zone and surface values should help to improve matters; however, the errors could easily become unacceptable when there are rapid changes over the depth range in question. Some subjectivity and uncertainty is always involved in such a process. Furthermore, the errors are additive and combined effects of ray-path approximations and errors in values could become excessive. Therefore, an obvious method of simplifying the computational process, as well as improving the overall accuracy, is to integrate loss over all the ray paths using an appropriate profile for the region.

In the following sections, all of the GEOSECS data are analyzed for the purpose of assessing the accuracy of the K contour charts. The second and perhaps major purpose is to investigate K-profile estimation methods for incorporation in existing computer programs for propagation loss.

GEOSECS Data Analysis

The Geochemical Ocean Sections Study (GEOSECS) [16] atlas volumes contain records of the oceanographic data taken during the International Decade of Ocean Exploration (IDOE) 1970-1980. The areas covered include the Atlantic, Pacific and Indian Oceans. The expedition tracks followed depth contours of 4 km or more and coverage is not comprehensive. Data are missing for many of the stations also, particularly the first part of the North Atlantic track.

The Carbonate Chemistry sections of each volume contain the tables of temperature, salinity, pH and associated parameters vs depth. The pH data is the primary concern in this work. Procedures and method of pH analysis are discussed in the atlases and references. Values corrected to *in-situ* temperature and pressure are included and are used in this report.

Data for the three oceans are presented in sections, each beginning with a track chart showing the station numbers. Station sequence is followed except for the Indian Ocean section where the profiles 404-407, for the Mediterranean Sea, the Red Sea and the Gulf of Aden, are placed at the end in reversed order.

The graphs at the top of the figures following contain 5 sequential pH vs depth profiles. Depth intervals were chosen to give the minimum required detail and the original data were interpolated to obtain the values when necessary. Any fine structure present was minimized by smoothing. The pH scale for each station is indicated by solid vertical lines with the value pH8.0 at the top. The tick marks are 0.1 pH units and successive profiles are displaced two units to the right. The tables below the graphs show the station numbers, station coordinates and calculated K values vs depth.

The K contours at five selected depths 0, 0.5, 1, 2 and 4 km are shown in Figures 41-45 The contours were derived by plotting the K values on the charts and adjusting for "best-fit", taking into consideration values and trends indicated by the Russian profiles. Note that the K values refer to regions separated by contour lines and not the contour lines themselves, as in the earlier charts. This simplifies selection of values in the regions of gradual change and serves to identify problem regions of rapid change as well.

The five K values provided by the charts should permit quite accurate estimation of the K profiles in regions where no data are available. In later sections, several alternative methods for formulating profiles are proposed. The expected error in predicted loss due to profile estimation errors is also considered.

TRACK OF R/V KNORR,
GEOSECS ATLANTIC EXPEDITION, 1972-73
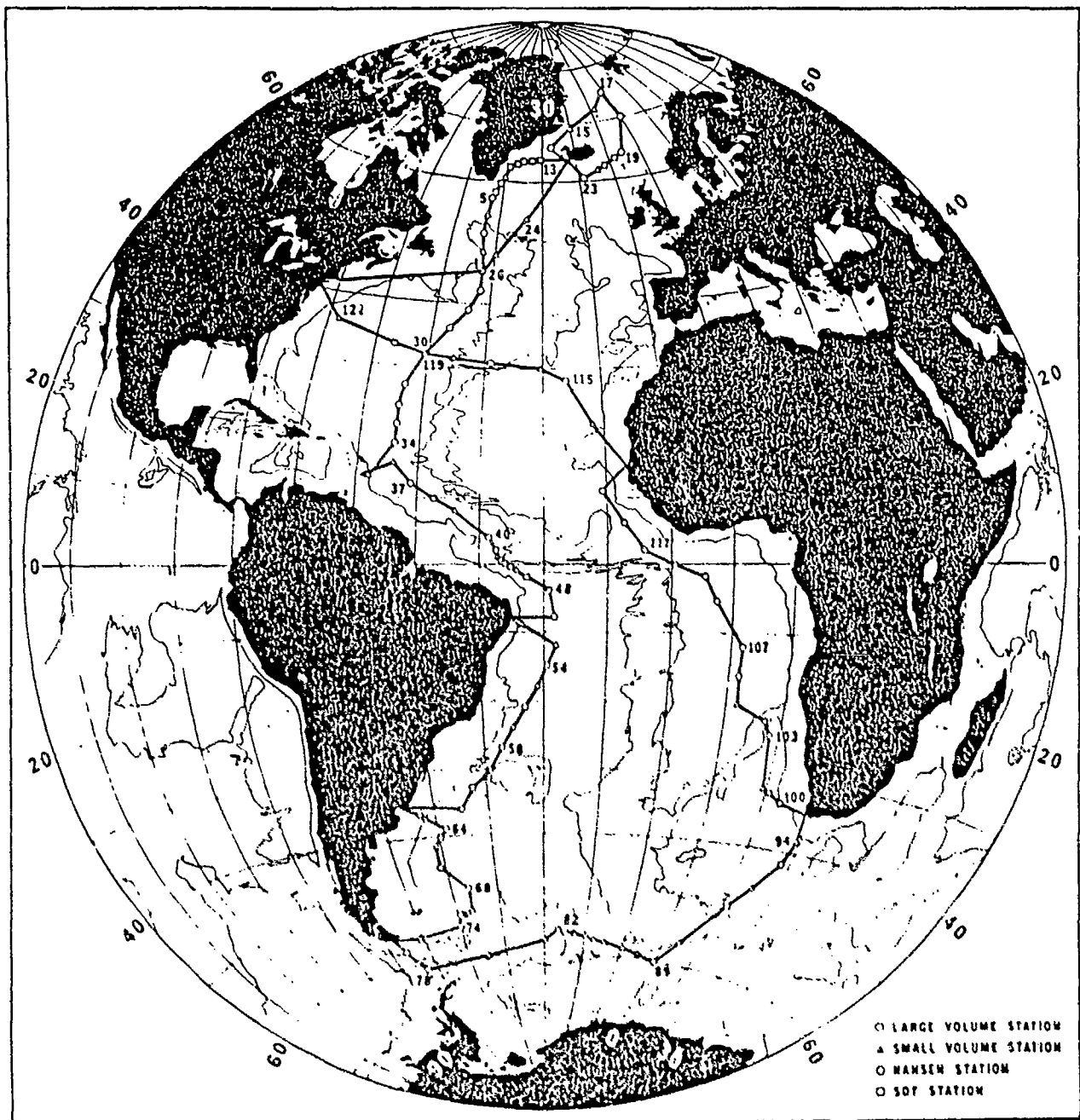
Figure 9: Atlantic track.
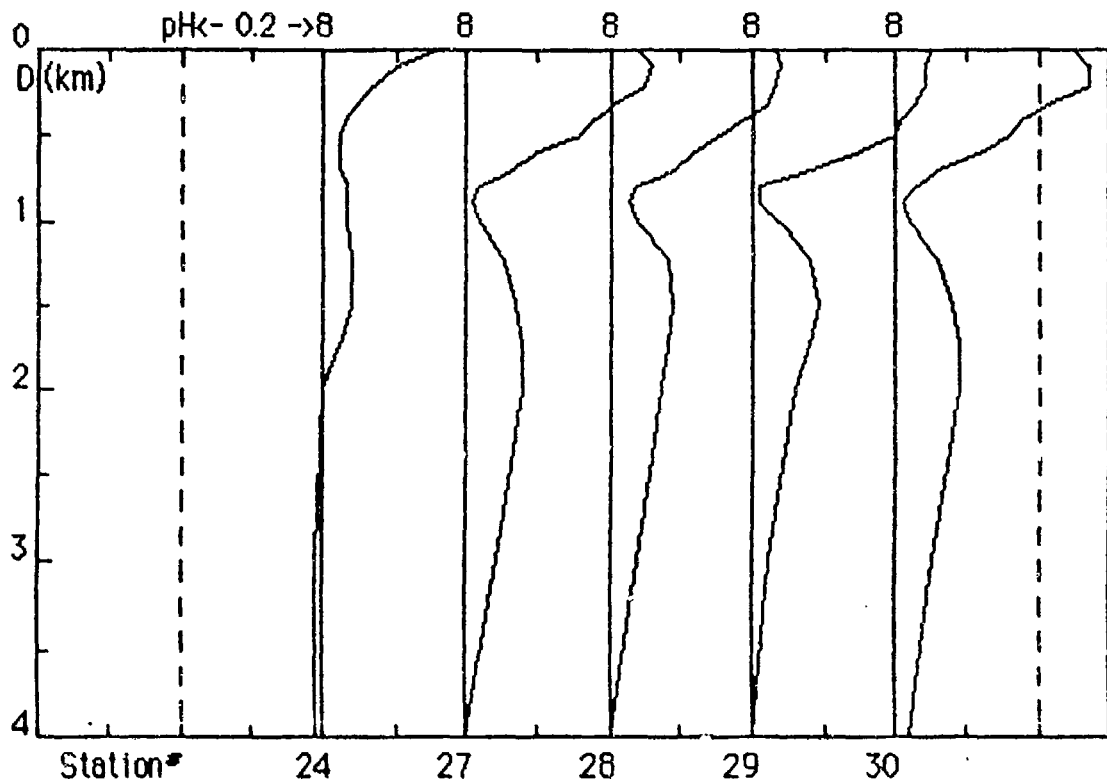
Station#>	24 54°N 34°W	27 42°N 42°W	28 39°N 44°W	29 36°N 47°W	30 32°N 51°W
Depth(km)					
0.00	1.45	1.74	1.70	1.78	1.78
0.10	1.26	1.82	1.74	1.74	1.86
0.20	1.17	1.78	1.70	1.74	1.06
0.30	1.12	1.62	1.66	1.70	1.66
0.40	1.07	1.51	1.55	1.62	1.51
0.50	1.05	1.45	1.41	1.58	1.45
0.60	1.05	1.26	1.32	1.41	1.32
0.70	1.05	1.15	1.23	1.20	1.15
0.80	1.07	1.05	1.10	1.02	1.07
0.90	1.07	1.02	1.07	1.02	1.02
1.00	1.07	1.05	1.10	1.10	1.05
1.25	1.10	1.12	1.20	1.20	1.15
1.50	1.10	1.17	1.23	1.23	1.20
1.75	1.05	1.20	1.20	1.20	1.23
2.00	1.00	1.20	1.17	1.15	1.23
3.00	0.98	1.10	1.10	1.05	1.12
4.00	0.98	1.00	1.00	1.00	1.05

Figure 10: Atlantic Ocean stations.
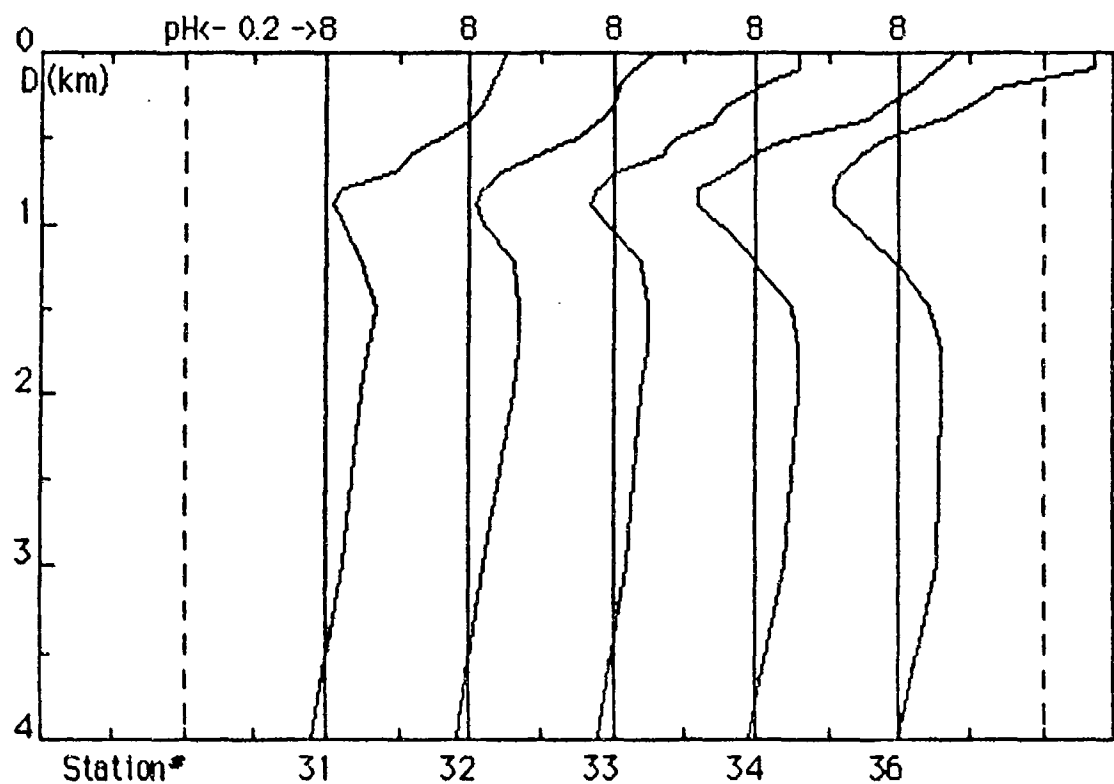
Station#>	31 27°N 54°W	32 24°N 54°W	33 21°N 54°W	34 18°N 54°W	36 15°N 54°W
Depth(km)					
0.00	1.78	1.82	1.82	1.91	1.86
0.10	1.74	1.70	1.82	1.78	1.86
0.20	1.70	1.62	1.58	1.66	1.35
0.30	1.66	1.58	1.45	1.51	1.26
0.40	1.58	1.51	1.38	1.41	1.12
0.50	1.45	1.41	1.23	1.12	0.95
0.60	1.32	1.26	1.17	1.00	0.89
0.70	1.23	1.10	1.00	0.91	0.83
0.80	1.05	1.05	0.95	0.83	0.81
0.90	1.02	1.02	0.93	0.83	0.81
1.00	1.05	1.05	0.98	0.89	0.87
1.25	1.12	1.15	1.10	1.00	1.00
1.50	1.17	1.17	1.12	1.12	1.10
1.75	1.15	1.17	1.12	1.15	1.15
2.00	1.12	1.15	1.10	1.15	1.15
3.00	1.05	1.05	1.05	1.10	1.12
4.00	0.95	0.95	0.95	0.98	1.00

Figure 11: Atlantic Ocean stations.

- 14 -
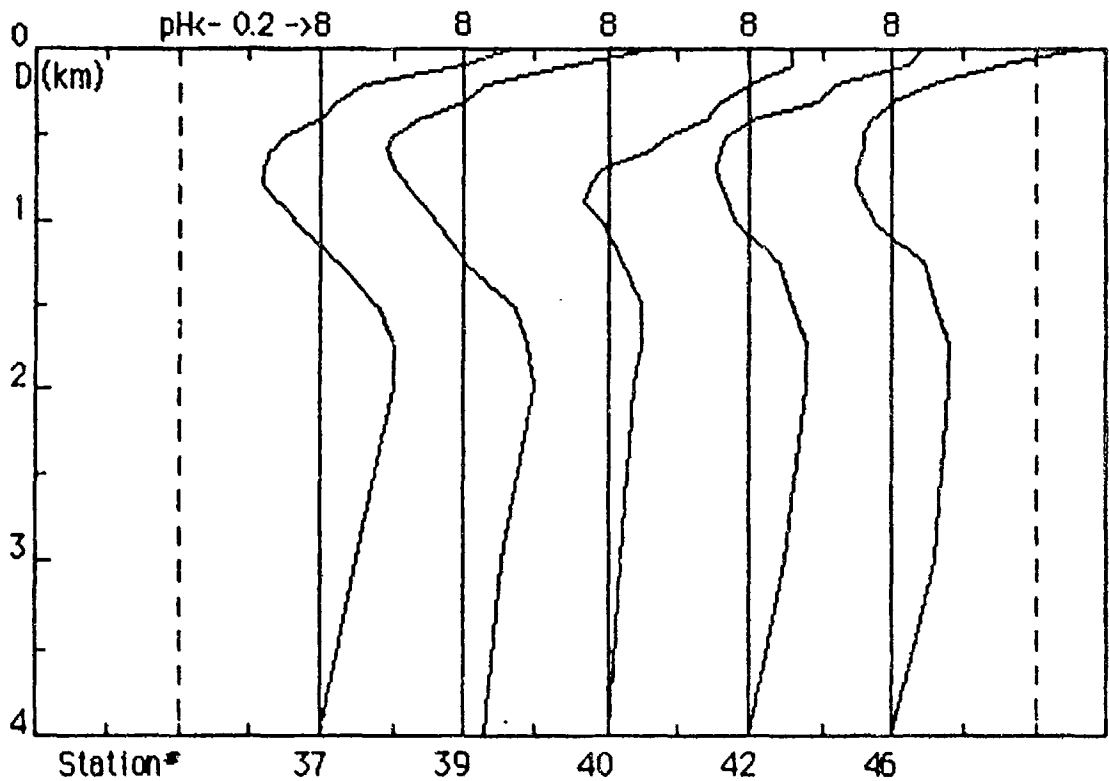
Station#>	37 12°N 51°W	39 08°N 44°W	40 04°N 39°W	42 01°N 37°W	46 01°S 34°W
Depth(km)					
0.00	1.86	1.86	1.82	1.74	1.86
0.10	1.58	1.41	1.82	1.66	1.41
0.20	1.15	1.07	1.58	1.32	1.12
0.30	1.05	1.00	1.45	1.23	1.00
0.40	1.00	0.87	1.38	1.02	0.93
0.50	0.89	0.79	1.23	0.93	0.91
0.60	0.85	0.78	1.15	0.91	0.91
0.70	0.83	0.79	0.98	0.89	0.89
0.80	0.83	0.83	0.95	0.91	0.89
0.90	0.87	0.87	0.93	0.93	0.91
1.00	0.91	0.91	0.98	0.95	0.93
1.25	1.05	1.00	1.05	1.10	1.10
1.50	1.20	1.17	1.12	1.15	1.15
1.75	1.26	1.23	1.12	1.20	1.20
2.00	1.26	1.26	1.10	1.20	1.20
3.00	1.12	1.12	1.05	1.12	1.15
4.00	1.00	1.07	1.00	1.00	1.00

Figure 12: Atlantic Ocean stations.
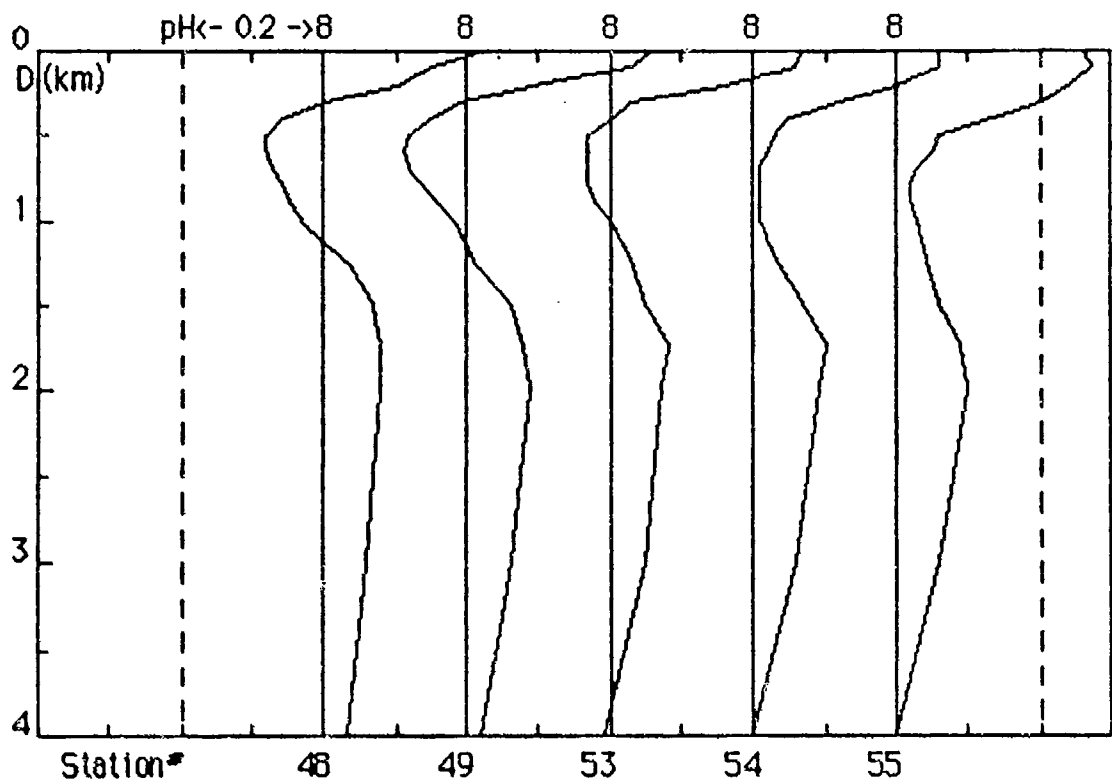
Station#>	48 04°S 29°W	49 06°S 28°W	53 12°S 28°W	54 15°S 30°W	55 18°S 31°W
Depth(km)					
0.00	1.70	1.82	1.86	1.82	1.82
0.10	1.41	1.70	1.82	1.82	1.66
0.20	1.26	1.23	1.45	1.58	1.74
0.30	1.00	0.98	1.07	1.32	1.58
0.40	0.87	0.89	1.00	1.12	1.35
0.50	0.83	0.83	0.93	1.07	1.15
0.60	0.83	0.81	0.93	1.05	1.12
0.70	0.85	0.83	0.93	1.02	1.07
0.80	0.67	0.87	0.93	1.02	1.05
0.90	0.89	0.91	0.95	1.02	1.05
1.00	0.93	0.95	1.00	1.02	1.07
1.25	1.07	1.02	1.07	1.07	1.10
1.50	1.17	1.15	1.12	1.17	1.15
1.75	1.20	1.20	1.20	1.26	1.23
2.00	1.20	1.23	1.17	1.23	1.26
3.00	1.15	1.15	1.12	1.15	1.15
4.00	1.07	1.05	0.98	1.00	1.00

Figure 13: Atlantic Ocean stations.
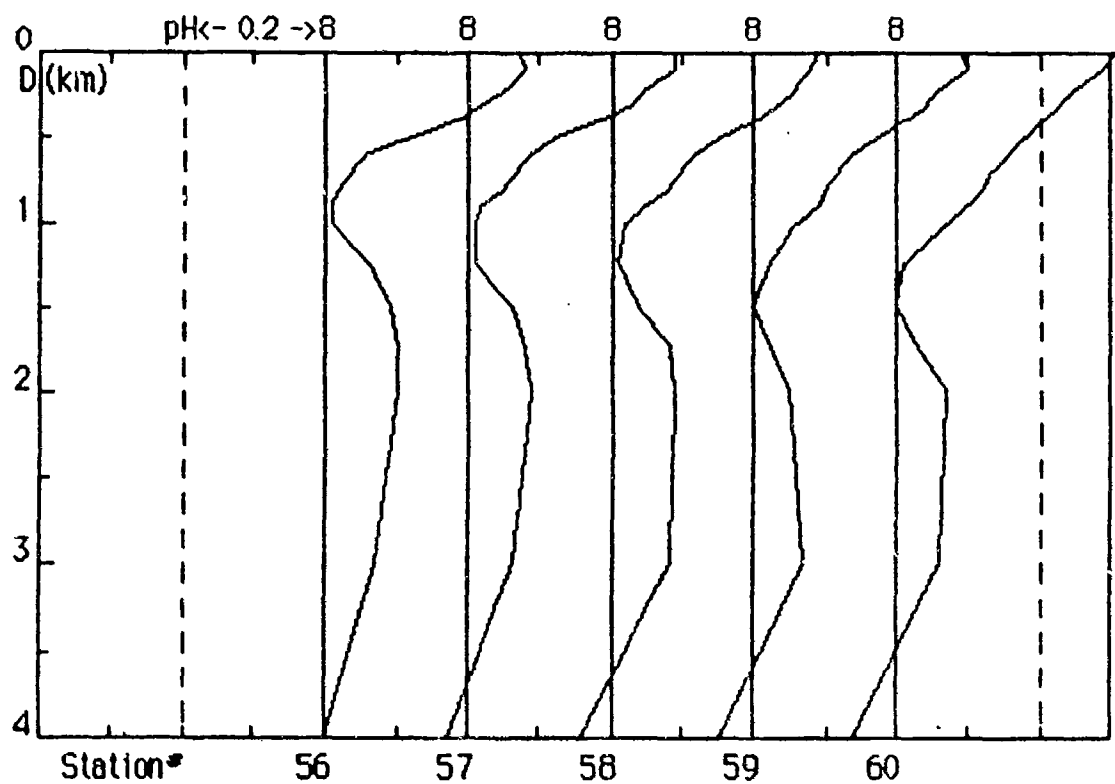
Station#>	56 21°S 33°W	57 24°S 35°W	58 27°S 37°W	59 30°S 39°W	60 33°S 42°W
Depth(km)					
0.00	1.86	1.95	1.95	1.95	2.04
0.10	1.91	1.95	1.91	2.00	1.95
0.20	1.78	1.78	1.82	1.82	1.78
0.30	1.66	1.70	1.70	1.74	1.70
0.40	1.51	1.51	1.58	1.62	1.58
0.50	1.32	1.32	1.41	1.48	1.51
0.60	1.15	1.23	1.32	1.38	1.45
0.70	1.10	1.17	1.26	1.32	1.35
0.80	1.05	1.12	1.20	1.26	1.32
0.90	1.02	1.05	1.12	1.23	1.26
1.00	1.02	1.02	1.05	1.15	1.17
1.25	1.15	1.02	1.02	1.05	1.02
1.50	1.23	1.15	1.10	1.00	1.00
1.75	1.26	1.20	1.20	1.05	1.07
2.00	1.26	1.23	1.23	1.12	1.17
3.00	1.17	1.15	1.20	1.17	1.15
4.00	1.00	0.93	0.91	0.89	0.87

Figure 14: Atlantic Ocean stations.
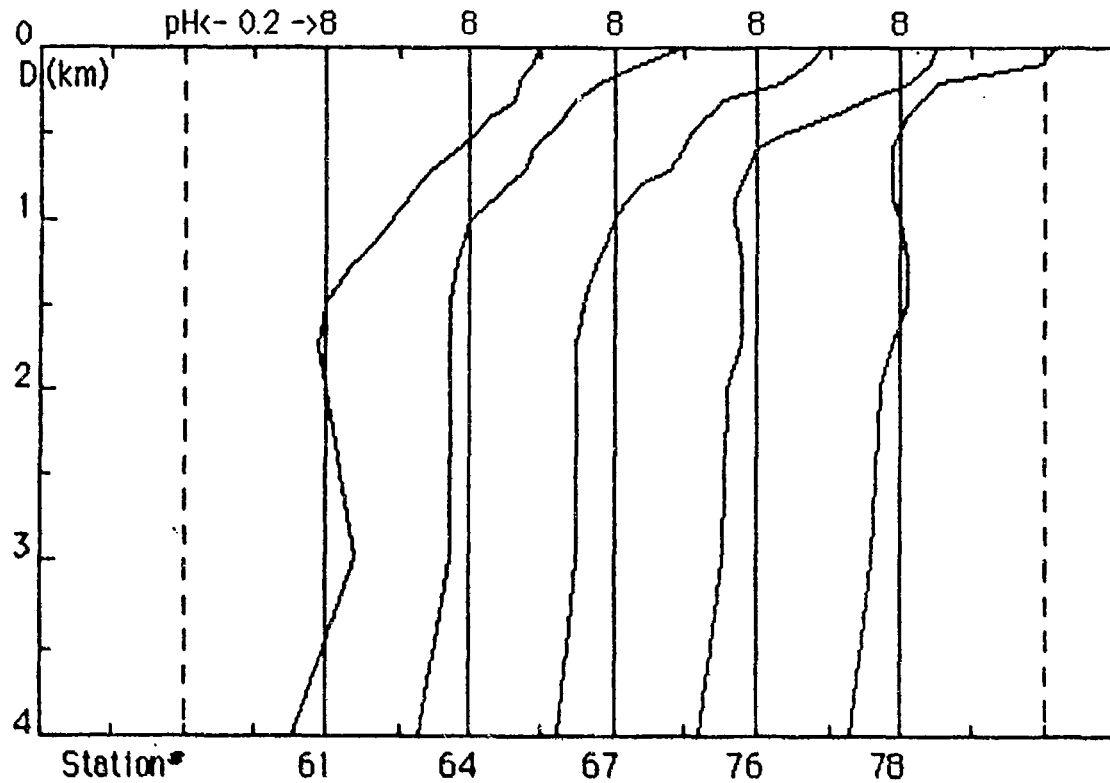
Station*>	61 36°S 45°W	64 39°S 49°W	67 45°S 51°W	76 58°S 66°W	78 61°S 63°W
Depth(km)					
0.00	2.00	2.00	1.95	1.78	1.66
0.10	1.95	1.74	1.86	1.74	1.58
0.20	1.86	1.51	1.70	1.62	1.12
0.30	1.82	1.41	1.41	1.41	1.07
0.40	1.70	1.35	1.35	1.26	1.02
0.50	1.62	1.29	1.29	1.10	1.00
0.60	1.51	1.23	1.26	1.00	0.98
0.70	1.41	1.20	1.20	0.98	0.98
0.80	1.35	1.12	1.10	0.95	0.98
0.90	1.29	1.07	1.05	0.93	0.98
1.00	1.23	1.00	1.00	0.93	1.00
1.25	1.10	0.95	0.95	0.95	1.02
1.50	1.00	0.93	0.91	0.95	1.02
1.75	0.98	0.93	0.89	0.95	0.98
2.00	1.00	0.93	0.89	0.91	0.93
3.00	1.10	0.93	0.89	0.89	0.91
4.00	0.89	0.85	0.83	0.83	0.85

Figure 15: Atlantic Ocean stations.
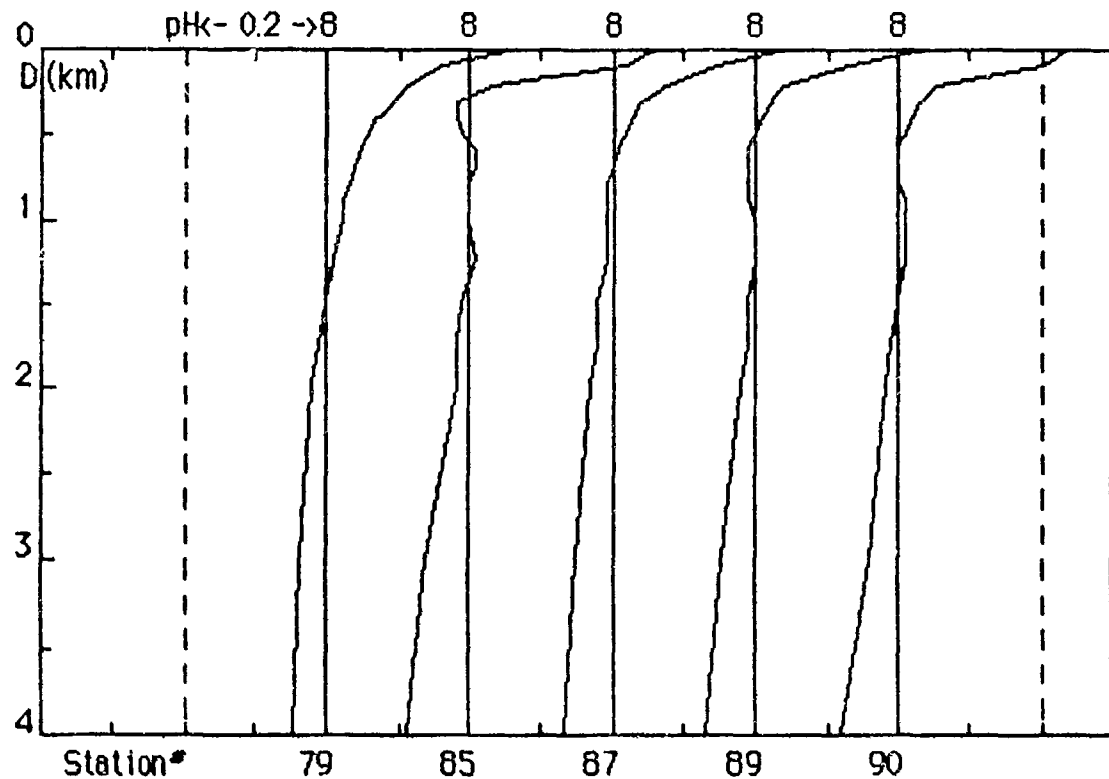
Station#>	79 60°S 45°W	85 57°S 17°W	87 59°S 09°W	89 60°S 00°E	90 56°S 05°E
Depth(km)					
0.00	1.86	1.82	1.78	1.74	1.74
0.10	1.45	1.66	1.36	1.35	1.58
0.20	1.29	1.07	1.17	1.10	1.12
0.30	1.23	0.95	1.10	1.05	1.07
0.40	1.17	0.95	1.07	1.02	1.05
0.50	1.15	0.98	1.05	1.00	1.02
0.60	1.12	1.02	1.02	0.98	1.00
0.70	1.10	1.02	1.00	0.98	1.00
0.80	1.07	1.00	0.98	0.98	1.00
0.90	1.05	1.00	0.98	0.98	1.02
1.00	1.05	1.00	0.98	1.00	1.02
1.25	1.02	1.02	0.98	1.00	1.02
1.50	1.00	0.98	0.95	0.98	1.00
1.75	0.98	0.95	0.95	0.98	0.98
2.00	0.95	0.95	0.93	0.95	0.95
3.00	0.91	0.87	0.89	0.89	0.91
4.00	0.89	0.81	0.85	0.85	0.83

Figure 16: Atlantic Ocean stations.
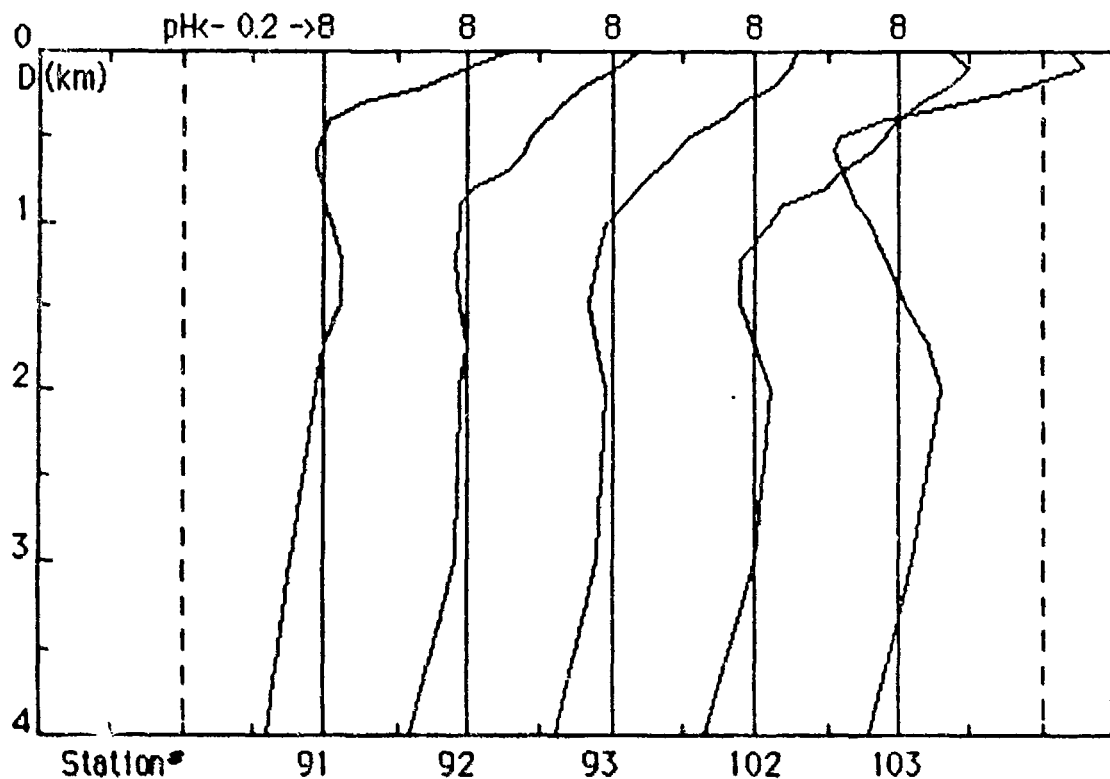
Station#>	91 50°S 11°E	92 46°S 15°E	93 42°S 18°E	102 32°S 09°E	103 24°S 08°E
Depth(km)					
0.00	1.82	1.74	1.82	1.86	1.74
0.10	1.58	1.62	1.78	2.00	1.62
0.20	1.38	1.45	1.66	1.86	1.51
0.30	1.12	1.35	1.51	1.70	1.23
0.40	1.02	1.29	1.41	1.58	0.95
0.50	1.00	1.23	1.29	1.51	0.83
0.60	0.98	1.20	1.23	1.45	0.81
0.70	0.98	1.12	1.15	1.32	0.83
0.80	1.00	1.02	1.10	1.26	0.85
0.90	1.00	0.98	1.05	1.10	0.87
1.00	1.02	0.98	0.98	1.05	0.91
1.25	1.05	0.95	0.95	0.95	0.95
1.50	1.05	0.98	0.93	0.95	1.02
1.75	1.00	1.00	0.95	1.00	1.10
2.00	0.98	0.98	0.98	1.05	1.15
3.00	0.89	0.95	0.95	1.00	1.05
4.00	0.83	0.83	0.83	0.85	0.91

Figure 17: Atlantic Ocean stations.

Figure 18: Atlantic Ocean stations.
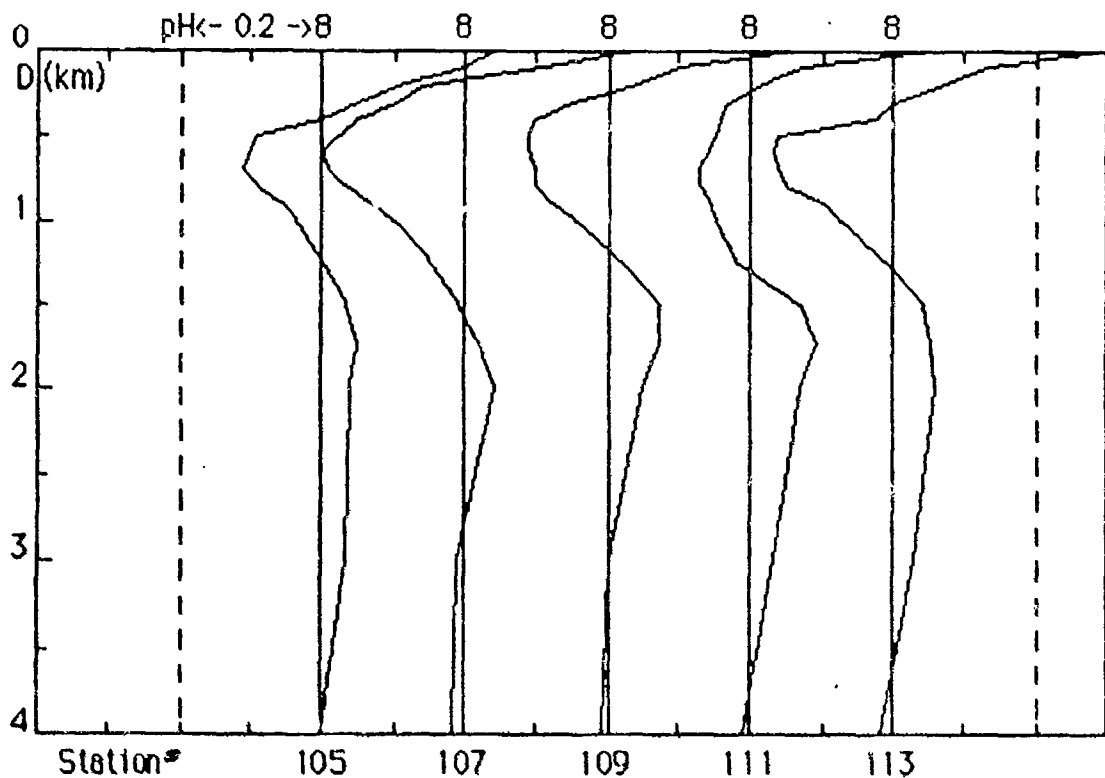
Station#>	105 20°S 02°E	107 12°S 02°E	109 02°S 04°W	111 02°N 14°W	113 11°N 21°W
Depth(km)					
0.00	1.74	1.74	1.86	1.82	2.00
0.10	1.58	1.29	1.26	1.17	1.35
0.20	1.26	0.87	1.07	1.02	1.15
0.30	1.12	0.79	0.89	0.93	1.00
0.40	1.00	0.71	0.79	0.91	0.93
0.50	0.81	0.66	0.78	0.89	0.69
0.60	0.79	0.63	0.78	0.87	0.68
0.70	0.78	0.65	0.79	0.85	0.69
0.80	0.81	0.68	0.79	0.85	0.71
0.90	0.87	0.74	0.83	0.87	0.79
1.00	0.91	0.79	0.91	0.89	0.85
1.25	1.00	0.89	1.05	0.95	0.98
1.50	1.07	0.98	1.17	1.17	1.10
1.75	1.12	1.05	1.17	1.23	1.12
2.00	1.10	1.10	1.12	1.17	1.15
3.00	1.07	0.98	1.00	1.07	1.07
4.00	1.00	0.95	0.98	0.98	0.95
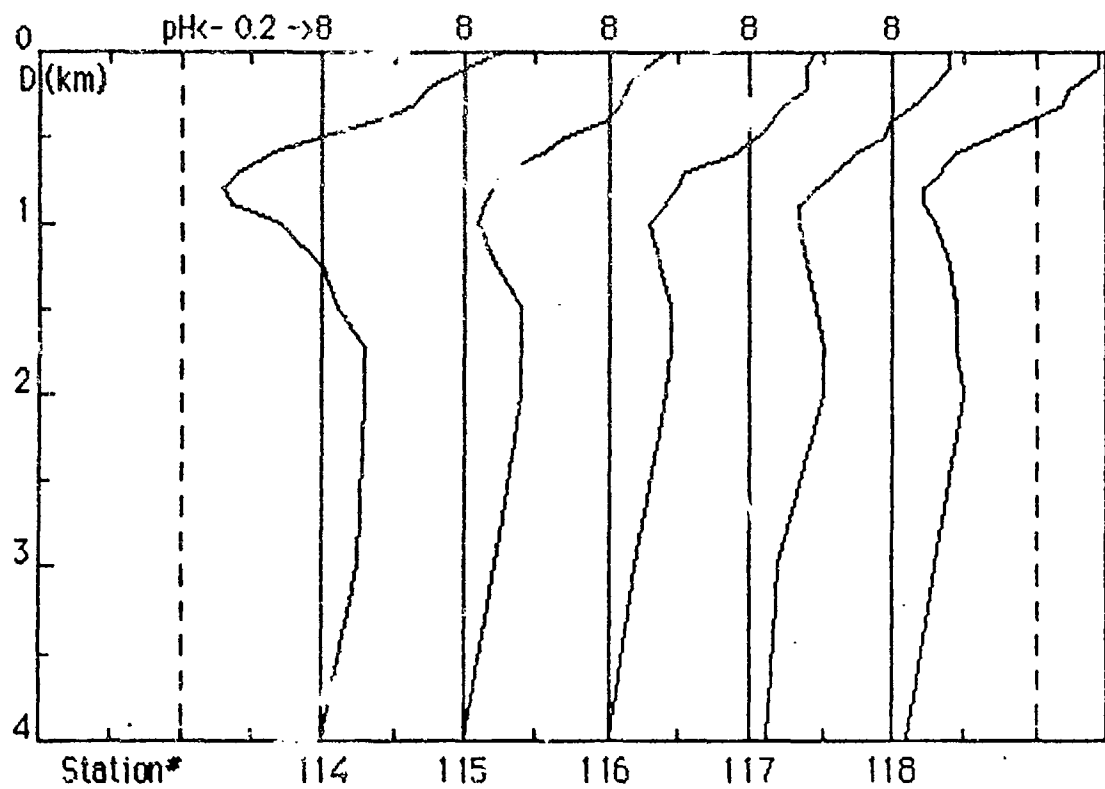
Station ->	114 21°N 22°W	115 28°N 26°W	116 30°N 30°W	117 31°N 39°W	118 31°N 46°W
Depth(km)					
0.00	1.78	1.91	1.95	1.91	1.95
0.10	1.58	1.78	1.91	1.91	1.95
0.20	1.41	1.70	1.91	1.78	1.78
0.30	1.35	1.66	1.78	1.70	1.74
0.40	1.20	1.58	1.70	1.58	1.55
0.50	1.00	1.38	1.62	1.55	1.38
0.60	0.85	1.29	1.51	1.41	1.23
0.70	0.76	1.12	1.29	1.32	1.17
0.80	0.72	1.10	1.26	1.23	1.10
0.90	0.74	1.07	1.20	1.17	1.10
1.00	0.87	1.05	1.15	1.17	1.15
1.25	1.00	1.10	1.17	1.20	1.20
1.50	1.05	1.20	1.23	1.23	1.23
1.75	1.15	1.20	1.23	1.26	1.23
2.00	1.15	1.20	1.20	1.26	1.26
3.00	1.12	1.10	1.10	1.10	1.15
4.00	1.00	1.00	1.00	1.05	1.05

Figure 19: Atlantic Ocean stations.

- 22 -
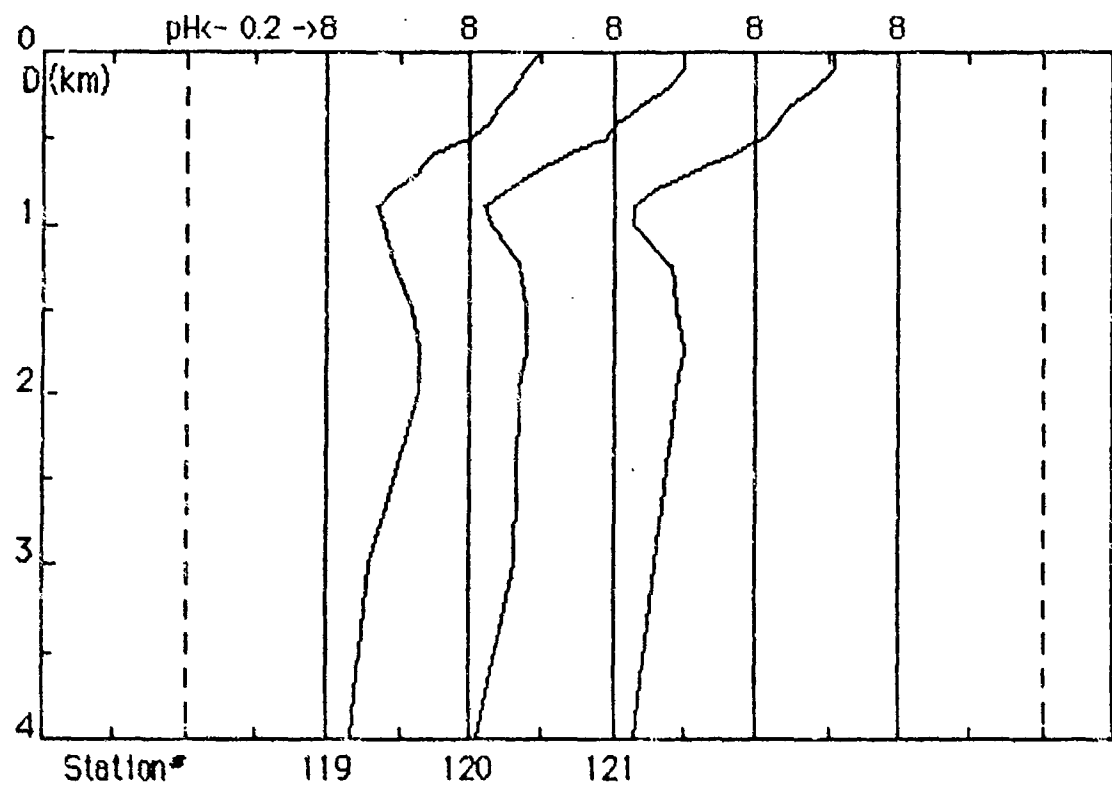
Station#>	119 32°N 51°W	120 33°N 57°W	121 36°N 68°W		
Depth(km)					
0.00	2.00	2.00	2.04		
0.10	1.91	2.00	2.04		
0.20	1.82	1.86	1.91		
0.30	1.74	1.74	1.78		
0.40	1.70	1.62	1.70		
0.50	1.58	1.55	1.62		
0.60	1.41	1.38	1.48		
0.70	1.35	1.23	1.29		
0.80	1.23	1.12	1.15		
0.90	1.17	1.05	1.07		
1.00	1.20	1.07	1.07		
1.25	1.23	1.17	1.20		
1.50	1.32	1.20	1.23		
1.75	1.35	1.20	1.26		
2.00	1.35	1.17	1.23		
3.00	1.15	1.15	1.15		
4.00	1.07	1.02	1.07		

Figure 20: Atlantic Ocean stations.

- 23 -

TRACK OF R/V MELVILLE,
GEOSECS PACIFIC EXPEDITION, 1973-74
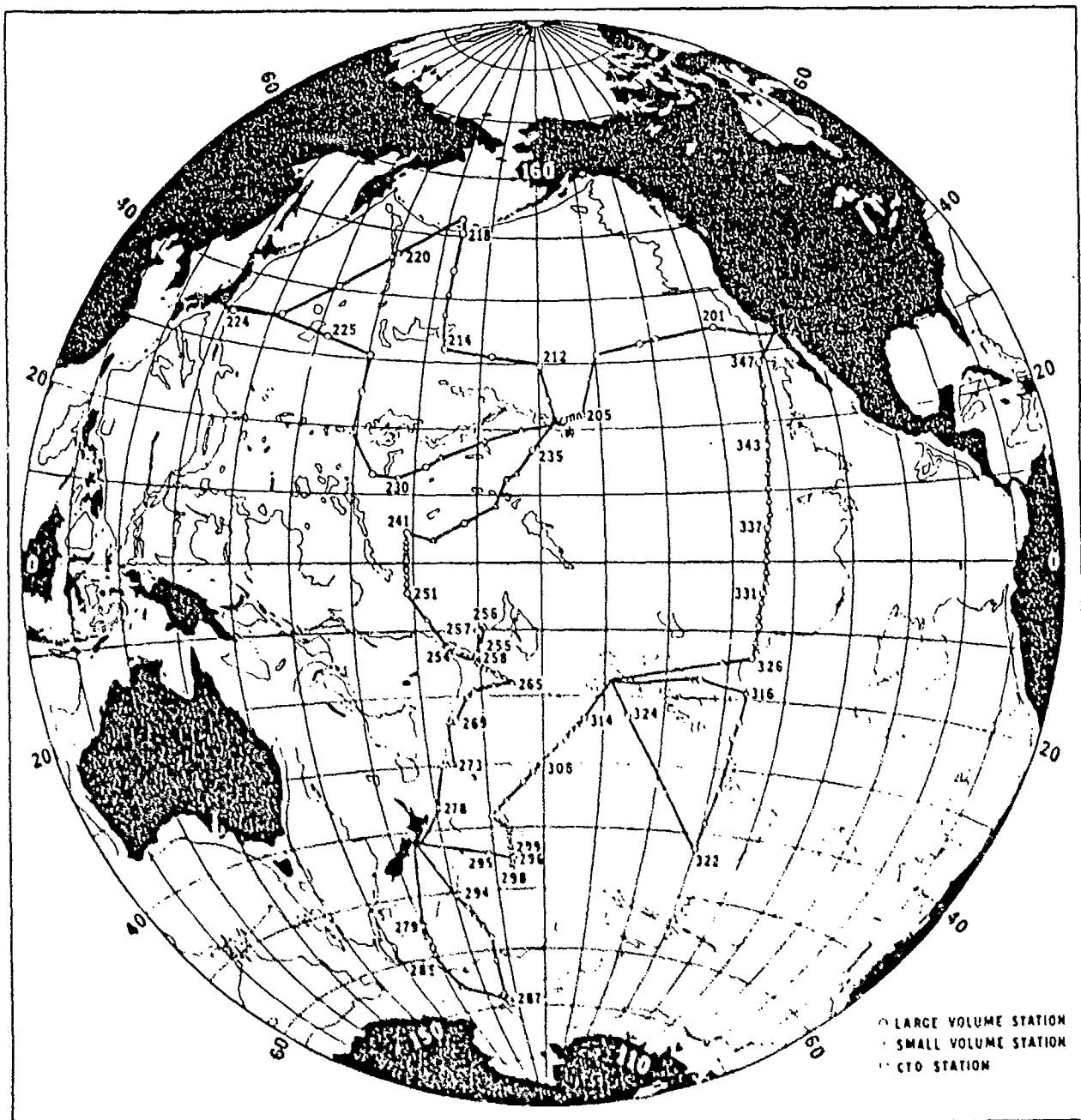
Figure 21: Pacific track.
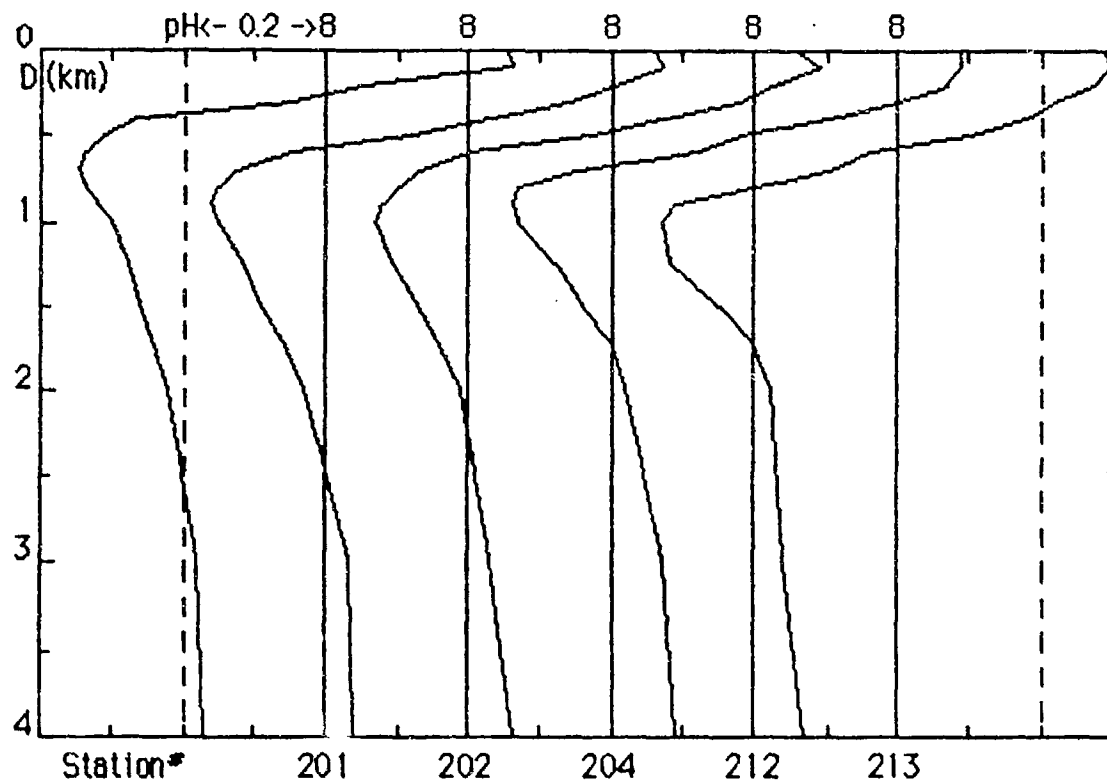
| Station#> | 201 | 202 | 204 | 212 | 213 |
| | 34°N | 33°N | 31°N | 30°N | 31°N |
Depth(km)	128°W	140°W	150°W	160°W	169°W
0.00	1.78	1.82	1.82	1.95	1.95
0.10	1.82	1.86	1.95	1.95	2.00
0.20	1.12	1.58	1.66	1.86	1.86
0.30	0.89	1.38	1.51	1.58	1.66
0.40	0.54	1.07	1.17	1.26	1.51
0.50	0.49	0.83	0.93	0.95	1.26
0.60	0.46	0.56	0.63	0.83	0.91
0.70	0.45	0.47	0.54	0.56	0.79
0.80	0.46	0.45	0.50	0.47	0.63
0.90	0.48	0.44	0.48	0.46	0.49
1.00	0.50	0.45	0.47	0.47	0.47
1.25	0.52	0.48	0.49	0.52	0.48
1.50	0.55	0.51	0.54	0.58	0.56
1.75	0.58	0.55	0.58	0.63	0.63
2.00	0.60	0.59	0.62	0.66	0.66
3.00	0.66	0.68	0.68	0.74	0.69
4.00	0.68	0.69	0.72	0.78	0.74

Figure 22: Pacific Ocean stations.
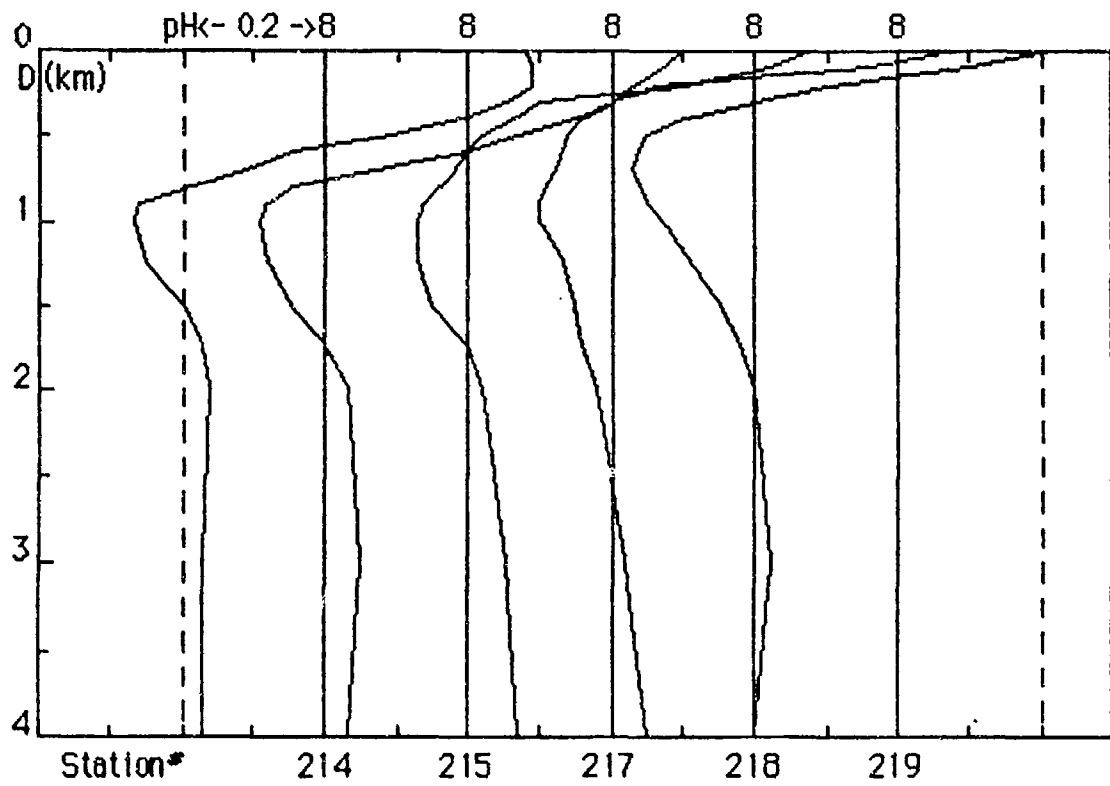
Station#>	214 32°N 177°W	215 37°N 177°W	217 45°N 177°W	218 50°N 177°W	219 53°N 177°W
Depth(km)					
0.00	1.91	2.00	1.91	1.95	1.66
0.10	1.95	1.86	1.66	1.45	1.26
0.20	1.95	1.70	1.26	0.72	0.79
0.30	1.78	1.58	0.79	0.63	0.63
0.40	1.55	1.41	0.72	0.58	0.50
0.50	1.23	1.17	0.66	0.55	0.45
0.60	0.89	1.00	0.63	0.54	0.44
0.70	0.78	0.74	0.60	0.52	0.43
0.80	0.65	0.56	0.58	0.51	0.44
0.90	0.55	0.52	0.55	0.50	0.45
1.00	0.54	0.51	0.54	0.50	0.47
1.25	0.56	0.52	0.54	0.54	0.51
1.50	0.63	0.56	0.56	0.56	0.56
1.75	0.68	0.63	0.63	0.58	0.60
2.00	0.69	0.68	0.66	0.60	0.63
3.00	0.68	0.71	0.71	0.66	0.66
4.00	0.68	0.68	0.74	0.71	0.63

Figure 23: Pacific Ocean stations.
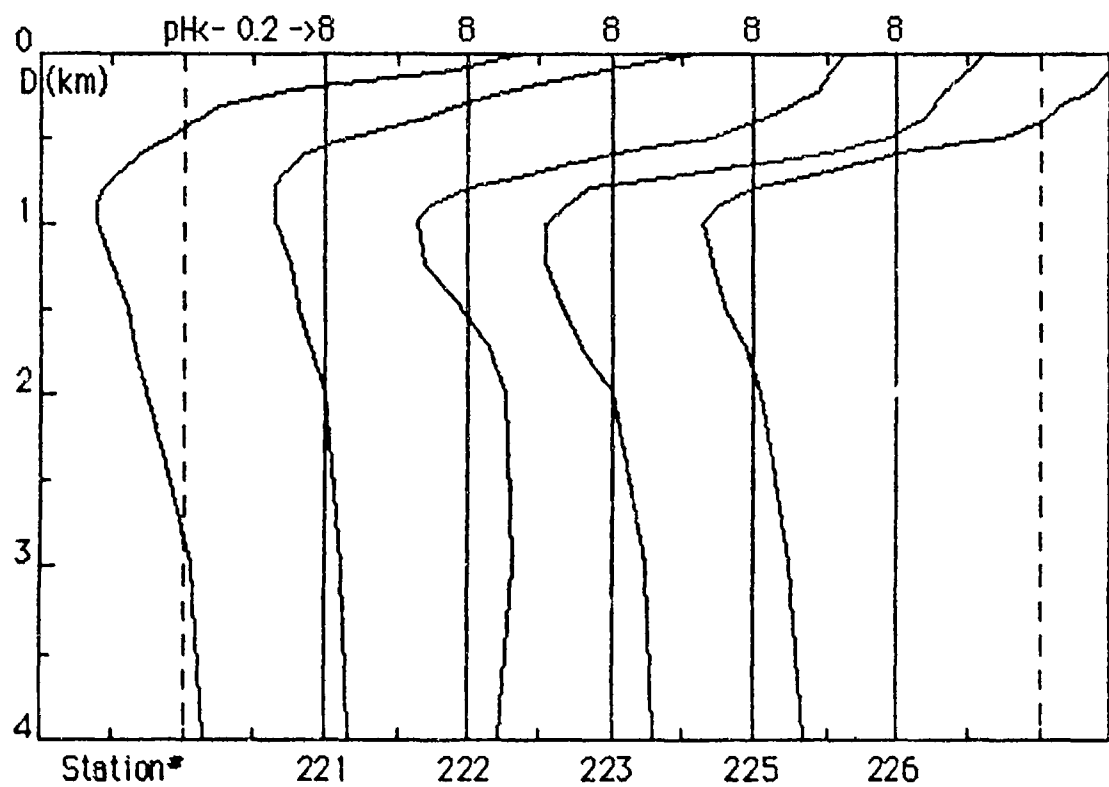
Station*>	221 45°N 169°W	222 40°N 160°W	223 35°N 152°W	225 33°N 162°W	226 31°N 171°W
Depth(km)					
0.00	1.91	2.09	2.14	2.09	2.00
0.10	1.51	1.55	2.04	2.00	2.00
0.20	0.89	1.15	1.95	1.86	1.86
0.30	0.71	0.95	1.78	1.78	1.70
0.40	0.65	0.83	1.58	1.70	1.58
0.50	0.60	0.68	1.38	1.55	1.41
0.60	0.55	0.59	1.00	1.26	1.00
0.70	0.51	0.55	0.79	0.85	0.79
0.80	0.49	0.54	0.63	0.59	0.63
0.90	0.48	0.54	0.56	0.55	0.56
1.00	0.48	0.54	0.54	0.51	0.54
1.25	0.50	0.56	0.55	0.51	0.55
1.50	0.52	0.58	0.62	0.54	0.58
1.75	0.54	0.60	0.66	0.58	0.62
2.00	0.56	0.63	0.71	0.63	0.65
3.00	0.65	0.66	0.72	0.71	0.71
4.00	0.68	0.68	0.69	0.72	0.74

Figure 24: Pacific Ocean stations.
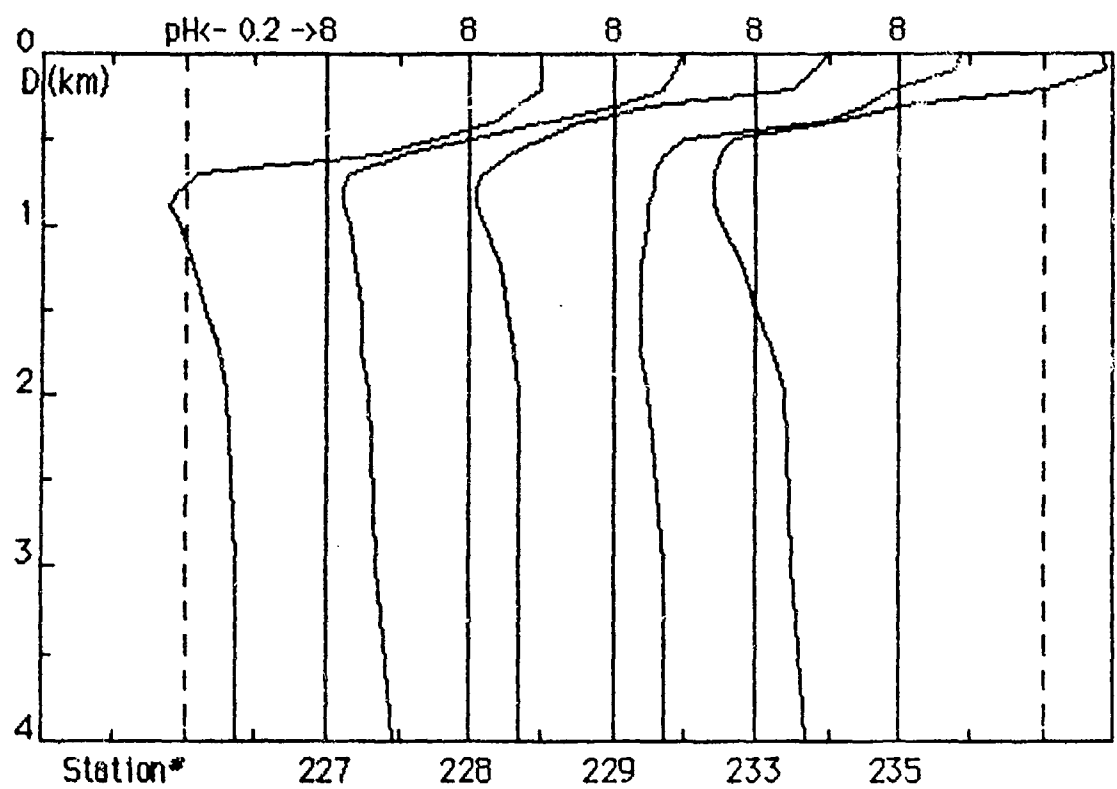
Station#>	227 25°N 170°W	228 19°N 169°W	229 13°N 173°W	233 18°N 169°W	235 17°N 161°W
Depth(km)					
0.00	2.00	2.00	2.00	1.95	1.91
0.10	2.00	1.95	1.91	1.91	1.95
0.20	2.00	1.86	1.78	1.55	1.58
0.30	1.82	1.58	1.12	1.41	1.00
0.40	1.70	1.26	0.89	1.23	0.79
0.50	1.41	1.00	0.79	0.79	0.59
0.60	1.17	0.79	0.71	0.74	0.56
0.70	0.66	0.68	0.66	0.72	0.55
0.80	0.62	0.66	0.65	0.72	0.55
0.90	0.60	0.66	0.65	0.71	0.55
1.00	0.62	0.68	0.66	0.71	0.56
1.25	0.65	0.69	0.69	0.69	0.60
1.50	0.68	0.71	0.71	0.69	0.63
1.75	0.71	0.71	0.72	0.69	0.66
2.00	0.72	0.72	0.74	0.71	0.69
3.00	0.74	0.74	0.74	0.74	0.71
4.00	0.74	0.78	0.74	0.74	0.74

Figure 25: Pacific Ocean stations.
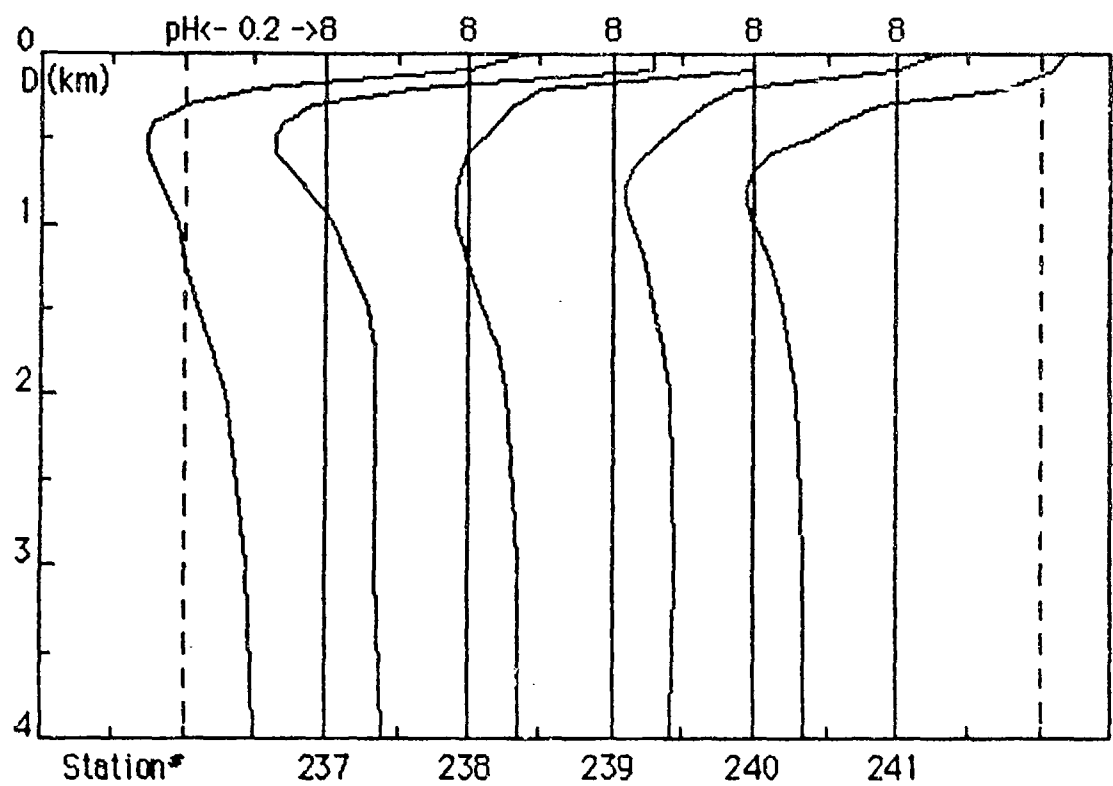
Station#>	237 12°N 165°W	238 08°N 167°W	239 06°N 172°W	240 03°N 177°W	241 05°N 179°E
Depth(km)					
0.00	1.95	1.82	1.58	1.82	1.74
0.10	1.58	1.82	1.58	1.58	1.66
0.20	0.79	0.83	0.79	0.93	1.41
0.30	0.63	0.60	0.72	0.85	0.93
0.40	0.58	0.55	0.69	0.79	0.83
0.50	0.56	0.54	0.66	0.74	0.76
0.60	0.56	0.54	0.63	0.71	0.66
0.70	0.58	0.56	0.62	0.68	0.63
0.80	0.59	0.59	0.60	0.66	0.62
0.90	0.60	0.62	0.60	0.66	0.62
1.00	0.62	0.65	0.60	0.68	0.63
1.25	0.63	0.68	0.63	0.71	0.66
1.50	0.66	0.72	0.66	0.72	0.69
1.75	0.69	0.74	0.69	0.74	0.71
2.00	0.72	0.74	0.71	0.76	0.72
3.00	0.78	0.74	0.74	0.78	0.74
4.00	0.79	0.76	0.74	0.76	0.74

Figure 26: Pacific Ocean stations.
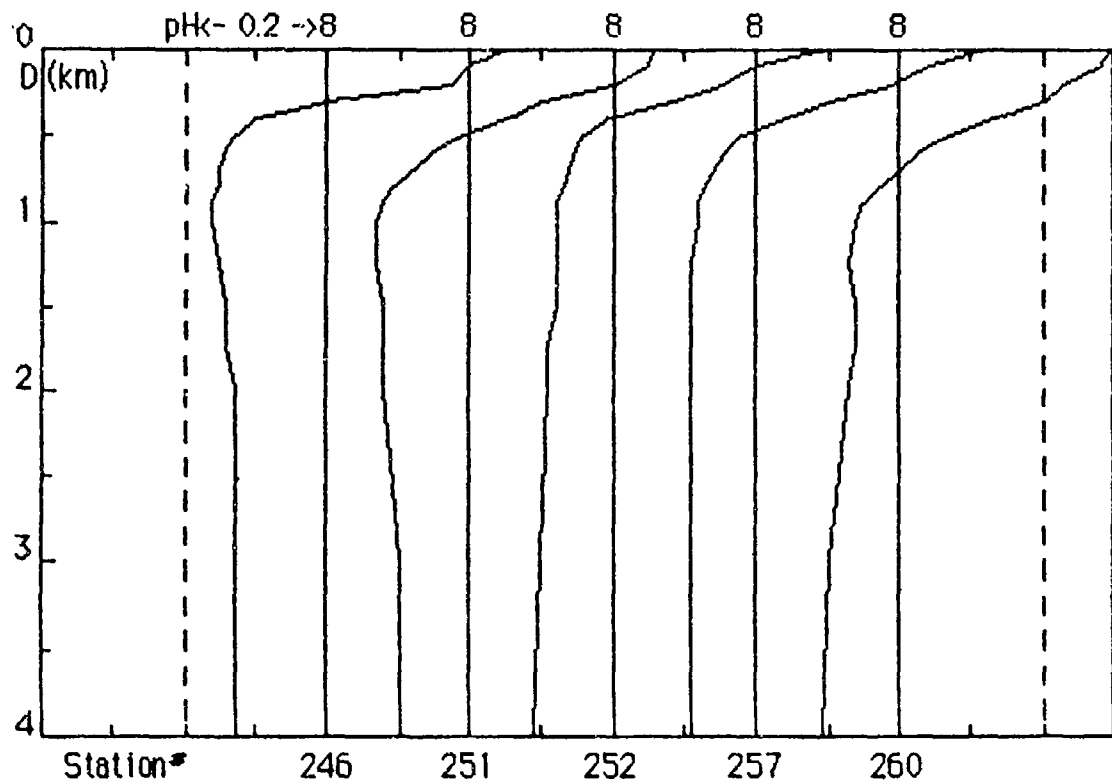
Station#>	246 00°S 179°E	251 05°S 179°E	252 08°S 178°W	257 19°S 170°W	260 15°S 170°W
Depth(km)					
0.00	1.78	1.82	2.00	2.09	2.00
0.10	1.58	1.78	1.58	1.74	1.91
0.20	1.48	1.58	1.41	1.55	1.70
0.30	1.00	1.26	1.20	1.26	1.58
0.40	0.79	1.12	0.98	1.10	1.35
0.50	0.74	0.98	0.91	0.95	1.17
0.60	0.72	0.89	0.89	0.91	1.07
0.70	0.71	0.83	0.87	0.87	1.00
0.80	0.71	0.78	0.85	0.85	0.93
0.90	0.69	0.76	0.83	0.83	0.89
1.00	0.69	0.74	0.83	0.83	0.87
1.25	0.71	0.74	0.83	0.81	0.85
1.50	0.72	0.76	0.83	0.81	0.87
1.75	0.72	0.76	0.81	0.81	0.87
2.00	0.74	0.76	0.81	0.81	0.85
3.00	0.74	0.79	0.79	0.81	0.79
4.00	0.74	0.79	0.78	0.81	0.78

Figure 27: Pacific Ocean stations.
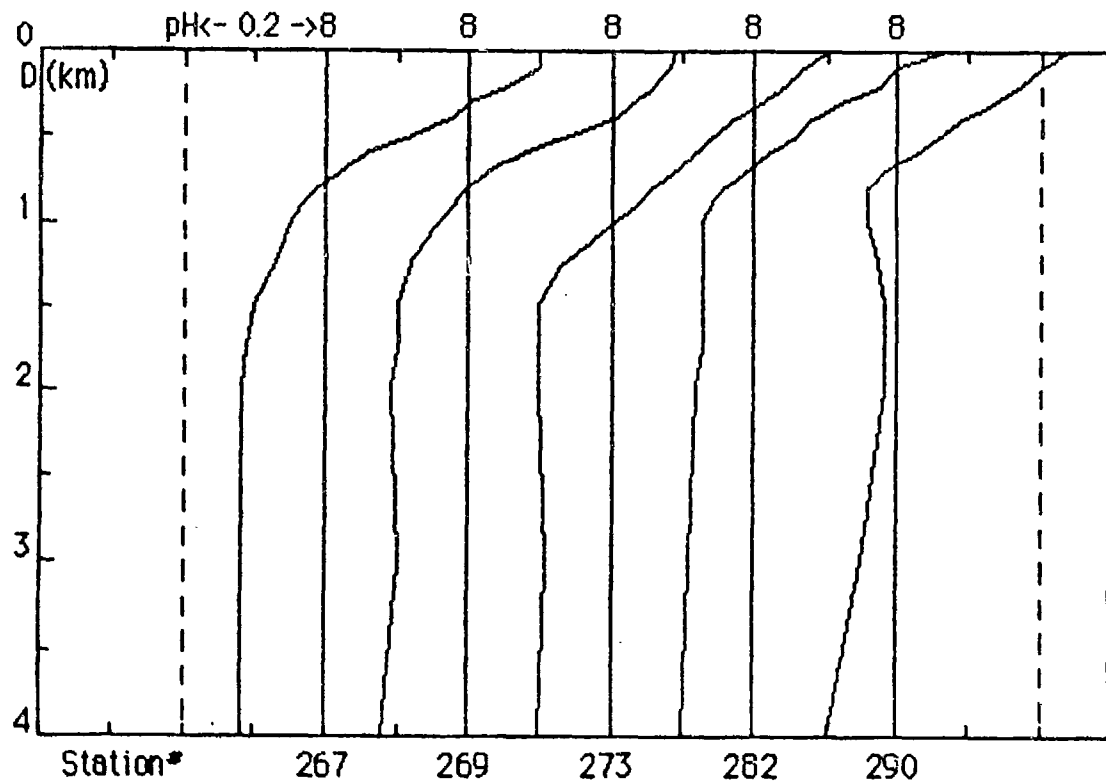
Station#>	267 19°S 171°W	269 24°S 175°W	273 30°S 176°W	282 58°S 170°E	290 58°S 174°W
Depth(km)					
0.00	2.00	1.95	2.00	1.66	1.74
0.10	2.00	1.91	1.86	1.58	1.58
0.20	1.78	1.82	1.74	1.48	1.48
0.30	1.58	1.70	1.62	1.32	1.35
0.40	1.48	1.58	1.48	1.20	1.23
0.50	1.32	1.38	1.38	1.15	1.15
0.60	1.15	1.20	1.32	1.05	1.07
0.70	1.05	1.07	1.23	0.98	0.95
0.80	0.98	1.00	1.15	0.91	0.91
0.90	0.93	0.95	1.10	0.87	0.91
1.00	0.89	0.91	1.00	0.85	0.91
1.25	0.85	0.83	0.85	0.85	0.93
1.50	0.79	0.79	0.79	0.85	0.95
1.75	0.78	0.79	0.79	0.85	0.95
2.00	0.76	0.78	0.79	0.83	0.95
3.00	0.76	0.79	0.81	0.81	0.89
4.00	0.76	0.76	0.79	0.79	0.79

Figure 28: Pacific Ocean stations.
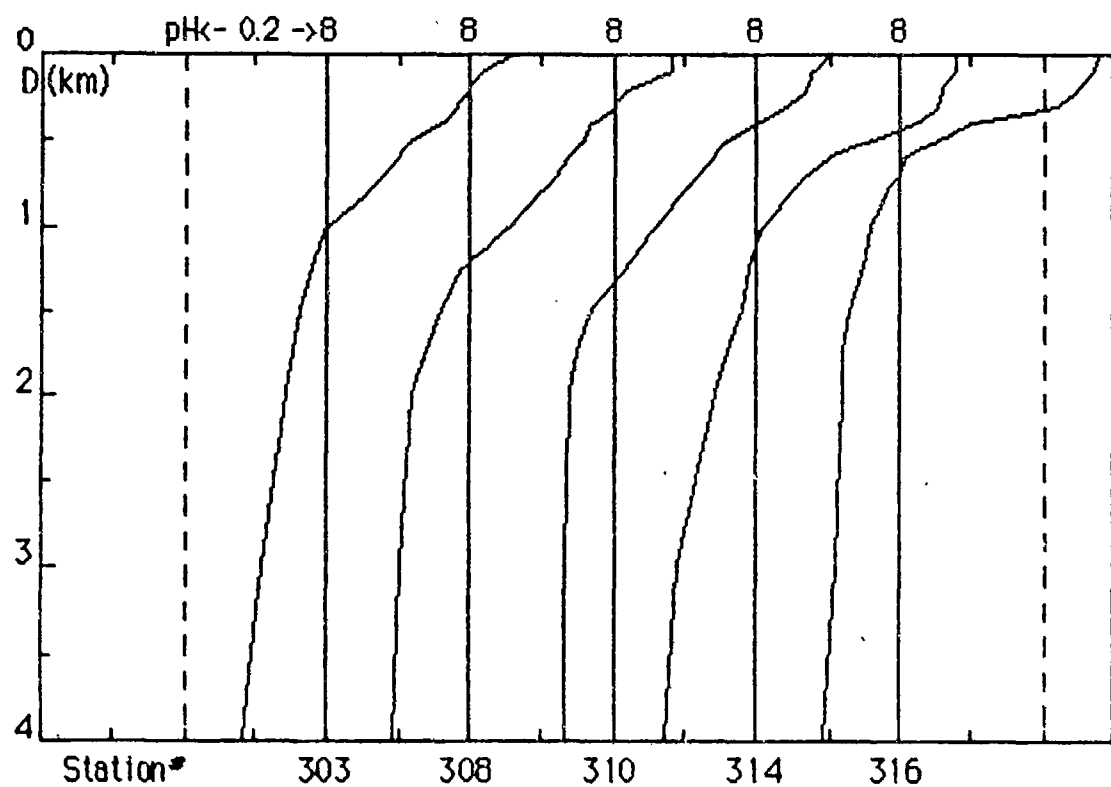
Station#>	303 38°S 170°W	308 30°S 160°W	310 27°S 157°W	314 24°S 154°W	316 19°S 127°W
Depth(km)					
0.00	1.82	1.91	2.00	1.91	1.91
0.10	1.66	1.91	1.91	1.91	1.86
0.20	1.58	1.66	1.86	1.82	1.78
0.30	1.51	1.58	1.74	1.78	1.66
0.40	1.45	1.48	1.58	1.66	1.26
0.50	1.32	1.45	1.45	1.45	1.12
0.60	1.26	1.38	1.38	1.26	1.02
0.70	1.20	1.32	1.32	1.17	1.00
0.80	1.15	1.26	1.26	1.12	0.95
0.90	1.07	1.20	1.20	1.07	0.93
1.00	1.00	1.12	1.15	1.02	0.91
1.25	0.95	0.98	1.05	0.98	0.89
1.50	0.91	0.91	0.93	0.95	0.85
1.75	0.89	0.87	0.89	0.91	0.83
2.00	0.87	0.83	0.87	0.87	0.83
3.00	0.81	0.79	0.85	0.78	0.81
4.00	0.76	0.78	0.85	0.74	0.78

Figure 29: Pacific Ocean stations.
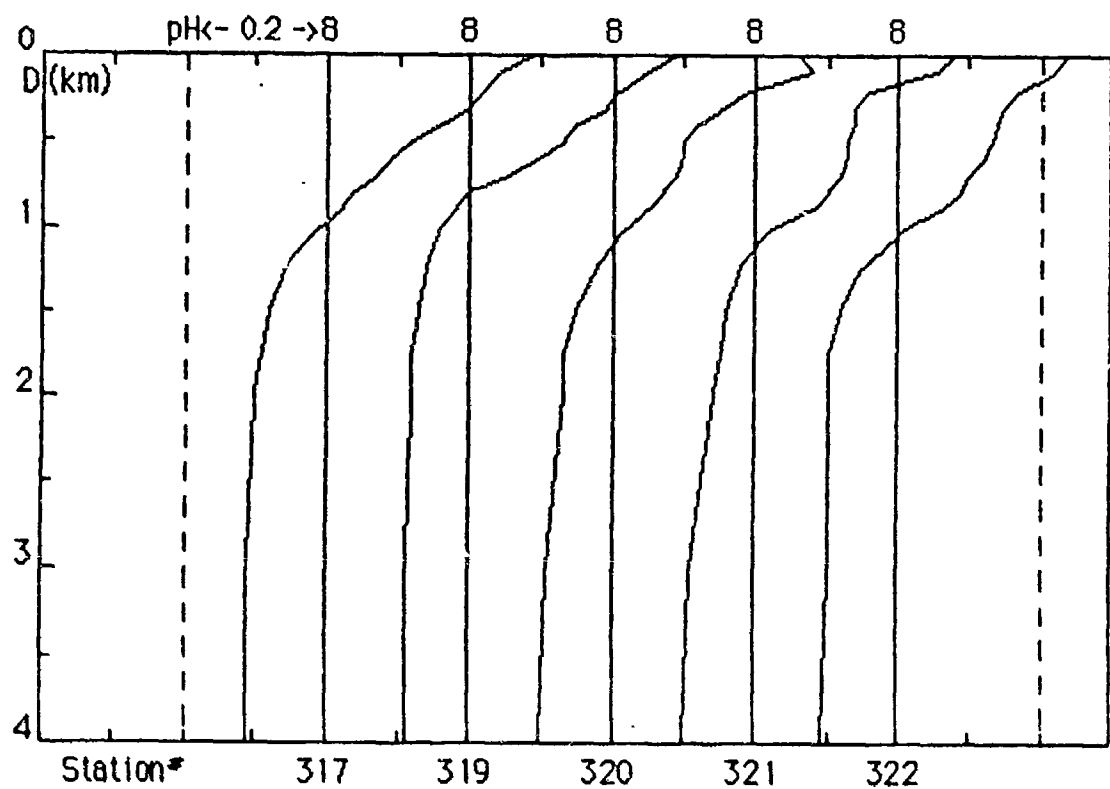
Station#>	317 24°S 128°W	319 28°S 128°W	320 33°S 126°W	321 39°S 129°W	322 43°S 130°W
Depth(km)					
0.00	1.95	1.95	1.82	1.91	1.74
0.10	1.74	1.78	1.91	1.78	1.66
0.20	1.66	1.62	1.55	1.45	1.48
0.30	1.58	1.55	1.41	1.38	1.41
0.40	1.45	1.41	1.32	1.38	1.38
0.50	1.32	1.35	1.26	1.35	1.35
0.60	1.23	1.26	1.26	1.35	1.32
0.70	1.17	1.12	1.23	1.32	1.26
0.80	1.10	1.00	1.17	1.26	1.23
0.90	1.05	0.95	1.12	1.20	1.15
1.00	0.98	0.91	1.05	1.05	1.02
1.25	0.87	0.87	0.95	0.95	0.89
1.50	0.83	0.85	0.89	0.91	0.83
1.75	0.81	0.83	0.85	0.89	0.79
2.00	0.79	0.83	0.85	0.87	0.79
3.00	0.78	0.81	0.81	0.81	0.79
4.00	0.78	0.81	0.79	0.79	0.78

Figure 30: Pacific Ocean stations.
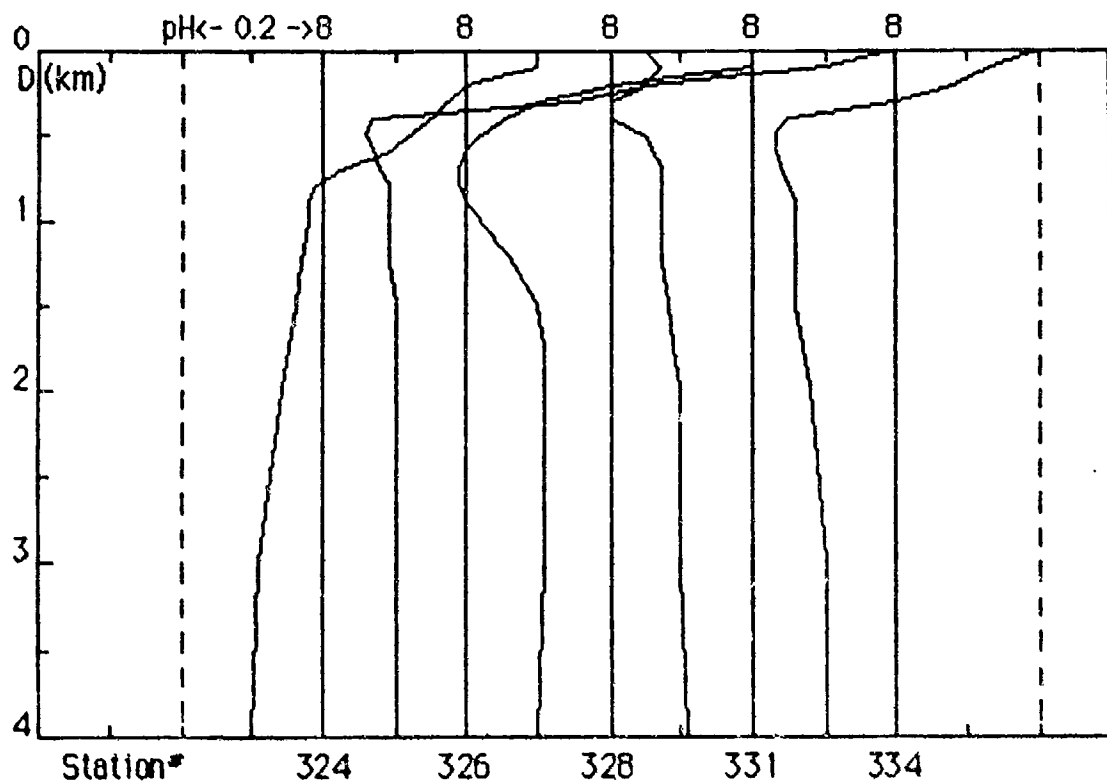
Station#>	324 23°S 146°W	326 14°S 126°W	328 09°S 126°W	331 05°S 125°W	334 00°N 125°W
Depth(km)					
0.00	2.00	1.78	1.58	1.58	1.58
0.10	2.00	1.86	1.58	1.26	1.35
0.20	1.58	1.78	1.00	0.71	1.20
0.30	1.48	1.41	0.79	0.63	1.00
0.40	1.41	0.74	0.71	0.63	0.71
0.50	1.32	0.72	0.66	0.71	0.68
0.60	1.23	0.74	0.63	0.72	0.68
0.70	1.05	0.76	0.62	0.74	0.69
0.80	0.98	0.78	0.62	0.74	0.71
0.90	0.95	0.78	0.63	0.74	0.72
1.00	0.95	0.78	0.66	0.74	0.72
1.25	0.93	0.78	0.72	0.74	0.72
1.50	0.91	0.79	0.79	0.76	0.72
1.75	0.89	0.79	0.81	0.78	0.74
2.00	0.87	0.79	0.81	0.79	0.76
3.00	0.81	0.79	0.81	0.79	0.79
4.00	0.79	0.79	0.79	0.81	0.79

Figure 31: Pacific Ocean stations.
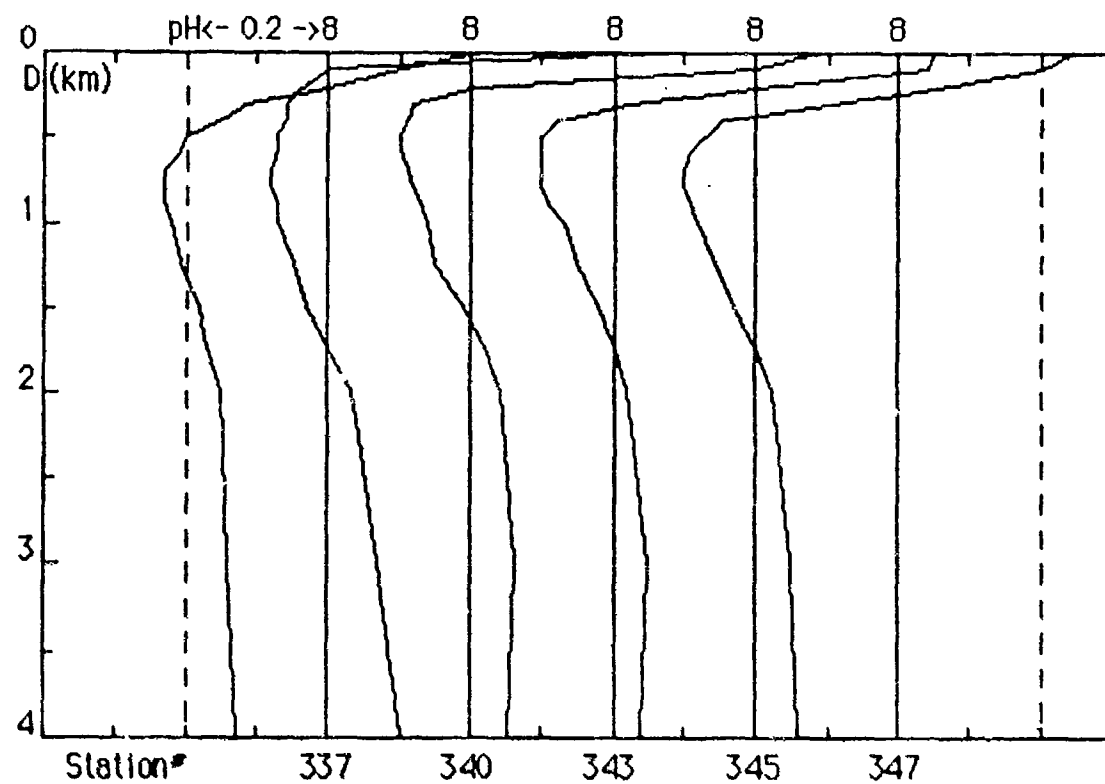
Station#>	337 06°N 124°W	340 10°N 124°W	343 17°N 123°W	345 23°N 122°W	347 29°N 121°W
Depth(km)					
0.00	1.66	1.91	1.95	1.78	1.78
0.10	1.26	0.63	1.58	1.74	1.58
0.20	1.00	0.58	0.63	1.00	1.12
0.30	0.76	0.55	0.52	0.66	0.79
0.40	0.71	0.55	0.51	0.52	0.56
0.50	0.63	0.54	0.50	0.50	0.54
0.60	0.62	0.54	0.50	0.50	0.51
0.70	0.59	0.52	0.51	0.50	0.50
0.80	0.59	0.52	0.52	0.50	0.50
0.90	0.59	0.54	0.54	0.51	0.51
1.00	0.60	0.54	0.55	0.54	0.52
1.25	0.62	0.56	0.56	0.56	0.55
1.50	0.66	0.59	0.62	0.60	0.59
1.75	0.68	0.63	0.66	0.63	0.63
2.00	0.71	0.68	0.69	0.66	0.66
3.00	0.72	0.74	0.72	0.71	0.71
4.00	0.74	0.79	0.71	0.69	0.72

Figure 32: Pacific Ocean stations.

# TRACK OF R/V MELVILLE,
GEOSECS INDIAN OCEAN EXPEDITION, 1977-78
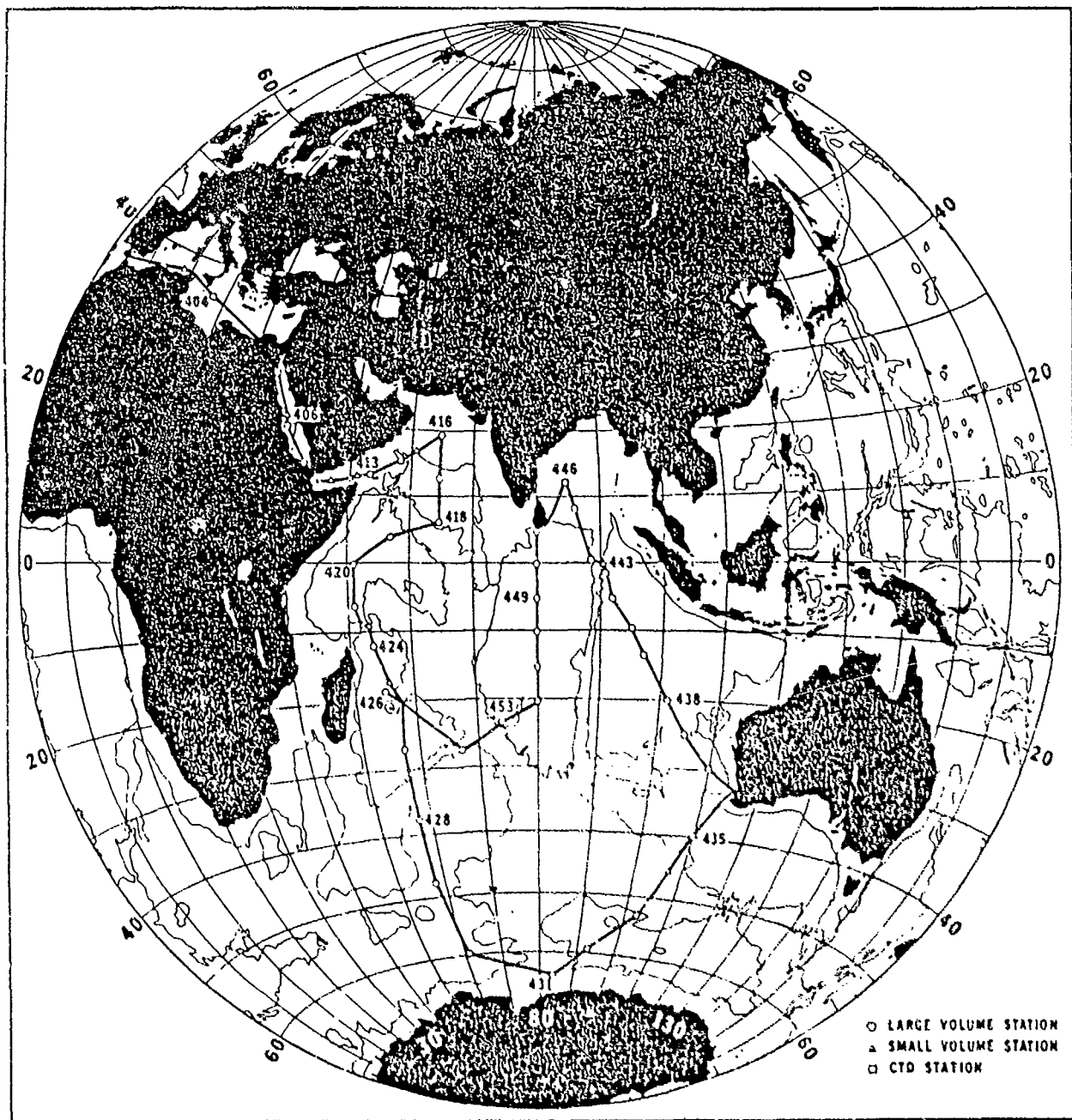


Figure 33: Indian Ocean track.

Figure 34: Indian Ocean stations.
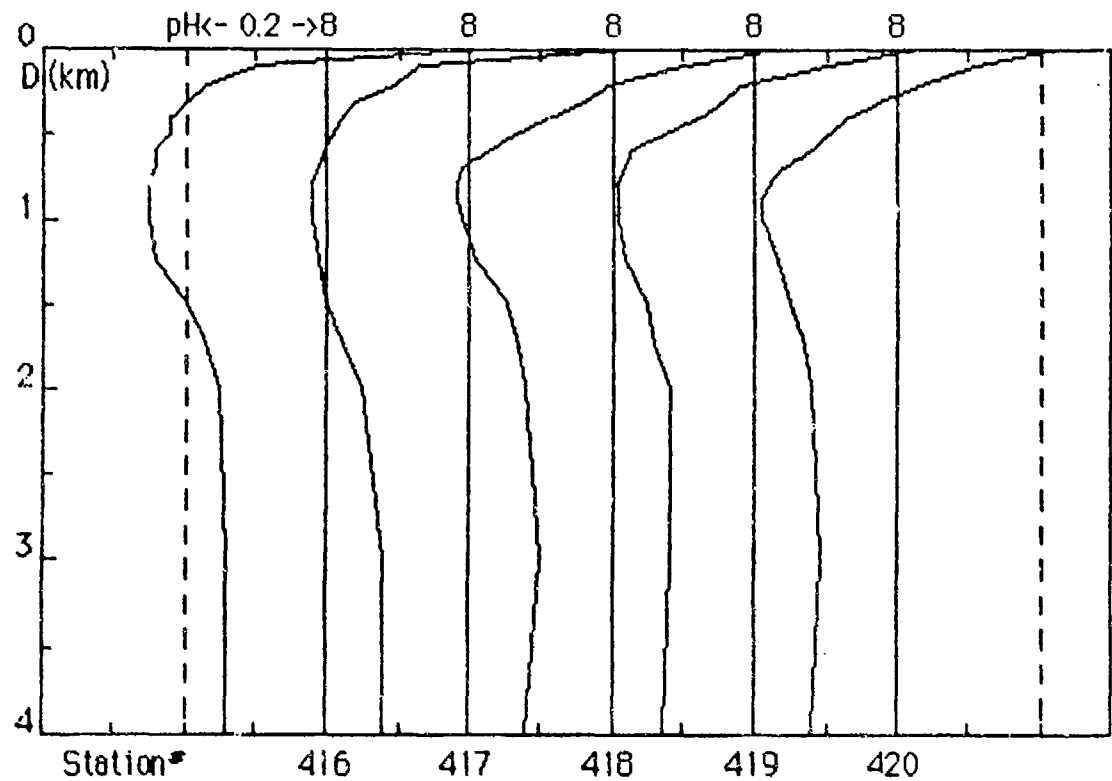
Station#>	416 20°N 65°E	417 13°N 64°E	418 06°N 64°E	419 04°N 57°E	420 00°S 51°E
Depth(km)					
0.00	1.70	1.70	1.74	1.70	1.70
0.10	0.79	0.85	1.26	1.26	1.29
0.20	0.68	0.78	0.98	0.95	1.07
0.30	0.63	0.69	0.91	0.69	0.93
0.40	0.60	0.66	0.81	0.83	0.85
0.50	0.60	0.65	0.72	0.74	0.79
0.60	0.58	0.63	0.68	0.68	0.76
0.70	0.58	0.62	0.62	0.66	0.69
0.80	0.56	0.60	0.60	0.65	0.66
0.90	0.56	0.60	0.60	0.65	0.65
1.00	0.56	0.60	0.62	0.65	0.65
1.25	0.58	0.62	0.65	0.66	0.68
1.50	0.63	0.63	0.71	0.71	0.71
1.75	0.68	0.66	0.74	0.72	0.74
2.00	0.71	0.71	0.76	0.76	0.76
3.00	0.72	0.76	0.79	0.76	0.78
4.00	0.72	0.76	0.76	0.74	0.76

Station#>	421 06°S 51°E	424 12°S 54°E	425 17°S 56°E	427 27°S 57°E	428 38°S 58°E
Depth(km)					
0.00	1.74	1.78	1.82	1.82	1.82
0.10	1.29	1.48	1.78	1.70	1.74
0.20	1.12	1.32	1.66	1.62	1.66
0.30	1.05	1.23	1.55	1.55	1.62
0.40	0.98	1.17	1.41	1.51	1.55
0.50	0.89	1.05	1.26	1.45	1.51
0.60	0.79	1.00	1.00	1.35	1.41
0.70	0.76	0.91	0.93	1.26	1.26
0.80	0.74	0.85	0.91	1.17	1.17
0.90	0.72	0.79	0.89	1.00	1.15
1.00	0.72	0.78	0.87	0.95	1.10
1.25	0.72	0.79	0.87	0.89	1.00
1.50	0.74	0.79	0.87	0.87	0.89
1.75	0.78	0.79	0.87	0.87	0.85
2.00	0.79	0.81	0.85	0.87	0.85
3.00	0.78	0.79	0.79	0.81	0.83
4.00	0.76	0.76	0.76	0.78	0.79

Figure 35: Indian Ocean stations.
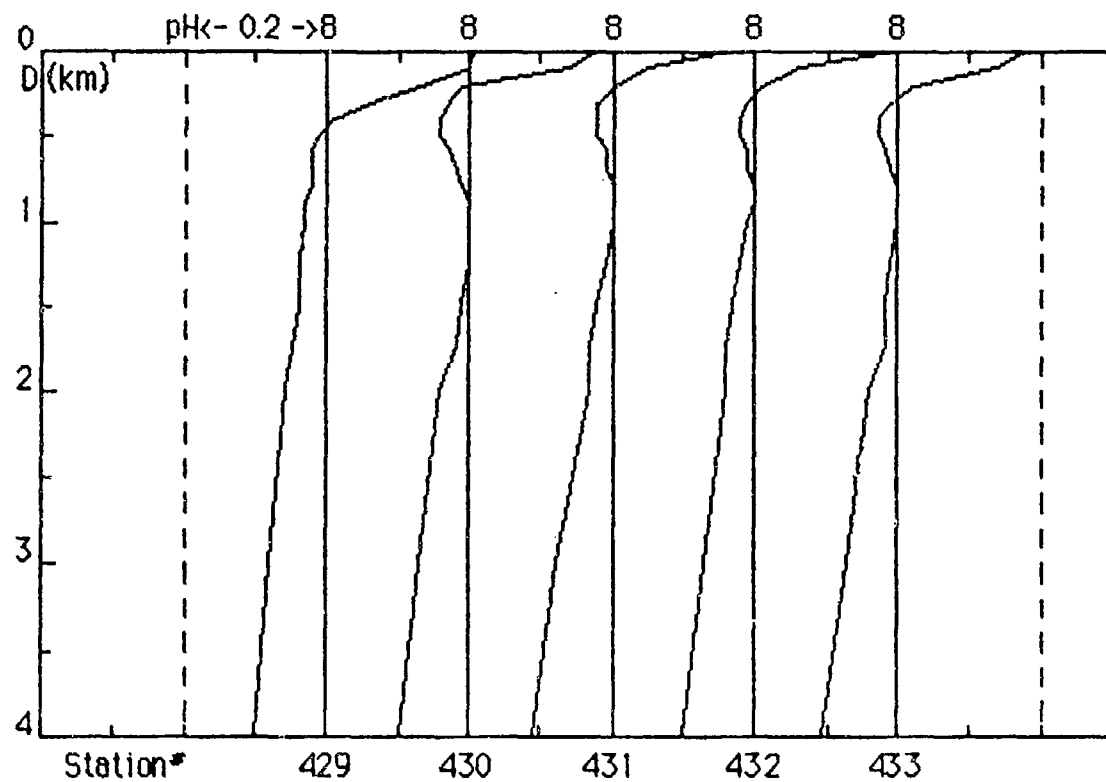
Station#>	429 48°S 58°E	430 60°S 61°E	431 64°S 84°E	432 59°S 93°E	433 53°S 103°E
Depth(km)					
0.00	1.62	1.51	1.48	1.58	1.51
0.10	1.58	1.38	1.12	1.15	1.38
0.20	1.35	0.98	1.00	1.02	1.05
0.30	1.15	0.93	0.95	0.98	0.98
0.40	1.02	0.91	0.95	0.95	0.93
0.50	0.98	0.91	0.95	0.95	0.93
0.60	0.95	0.93	0.98	0.98	0.95
0.70	0.95	0.95	0.98	0.98	0.98
0.80	0.95	0.98	1.00	1.00	1.00
0.90	0.93	1.00	1.00	1.00	1.00
1.00	0.93	1.00	1.00	0.98	1.00
1.25	0.91	1.00	0.98	0.95	0.98
1.50	0.91	0.98	0.95	0.93	0.95
1.75	0.89	0.95	0.93	0.91	0.95
2.00	0.87	0.91	0.93	0.91	0.91
3.00	0.83	0.85	0.83	0.85	0.85
4.00	0.79	0.79	0.78	0.79	0.78

Figure 36: Indian Ocean stations.
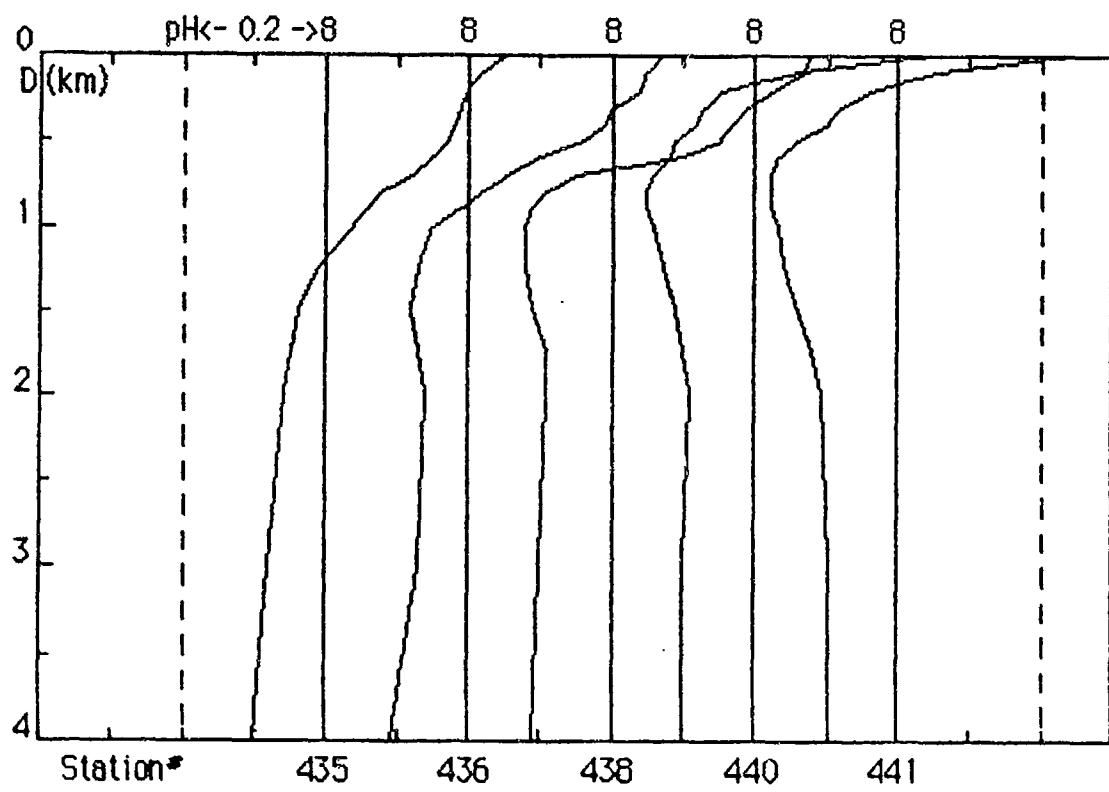
- 39 -

| Station#> | 435 | 436 | 438 | 440 | 441 |
| | 40°S | 29°S | 19°S | 09°S | 05°S |
Depth(km)	110°E	110°E	101°E	95°E	92°E
0.00	1.78	1.86	1.91	1.78	1.78
0.10	1.66	1.78	1.86	1.15	1.12
0.20	1.58	1.74	1.66	0.89	0.91
0.30	1.55	1.58	1.55	0.85	0.83
0.40	1.51	1.55	1.48	0.83	0.79
0.50	1.48	1.45	1.41	0.76	0.72
0.60	1.41	1.26	1.26	0.76	0.68
0.70	1.32	1.12	0.89	0.72	0.66
0.80	1.20	1.05	0.81	0.71	0.66
0.90	1.15	0.98	0.78	0.71	0.66
1.00	1.10	0.89	0.76	0.72	0.68
1.25	0.98	0.85	0.76	0.74	0.69
1.50	0.91	0.83	0.78	0.78	0.72
1.75	0.89	0.85	0.81	0.79	0.76
2.00	0.87	0.87	0.81	0.81	0.78
3.00	0.83	0.85	0.79	0.79	0.79
4.00	0.79	0.78	0.78	0.79	0.79

Figure 37: Indian Ocean stations.
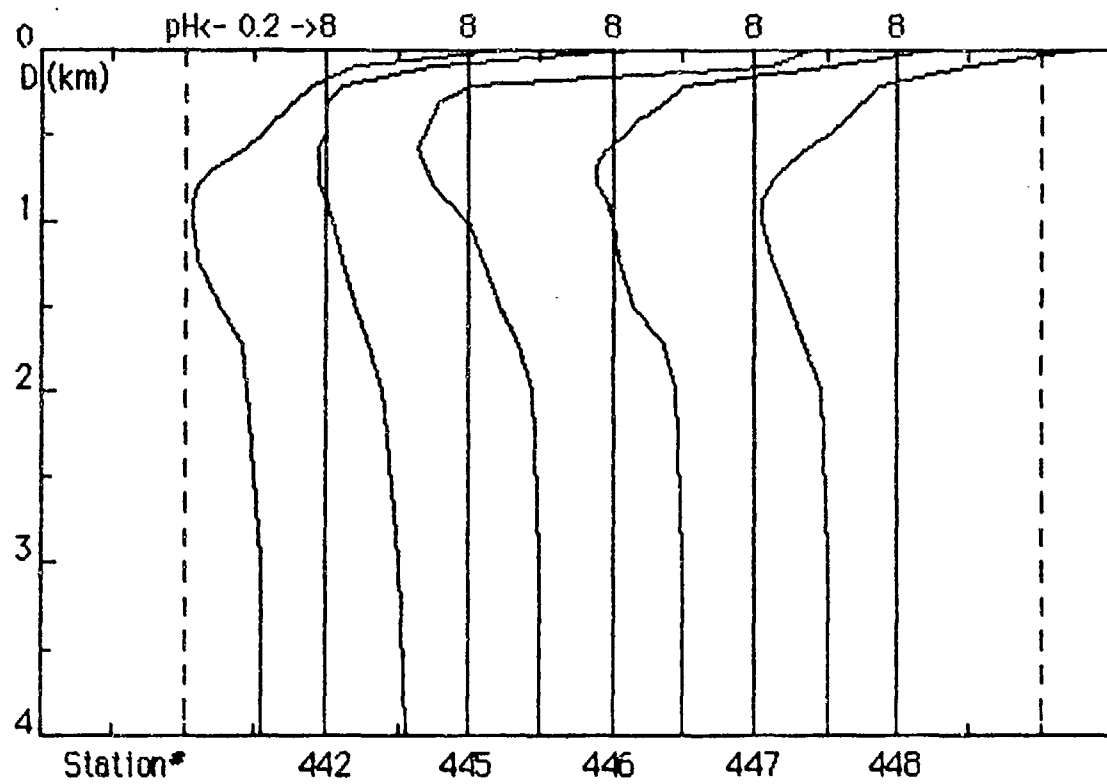
Station# >	442 01°S 91°E	445 09°N 86°E	446 13°N 85°E	447 05°N 80°E	448 00°N 80°E
Depth(km)					
0.00	1.82	1.74	1.91	1.82	1.82
0.10	1.10	0.89	1.66	1.26	1.26
0.20	0.95	0.66	0.63	0.79	0.93
0.30	0.89	0.63	0.58	0.74	0.89
0.40	0.85	0.63	0.56	0.69	0.85
0.50	0.81	0.63	0.55	0.66	0.79
0.60	0.76	0.62	0.54	0.62	0.74
0.70	0.69	0.62	0.55	0.60	0.69
0.80	0.66	0.62	0.56	0.60	0.66
0.90	0.65	0.63	0.59	0.62	0.65
1.00	0.65	0.65	0.63	0.63	0.65
1.25	0.66	0.66	0.66	0.65	0.66
1.50	0.71	0.69	0.69	0.68	0.71
1.75	0.76	0.72	0.74	0.74	0.74
2.00	0.78	0.76	0.78	0.78	0.78
3.00	0.81	0.79	0.79	0.79	0.79
4.00	0.81	0.81	0.79	0.79	0.79

Figure 38: Indian Ocean stations.
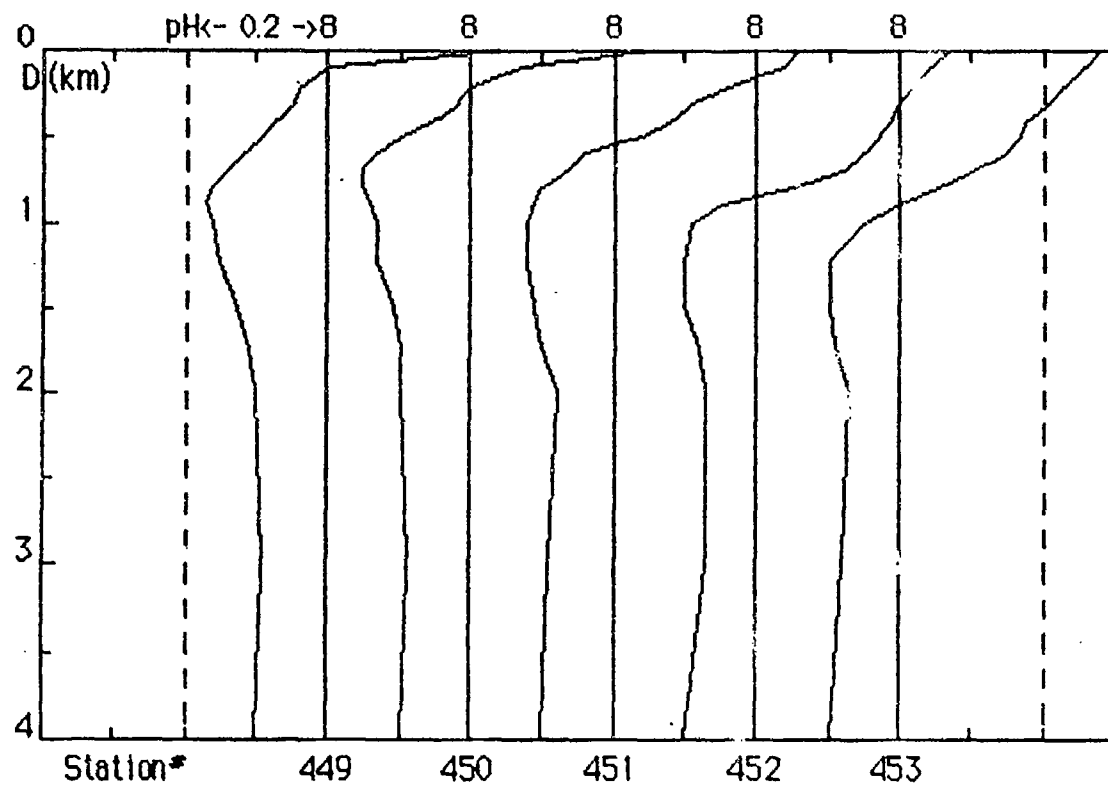
| Station#> | 449 | 450 | 451 | 452 | 453 |
| | 05°S | 10°S | 15°S | 20°S | 23°S |
Depth(km)	80°E	80°E	80°E	80°E	74°E
0.00	1.82	1.82	1.82	1.86	1.91
0.10	1.00	1.17	1.74	1.74	1.82
0.20	0.91	1.00	1.45	1.66	1.70
0.30	0.89	0.95	1.29	1.58	1.62
0.40	0.85	0.89	1.20	1.55	1.51
0.50	0.81	0.79	1.10	1.48	1.48
0.60	0.76	0.74	0.91	1.41	1.41
0.70	0.72	0.71	0.85	1.32	1.26
0.80	0.69	0.71	0.79	1.12	1.12
0.90	0.68	0.72	0.78	0.89	1.00
1.00	0.69	0.74	0.76	0.81	0.89
1.25	0.71	0.74	0.76	0.79	0.79
1.50	0.74	0.78	0.78	0.79	0.79
1.75	0.78	0.79	0.79	0.83	0.81
2.00	0.79	0.79	0.83	0.85	0.85
3.00	0.81	0.81	0.81	0.85	0.83
4.00	0.79	0.79	0.79	0.79	0.79

Figure 39: Indian Ocean stations.
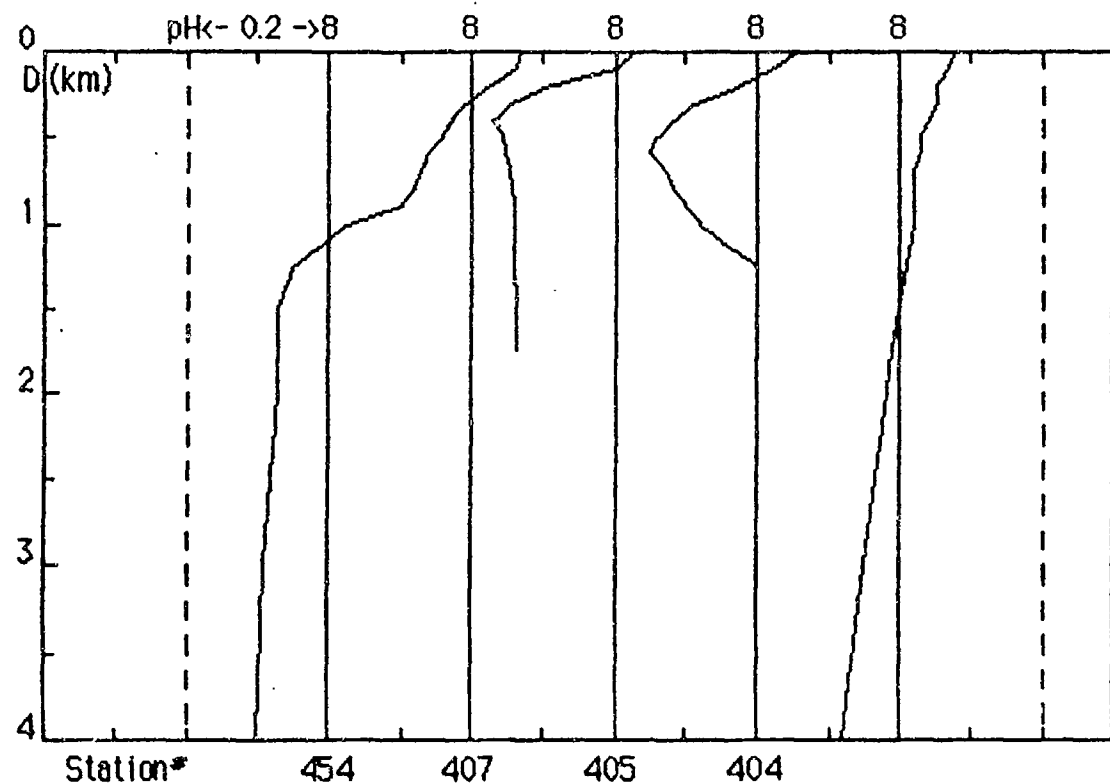
Station#>	454 27°S 67°E	407 20°N 38°E	405 27°N 35°E	404 36°N 17°E	
Depth(km)					
0.00	1.86	1.70	1.82	1.91	
0.10	1.82	1.58	1.66	1.86	
0.20	1.66	1.26	1.48	1.78	
0.30	1.55	1.12	1.29	1.78	
0.40	1.48	1.07	1.20	1.74	
0.50	1.45	1.10	1.15	1.70	
0.60	1.38	1.11	1.12	1.70	
0.70	1.35	1.12	1.17	1.66	
0.80	1.32	1.14	1.20	1.66	
0.90	1.26	1.14	1.26	1.66	
1.00	1.05	1.14	1.32	1.66	
1.25	0.89	1.15	1.58	1.62	
1.50	0.85	1.15		1.58	
1.75	0.85	1.15		1.55	
2.00	0.85			1.51	
3.00	0.81			1.41	
4.00	0.79			1.32	

Figure 40: Indian Ocean stations.

- 43 -
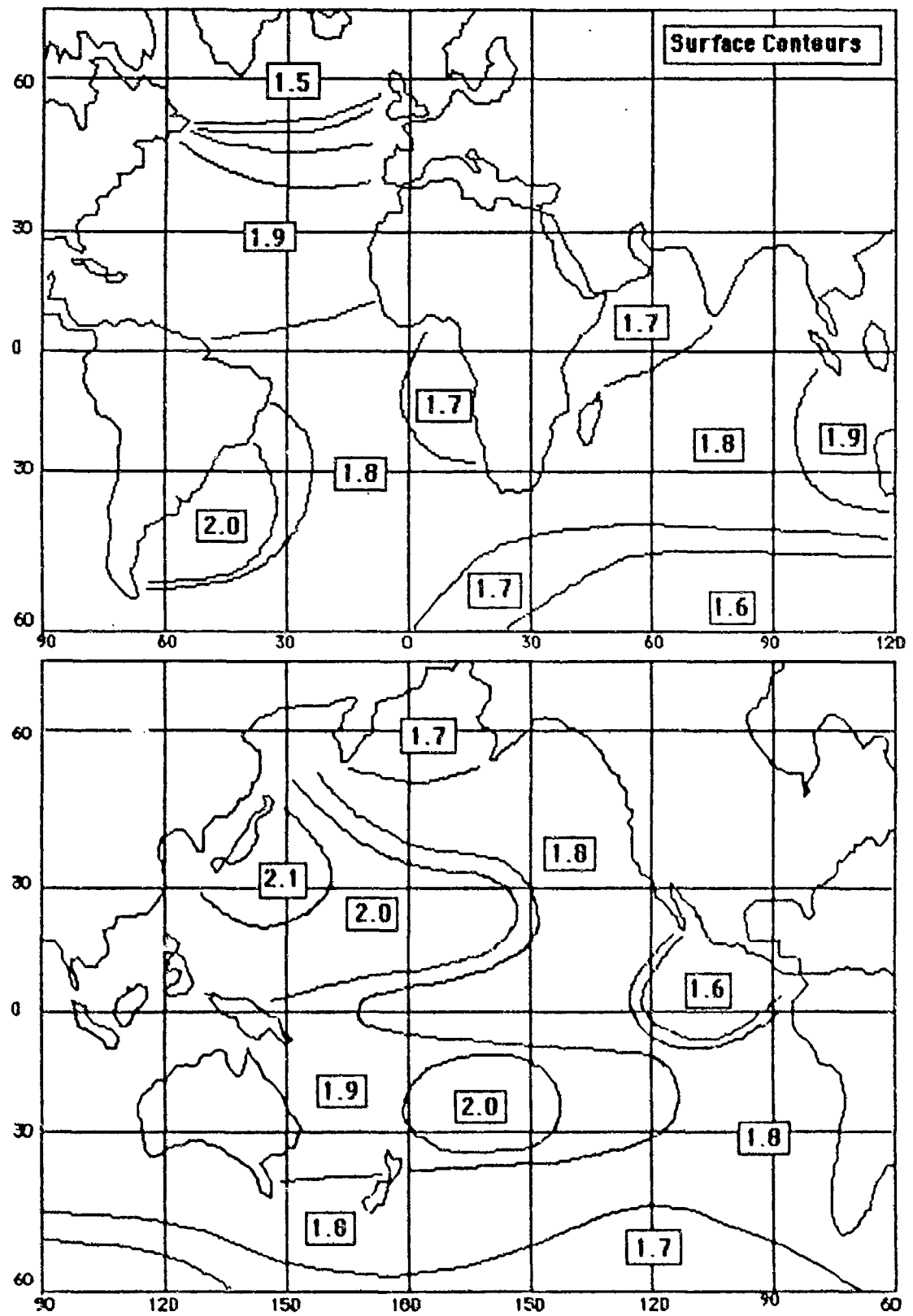
Figure 41: GEOSECS surface K contours.
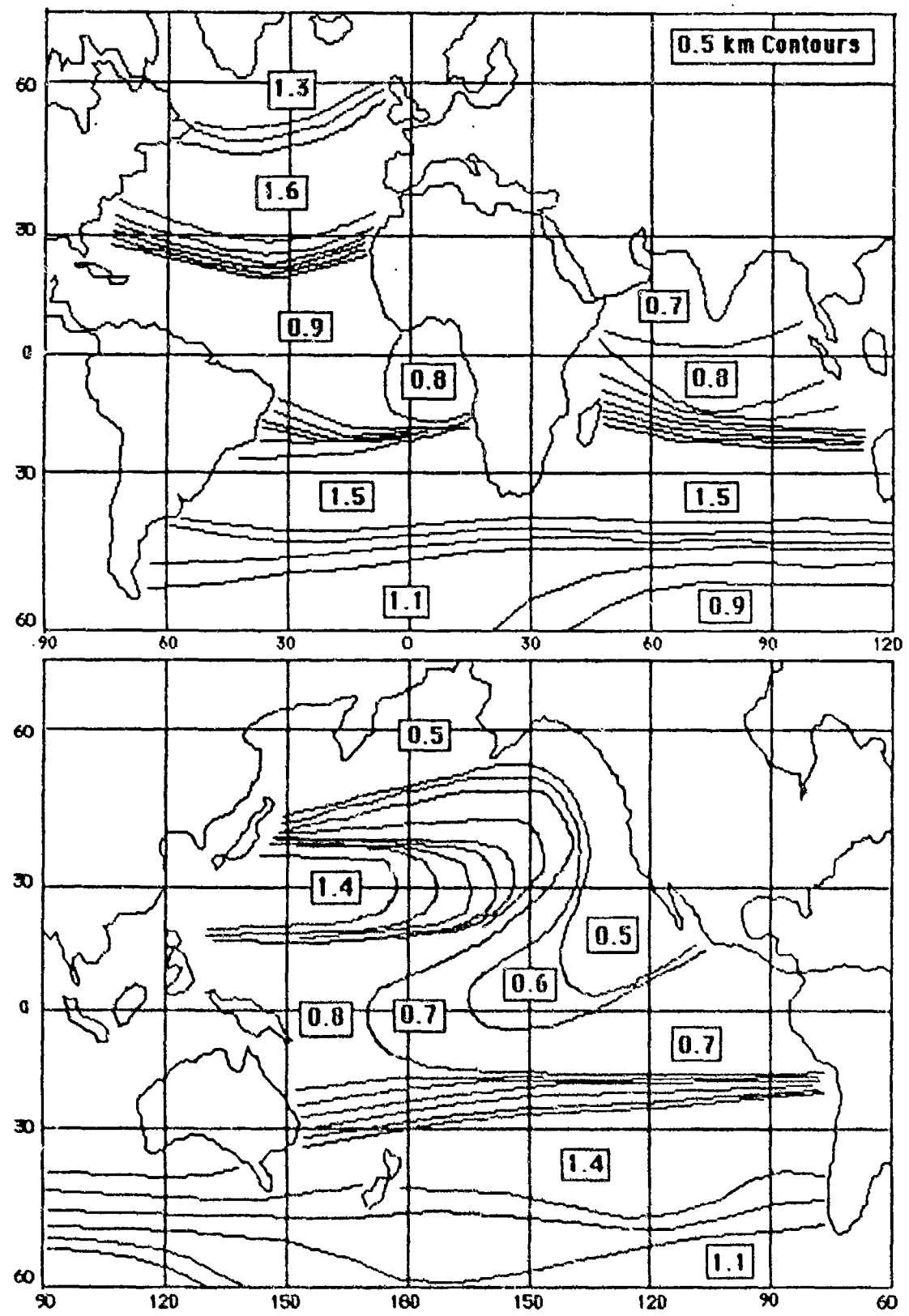
Figure 42: GEOSECS 0.5 km K contours.
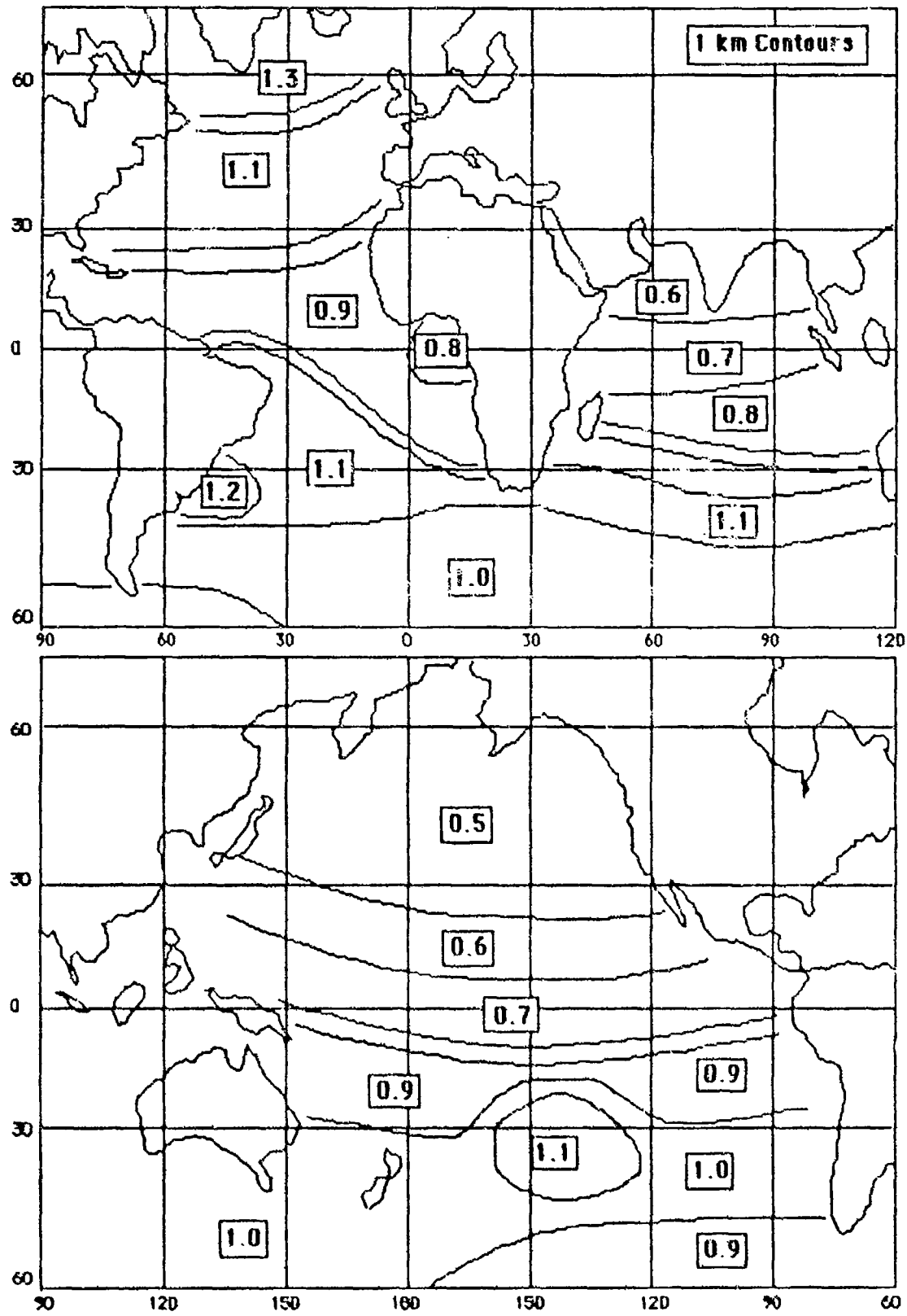
Figure 43: GEOSECS 1 km K contours.
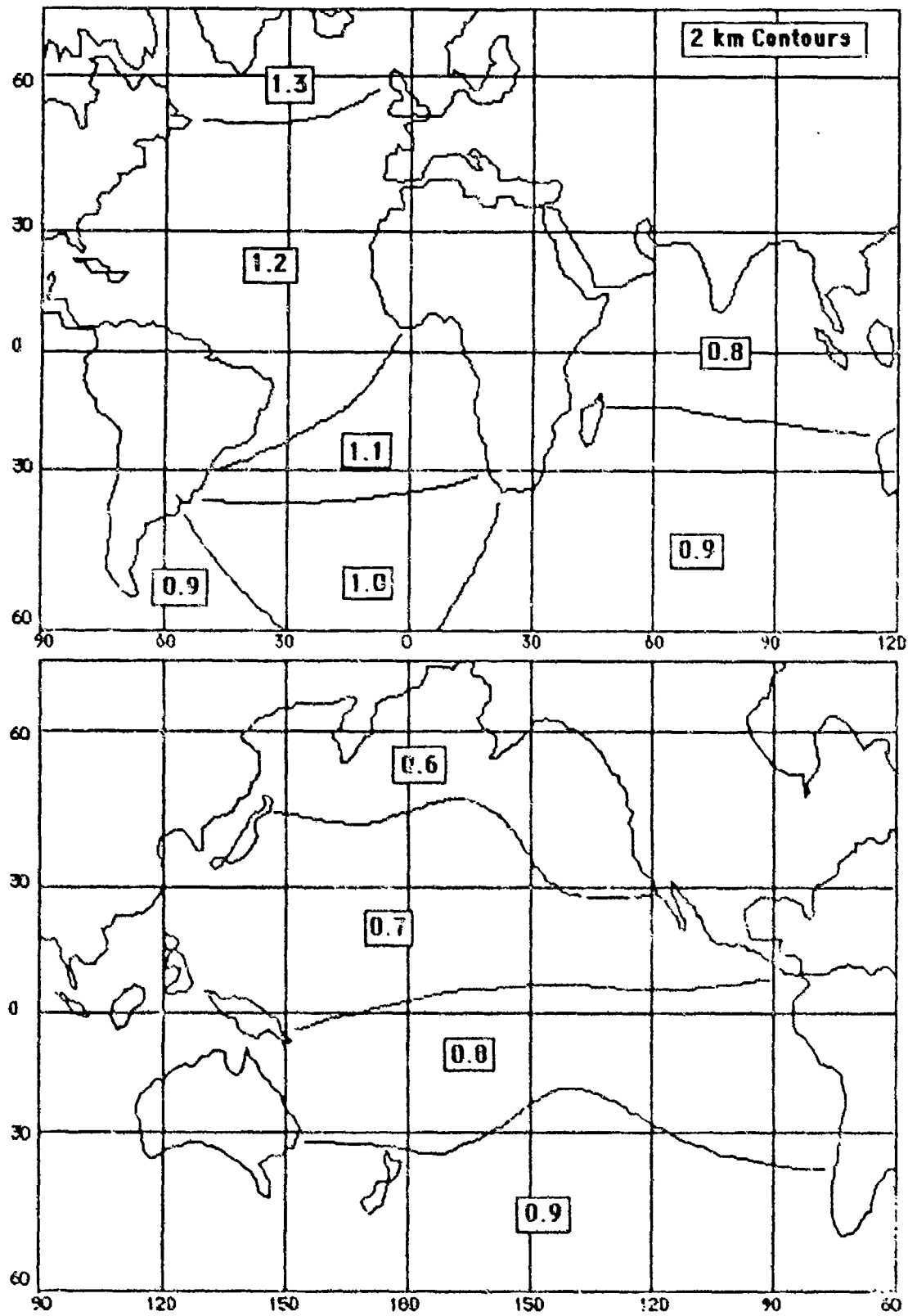
Figure 44. GEOSECS 2 km K contours.
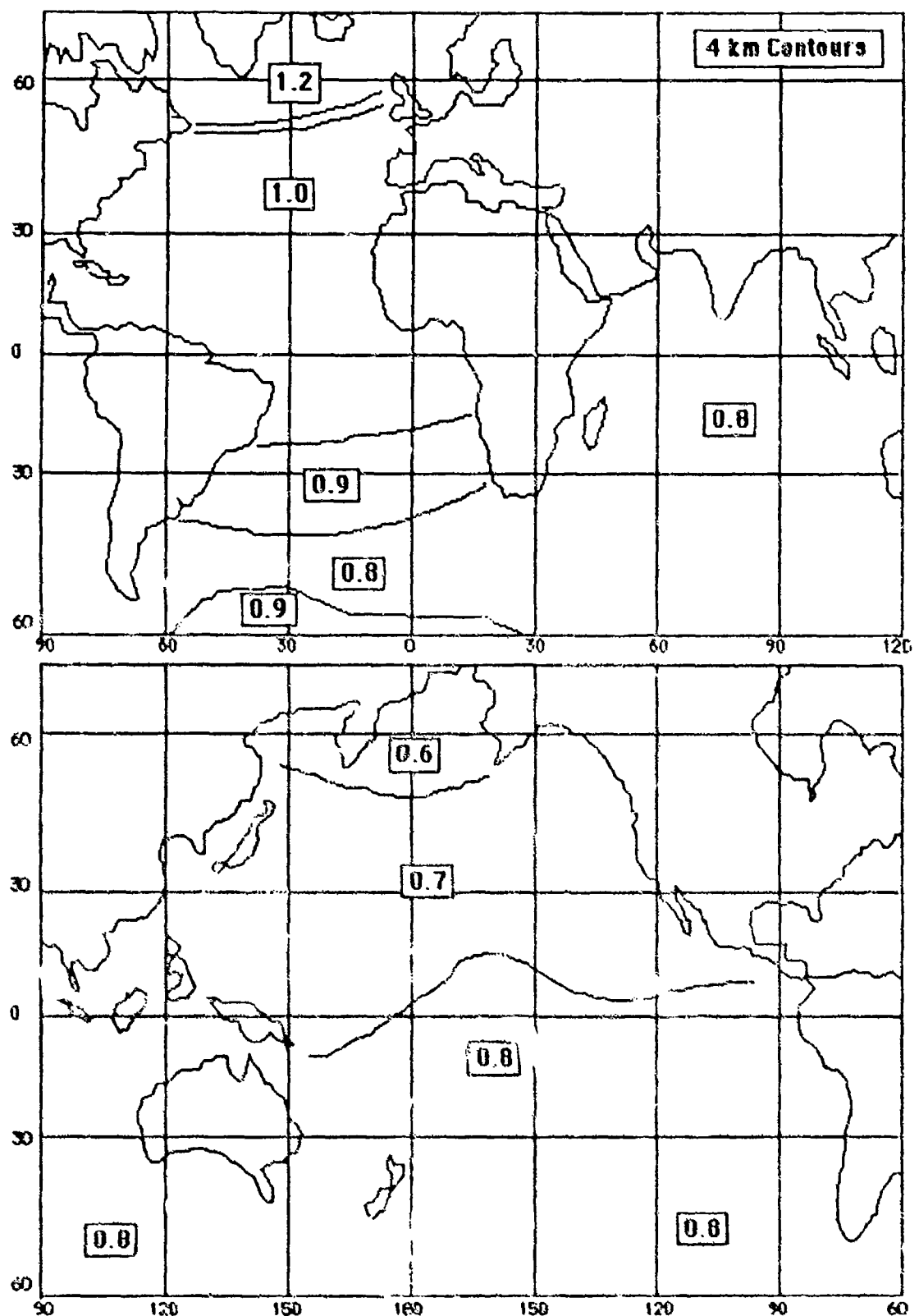
Figure 45 GEOSECS 4 km K contours.

K Profiles

Comparison of the K contours indicate no serious discrepencies between the new and earlier versions. However, adjustments of values and contours to fit the GEOSECS data should improve accuracy. Considerable uncertainty was involved in developing the earlier 2 km contours because the Pacific latitudes 165°E-130°W were not covered by Russian charts. Interpolation and pressure corrections were involved also. Therefore GEOSECS surface and 2 km charts should be the more accurate.

The K contours should also allow reasonably accurate of the profiles in most of the World Ocean. A graphic method is to connect the five points with a fair curve, which can be quite subjective. An automated method has been developed using an algorithm suggested by Dr. A. H. Nuttall, which has proved to give good results.

The five K points for depths D=0, 0.5, 1, 2, and 4 km are numbered 0-4 and the profile is fitted by the expression:

$$K(D)=K(4)+ [C_0 + C_1 D + C_2 D^2 + C_3 D^3 + C_4 D^4] \exp[-(a D)^b]$$

where $a=1/km$ and $b=1.5$ have been chosen by trial to obtain "best" results.
The five equations for n=0,1,2,3,4 to be solved are then given by:

$$C_0 + C_1 D_n + C_2 D_n^2 + C_3 D_n^3 + C_4 D_n^4 = [K(D_n) - K(4)] \exp(D_n^{1.5})$$

and solution for the coefficients can be obtained either algebraically or by writing the equations in matrix form and inverting.

Figures 46-49 show some results for the North Atlantic, North Pacific, Indian and Southern Oceans. The circles indicate the curve-fit to the five chart values for each region. A computer search is then made of the entire library to find the five GEOSECS profiles with least-square errors for the given points. The error Δ rms is shown for each case. Selected profiles are identified by station number and error. Since the error only indicates the goodness of fit at the five points, actual errors for particular ray paths can obviously be greater or less.

For the all the cases shown, the selected profiles fall within the regions in question and the errors appear to be minimal. In other cases where the method recovers profiles outside the area, the errors are equally small. An alternative procedure would be to select the profile with the best overall fit in place of the algorithm profile.
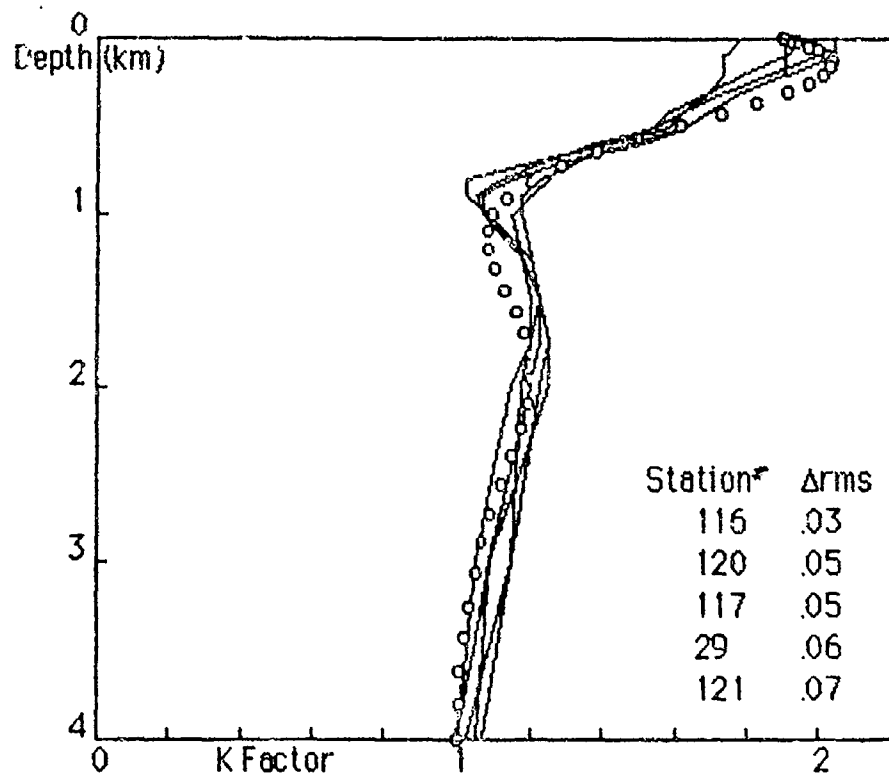
Figure 46: North Atlantic K profiles.

Station#	Δrms
116	.03
120	.05
117	.05
29	.06
121	.07
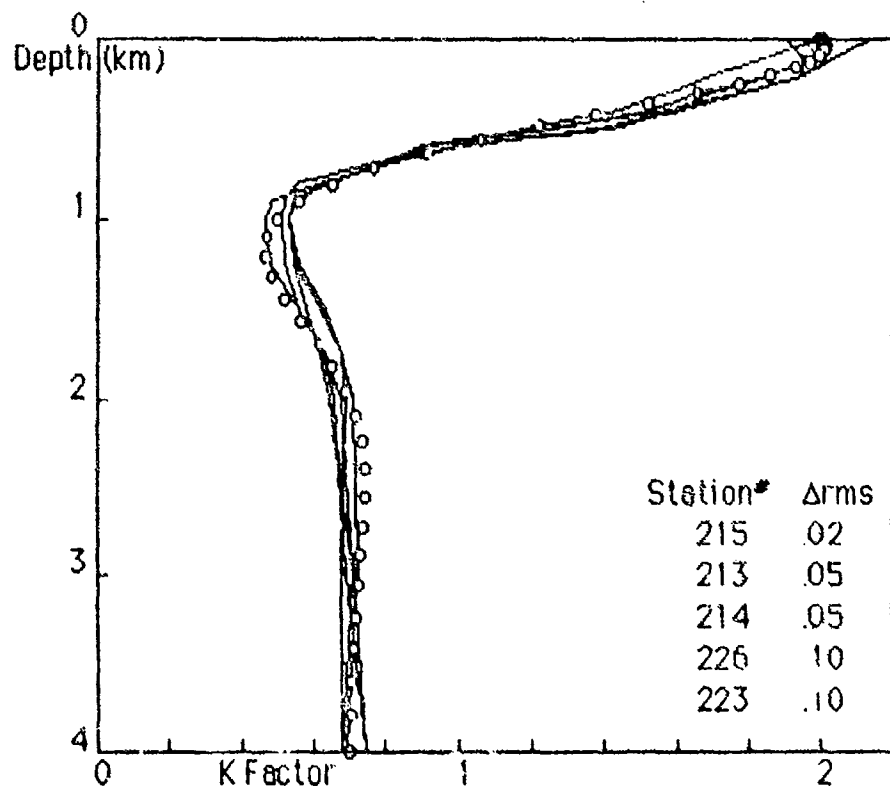
Figure 47: North Pacific K profiles.

Station#	Δrms
215	.02
213	.05
214	.05
226	.10
223	.10
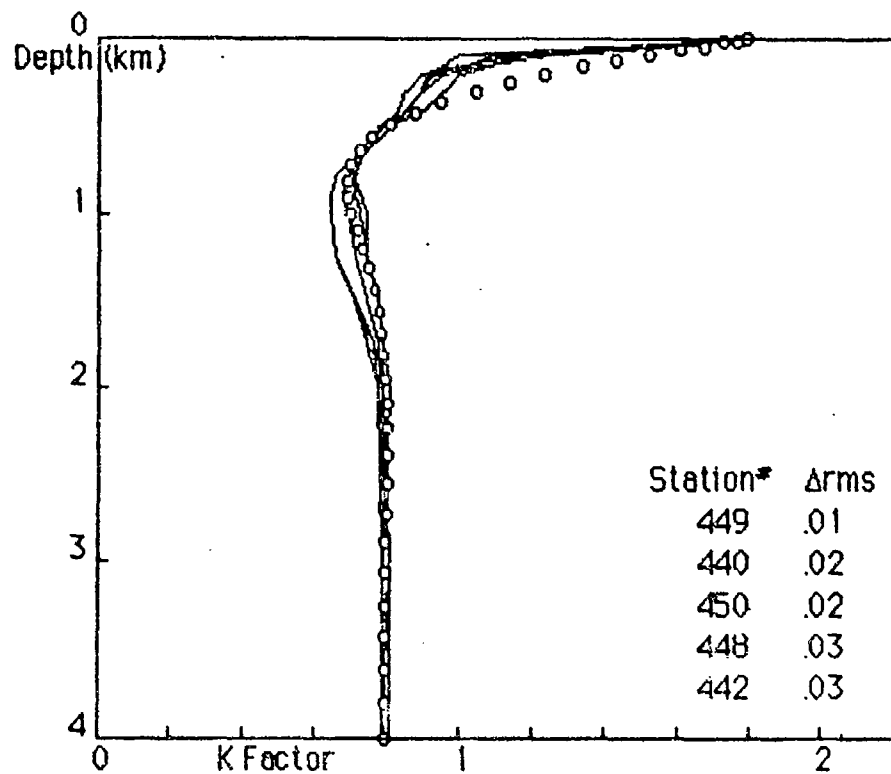
Figure 48: Indian Ocean K profiles.

Station#	Δrms
449	.01
440	.02
450	.02
448	.03
442	.03
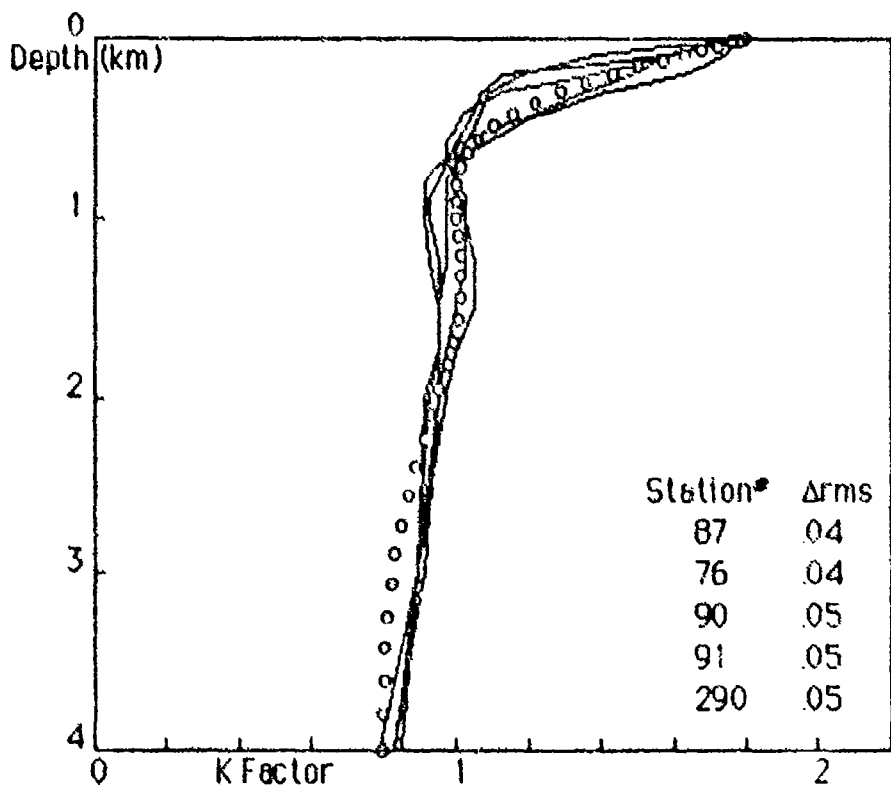
Figure 49: Southern Ocean K profiles.

Station#	Δrms
87	.04
76	.04
90	.05
91	.05
290	.05

## Temperature Profiles

Figure 50: Typical temperature profiles.

Temperature profiles are also required for the ray-integration method. Figure 50 shows some typical examples for the regions to be considered. Temperature profiles are obviously quite similar to K profiles and can be formulated by the same algorithm method. Salinity variations with depth are small and can be ignored.

Figures 51-53 show comparison of the temperature and K profiles for all reported stations in the three oceans. Station sequences read from left to right and are the same as before. Starting and ending station numbers are indicated on each graph. Note that the spacing has been increased in the lower Indian Ocean graph to eliminate overlap of the Gulf of Aden, Red Sea and Mediterranean Sea temperature profiles, which might otherwise cause confusion.

While there is a considerable degree of similarity between the profiles in many regions, the overall correlation is generally poor and clearly not sufficient to permit estimation of K profiles from temperature profiles with the required accuracy.

- 52 -
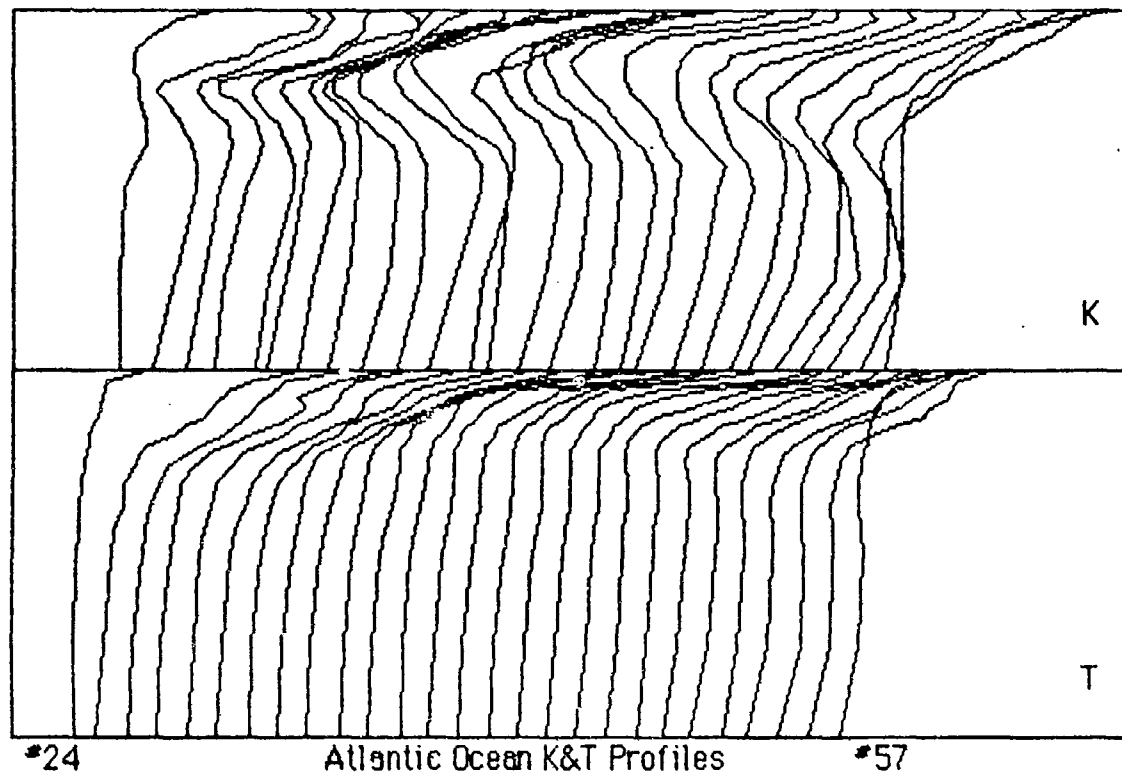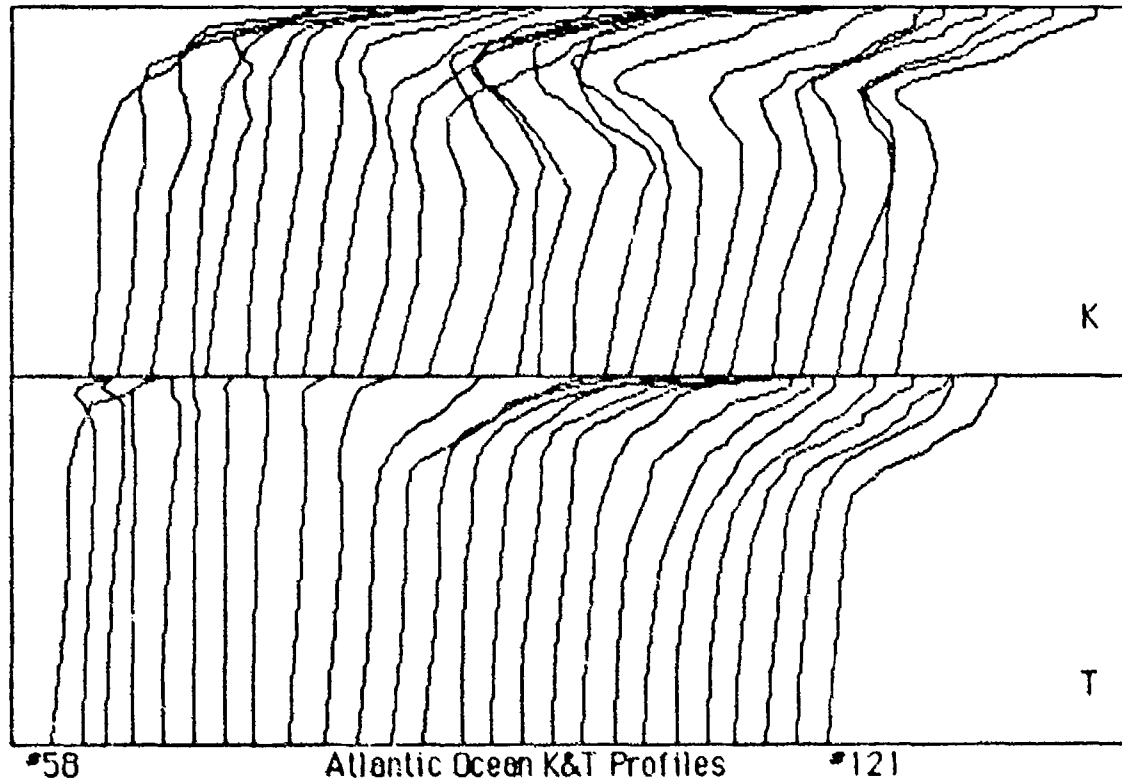
Figure 51: Temperature and K profile comparison.

K

T

#201   Pacific Ocean K&T Profiles   #251

K

T

#252   Pacific Ocean K&T Profiles   #347
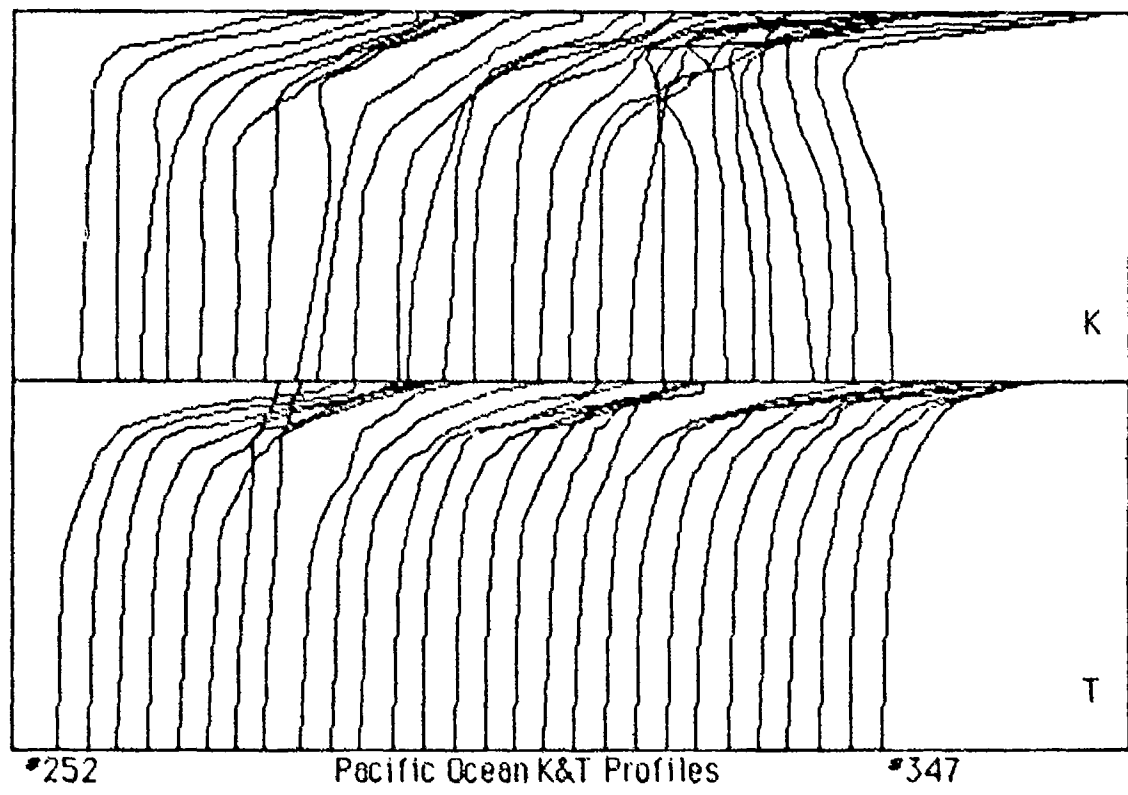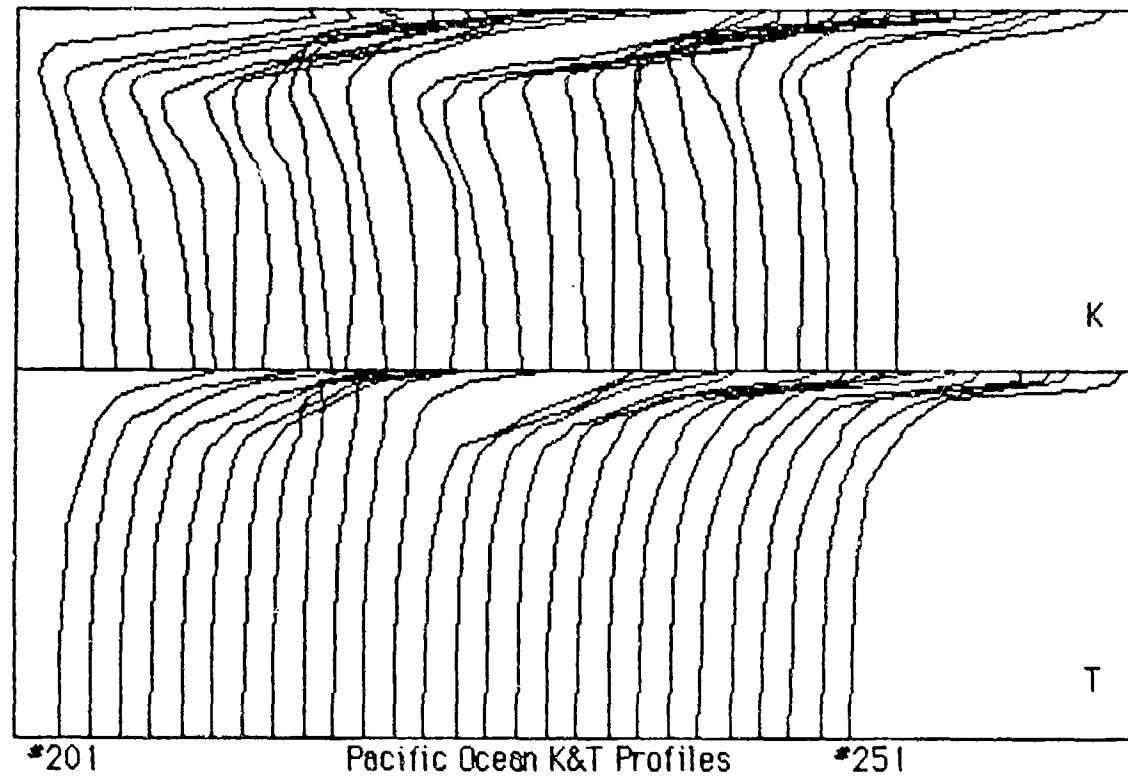
Figure 52: Temperature and K profile comparison.

K

T

#417   Indian Ocean K&T Profiles   #450

K

T

#451   Indian Ocean K&T Profiles   #404
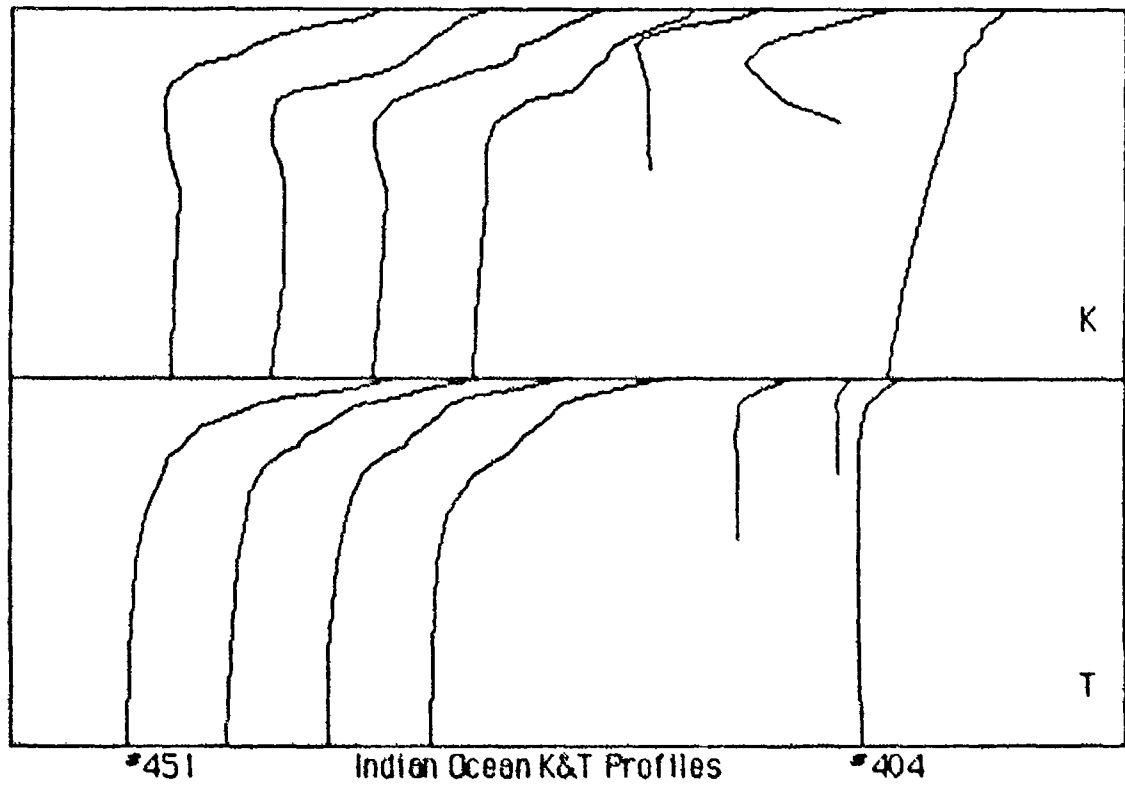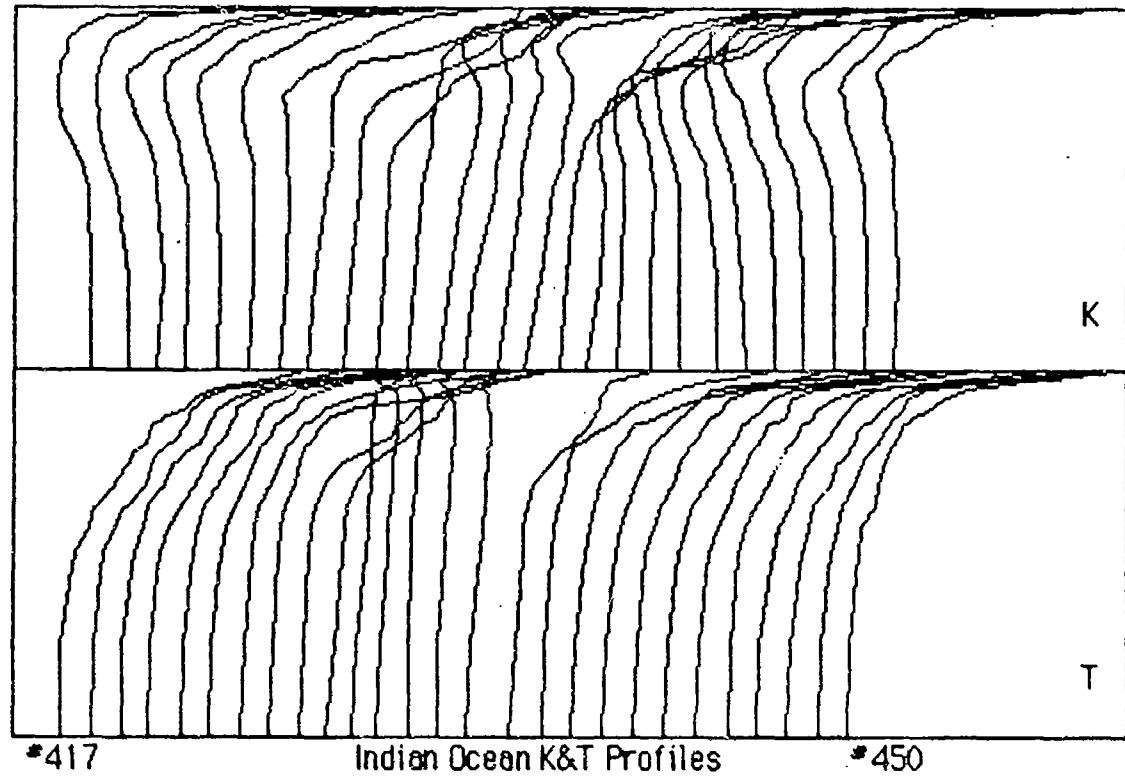
Figure 53: Temperature and K profile comparison.

Model Comparison

Absorption losses (dB) calculated by both the K model and Thorp equation for sound-channel, convergence and surface-duct propagation modes are shown in Figures 54-56. The differences Δ=A(Kmod)-A(Thorp) include the expected errors of the K model, indicating the degree of significance.

The K model calculations used ray integration and the algorithm profile. Values of K and temperature at the five depths were fitted to generate the profiles. Salinity was taken as constant S=35 except for the Mediterranean case where S=38 was used. Absorption loss at selected frequencies F(kHz) at ranges R(km) was calculated by integration over appropriate ray paths. Expected errors were calculated concurrently using $\Delta K=\pm0.05$ for the sound channels and CZ and $\Delta K=\pm0.1$ for the surface ducts. Thorp values were also calculated concurrently to minimize relative errors.

Figure 54 shows one-way sound-channel losses at R=500 km. The large range of Δ values reflects the regional pH variability at axial depths.

Figure 55 shows two-way absorption losses for active sonar in the CZ mode. Since the major part of the ray paths falls well below the depths of high pH variability, Δ values tend to be small in both magnitude and range.

Figure 56 shows two-way surface-duct losses at R=50 km. The Δ values are uniformly high because of the high surface pH.

Alpha (dB) SC		Atl. 30°N	Pac. 45°N	Pac. 50°S	Ind.10°S	E. Med.
F (kHz)	R (km)>	500	500	500	500	500
1.0	K mod.	33.3	17.5	47.6	21.9	51.6
	Thorp	32.7	32.7	32.7	32.7	32.7
	Δ	0.7±1.3	-15.2±1.4	15.0±1.4	-10.7±1.3	18.9±1.3
0.8	K mod.	24.6	12.9	36.1	16.1	36.8
	Thorp	24.7	24.7	24.7	24.7	24.7
	Δ	-0.2±1.0	-11.9±1.0	11.4±1.1	-8.7±1.0	12.1±1.0
0.6	K mod.	15.7	8.3	24.0	10.3	22.8
	Thorp	16.4	16.4	16.4	16.4	16.4
	Δ	-0.6±0.6	-8.1±0.7	7.6±0.7	-6.1±0.6	6.4±0.6
0.4	K mod.	7.8	4.2	12.3	5.1	10.9
	Thorp	8.4	8.4	8.4	8.4	8.4
	Δ	-0.6±0.3	-4.2±0.4	3.9±0.4	-3.3±0.3	2.5±0.3
0.2	K mod.	2.1	1.1	3.4	1.4	2.9
	Thorp	2.3	2.3	2.3	2.3	2.3
	Δ	-0.2±0.1	-1.2±0.1	1.1±0.1	-1.0±0.1	0.5±0.1

Figure 54: One-way sound-channel absorption values.

2Alpha (dB) CZ		Atl. 30°N	Pac. 45°N	Pac. 50°S	Ind.10°S	E. Med.
F (kHz)	R (km)>	74	64	36	74	47
3.5	K mod.	37.6	25.7	24.4	31.2	34.2
	Thorp	34.2	29.7	16.3	34.2	21.5
	Δ	3.4±1.0	-3.9±0.9	8.1±0.5	-3.0±1.0	12.7±0.8
3.0	K mod.	32.0	21.2	20.9	26.0	30.1
	Thorp	28.7	24.9	13.7	28.7	18.1
	Δ	3.3±0.9	-3.7±0.8	7.2±0.4	-2.7±0.9	12.1±0.7
2.5	K mod.	26.7	17.1	17.6	21.3	25.9
	Thorp	23.8	20.6	11.3	23.8	15.0
	Δ	2.9±0.8	-3.5±0.7	6.3±0.4	-2.5±0.8	10.9±0.6
2.0	K mod.	21.5	13.4	14.4	16.8	21.2
	Thorp	19.2	16.7	9.2	19.2	12.1
	Δ	2.2±0.7	-3.3±0.6	5.2±0.3	-2.5±0.7	9.1±0.5
1.5	K mod.	16.1	9.8	11.1	12.4	15.8
	Thorp	14.7	12.8	7.0	14.7	9.3
	Δ	1.4±0.6	-3.0±0.5	4.1±0.3	-2.4±0.6	6.6±0.4

Figure 55: Two-way convergence-zone absorption values.

2Alpha (dB) SD		Atl. 30°N	Pac. 45°N	Pac. 50°S	Ind.10°S	E. Med.
F (kHz)	R (km)>	50	50	50	50	50
3.5	K mod.	35.7	34.1	35.7	34.5	38.6
	Thorp	23.1	23.1	23.1	23.1	23.1
	Δ	12.6±1.6	11.0±1.4	12.5±1.4	11.3±1.7	15.4±1.7
3.0	K mod.	31.5	29.7	30.6	30.1	34.0
	Thorp	19.4	19.4	19.4	19.4	19.4
	Δ	12.0±1.5	10.3±1.3	11.2±1.3	10.7±1.5	14.6±1.5
2.5	K mod.	26.7	25.4	25.8	25.2	29.3
	Thorp	16.1	16.1	16.1	16.1	16.1
	Δ	10.6±1.3	9.3±1.2	9.7±1.1	9.1±1.3	13.2±1.4
2.0	K mod.	21.1	20.9	21.2	19.5	24.0
	Thorp	13.0	13.0	13.0	13.0	13.0
	Δ	8.1±1.0	7.9±1.0	8.2±1.0	6.5±1.0	10.9±1.1
1.5	K mod.	14.8	15.9	16.3	13.2	17.7
	Thorp	10.0	10.0	10.0	10.0	10.0
	Δ	4.8±0 7	6.0±0.8	6.4±0.8	3.3±0 7	7.7±0.9

Figure 56: Two-way surface-duct absorption values.

Conclusions and Recommendations

Two methods for estimating pH effects on sound absorption have been proposed for use in conjunction with the absorption formula of Figure 5. The interim method employs K contours for specific propagation modes; i.e. sound channel, CZ and surface duct (Figures 6-8). This method is useful for rapid calculation but involves judgement if there is no single dominant mode. The second method employs K profiles constructed from K-contour charts at five depths 0, 0.5, 1, 2 and 4 km (Figures 41-45). This method is useful for integrating loss over all ray paths by computer methods.

One purpose of the GEOSECS data analysis has been to investigate the consistency of the pH data. Results indicate agreement between the new K contours and the earlier versions. The sound-channel contours are in good agreement with Lovett's charts. Agreement with Russian charts at fixed depths is also good except for possible minor discrepencies in surface values, which may reflect seasonal variability. GEOSECS data were taken during warmer periods and surface temperatures appear to be consistently high, while the Russian data are seasonally averaged. Within these limits, errors for both surface charts appear comparable.

The second purpose has been to devise a simple procedure for estimating the K profiles required for propagation analysis by numerical methods. By integration losses over all ray paths using a profile, all uncertainty about what values to use is eliminated. The five points from the contour charts should allow reasonably accurate approximation of K profiles throughout most of the World Ocean in regions where no actual data can be found.

Profiles can be generated graphically by drawing a fair curve through the five points. Since making the fit consistent with actual profiles involves some subjectivity, the algorithm method may be preferred.

An alternative method is to do a computer search a library of profiles and select the one with least-square error for the five points in question. This procedure will usually recover a profile in the same general area. If not, discrepencies between known and recovered profiles are usually found to be minimal. Another alternative is to check the overall fit of the recovered profiles and arbitrarily pick the one that appears best suited to the region under consideration.

One of the main advantages of the library method is that additions can be made as new data become available. While some revisions of the contours may then be required, the extrapolation errors involved in approximating profiles should be reduced. This method also seems to be suitable for easy implementation in existing computer programs.

- 58 -

References

1. O. B. Wilson and R. W. Leonard, "Measurements of sound absorption in aqueous salt solutions by a resonator method", J. Acoust. Soc. Am. 26 223-228 (1954)

2. M. Eigen and K. Tamm, "Sound absorption in electrolytic solutions due to chemical relaxation", Z. Electrochem. 66 93-121 (1962)

3. M. Schulkin and H. W. Marsh, "Sound absorption in sea water", J. Acoust Soc. Am. 34 864-865 (1962)

4. W. H. Thorp, "Deep ocean sound attenuation in the sub and low kilocycle-per-second region", J. Acoust. Soc. Am. 38, 648-654 (1965)

5. W. H. Thorp, "Analytic description of the low-frequency attenuation coefficient" J. Acoust. Soc. Am. 42 270-271 (1967)

6. C. C. Leroy, "Sound propagation in the Mediterranean Sea", in Underwater Acoustics, ed. V. M. Albers (Plenum, 1967) Vol. 2, pp. 203-241.

7. R. H. Mellen and D. G. Browning, "Variability of low-frequency sound absorption: pH dependence", J. Acoust. Soc. Am. 61, 704-706 (1977)

8. E. Yeager, F. H. Fisher, J. Miceli and R. Bressel, "Origin of low-frequency sound absorption in sea water", J. Acoust. Soc. Am. 53, 1705-1707 (1973)

9. R. H. Mellen, D. G. Browning and V. P. Simmons, "Investigation of chemical sound absorption in sea water by the resonator method", J. Acoust. Soc Am. Part I, 68, 248-257 (1980)
Part II, 69, 1660-1662 (1981)
Part III, 70, 143-146 (1981)
Part IV, 74, 987-993 (1983)

10. R. H. Mellen, V. P. Simmons and D. G. Browning, "Sound absorption in sea water: a third chemical relaxation", J. Acoust. Soc. Am. 65, 923-925 (1974)

11. R. H. Mellen, "Global model for sound absorption in sea water" PSI Marine Sciences Report, August 1986.

12. Attenuation of Low Frequency Sound in the Sea,
NUSC Scientific and Engineering Studies, Volumes I & II
Published by the Naval Underwater Systems Center (1981)

13. F. H. Fisher and V. P. Simmons, "Sound absorption in sea water",
J. Acoust. Soc. Am. 62, 558-564 (1977)

14. R. H. Mellen and D. G. Browning, " Low-frequency sound absorption in the
Pacific Ocean", J. Acoust. Soc. Am. 59 700-702 (1976)

15. R. H. Mellen, T. Akal, E. H. Hug and D. G. Browning, Low-frequency sound
attenuation in the Mediterranean Sea", J. Acoust. Soc. Am. 78 S70 (1985)

16. GEOSECS Atlas, International Decade of Ocean Exploration (IDOE),
Published by National Science Foundation (1981)
Vol. 1, Atlantic Expediton 1972-1973
Vol. 3, Pacific Expedition 1973-1974
Vol. 5, Indian Ocean Expedition 1977-1978

17. World Ocean Atlas, edited by S. G. Gorshkov (Pergamon Press, New York)
Vol. 1, Pacific Ocean, pp.234-235 (1974),
Vol. 2, Atlantic and Indian Oceans, pp234-235 (1978)

19. J. R. Lovett, "Geographic variation of low-frequency sound absorption
in the Atlantic, Indian and Pacific Oceans",
J. Acoust. Soc. Am. 67 338-340 (1980)

19. Qiu Xinfang, Jiang Jiliang and Wan Shimin, "Sound absorption in sea
water due to low frequency chemical relaxations",
Chinese J Acoust. 2 71-80 (1983)

20. Qiu Xinfang, Jiang Jiliang and Wan Shimin, "Investigation of the
mechanism of sound absorption by the boric acid relaxation in sea water",
Chinese J. Acoust. 3 51-63 (1984)

EXTERNAL DISTRIBUTION LIST

Addressee	No. of Copies
CINCLANTFLT	1
CINPACFLT	1
COMMANDER SECOND FLT	1
COMMANDER THIRD FLT	1
SURF FORCE LANT	1
SURF FORCE PAC	1
SUB FORCE LANT (CDR Callahan)	1
SUB FORCE PAC (Staff Oceanographer)	1
TRAINING COMMAND LANT	1
TRAINING COMMAND PAC	1
SUBMARINE GROUP 2 (LT Arango)	1
SUBMARINE GROUP 6 (CDR Dantzler)	1
SUBMARINE DEV GROUP 1	1
SUBMARINE DEV SQUADRON 12 (CDR W. Stephenson)	2
DEFENSE TECH INFO CENTER	1
CNO - NOP-095, NOP-951, NOP-952, NOP-953, NOP-098 NOP-981, NOP-987, NOP-02, NOP-21, NOP-22, NOP-03, NOP-62	12
CNR - OCNR-00, OCNR-10, OCNR-11, OCNR-12, OCNR-122, OCNR-124, OCRN-125, OCNR-127, OCNR-13, OCNR-20	10
OFFICE OF NAVAL RESEARCH DETACHMENTS	1
ONR DET BAY ST. LOUIS	1
ONR DET BOSTON	1
ONR DET PASADENA	1
NAIR-03	1
SPAWAR-00, PDW-124, SPAWAR-05	3
SEA-62, SEA-63	2
NRL	2
NRL DET CHESAPEAKE	2
NRL UND SOUND REF DET ORLANDO	2
NRL SPEC PROJ DET PT. MUGU	2
NORDA	2
NEPRF	2
NADC	2
NCSC (Ms. A. Bagnell)	2
NOSC	2
NOSC DET HAWAII	2
NPRDC	2
DTNSRDC	2
DTNSRDC CARDEROCK LAB	1
DTNSRDC ANNAPOLIS LAB	1
DTNSRDC ACOUS RES DET BAYVIEW	1
DTNSRDC DET BREMERTON	1
NUSC	1
NUSC NEWPORT LAB	4
NUSC NEW LONDON LAB	2
NUSC DET AUTEC	2
NUSC DET WEST PALM BEACH	2
NUSC DET TUDOR HILL	2
NUSC DET FT. LAUDERDALE	2
NUSC DET SENECA LAKE	2

EXTERNAL DISTRIBUTION LIST

Addressee	No. of Copies
NAVAL OCEANOGRAPHY COMMAND	2
NAVAL OCEANOGRAPHIC OFFICE	2
FLEET NUMERICAL OCEANOGRAPHY CTR	2
NTSA	1
NPS	1
NWC	1
SURF WARFARE OFFICERS SCHOOL COMMAND	1
SUBMARINE SCHOOL (Code 10, CDR Almon)	1
APPLIED PHYSIC LAB, JOHNS HOPKINS	1
APPLIED PHYSICS LAB, U. WASHINGTON	1
APPLIED RESEARCH LAB, PENN STATE	1
APPLIED RESEARCH LAB, U. TEXAS	1
MARINE PHYSICAL LABORATORY SCRIPPS	1
WOODS HOLE OCEANOGRAPHIC INSTITUTION	1
UNIV. OF CT, MARINE SCIENCES (Dr. F. W. Bohlen)	1
UNIV. OF NH, EARTH SCIENCES (Dr. F. Anderson)	1
UNIV. OF RI	1
PLANNING SYSTEMS INC (Dr. R. H. Mellen)	10

Contract #N66604-87-M-B555